台灣二ＯＯ五年國際科學展覽會

科　　別：工程學

作品名稱：以熱聲效應改善微電子裝置散熱的研究

得獎獎項：大會獎第一名

　　美國團隊正選代表:參加美國第 56 屆國際科技展覽會

學　　校：臺北市立麗山高級中學

作　　者：邢本元、黃維綱

評語與建議事項：

利用電能轉換將過剩之熱能移除，構想非常好，實用性也很高，實驗之設計完整，能夠考慮將聲音造成噪音現象移除，提高其實用價值。可以將實驗建置於微小化環境，進一步探討使用於微電子裝置會碰到之問題及其解決方法。

2005 臺灣國際科學展覽會

作者黃維綱簡介

早在一年前，我們就研究過熱電半導體和風扇的降溫效果，也試著去改良它，很幸運在上屆國際科展入圍了。第一次做這麼大的專題，總會有點驕傲，自以爲了不起；但評審教授說了一句話：「大同風扇在市場上獨霸了五十年，沒有一個人打倒過它...，如果以後要有賣點，必須從電腦散熱著手...。」徹底打敗我的信心，當然也沒得獎啦。但經過他一番指點和指導之下，題目轉了個大彎，變成如今研究的熱聲散熱。老實說這個實驗連續做下來真的很累，還好我有認真負責的伴，讓我想偷懶的時候也不好意思偷懶。如今我們只做到一個段落而已，熱聲散熱裝置是個極具有淺力的東西，將來還有更多更多的現象及實驗等待人們去研究！

邢本元自傳

「…『邪』本元？」「有！」，頓時全班哄堂大笑，「是『邢』本元啦！」；首次教我的老師都可藉此多學一個字（國文老師除外）。重小到大，我就因姓名而被取過無數個外號，其中邢「粉圓」最爲常見。別說在國內造成誤會，到了國外每次向那些洋人解釋我的名子就得花上大半天的工夫。

我在民國八十二年的夏天到了美國檀香山就讀小學，一待就將近三年。我向來和歷史脫不了關係，父母皆爲歷史學者，邢家爲周公直系子孫，母方祖先爲清朝舉人，現在又到了 國父成立興中會的檀香山。

剛到達時，因爲完全不會英文而成爲大家的眾「笑」之的，備受歧視。幸虧當時在母親的教導與英語的環境之下學習英文，使我在三年後離開美國時可與同學們平起平坐、毫無隔閡。當時還被選入學校的資優課程，數學成績爲全班最高。旅美三年可說是我這生中的全盛時期吧，但也使我養成有些自負的性格 。

回到臺灣開始念小學四年級，也是第一次正式學注音符號。我那洋腔洋調的樣子連國字都不會寫，自然又成爲眾人消遣的對象。從這個角度來看，我在臺灣的小學後三年，似乎是美國的翻版。這二次的經驗都是由文化的差異與語言的隔閡所造成，我感覺到那兒都被當作外國人 ，這個滋味是多數人難以體會的。

國中又是另一個轉折點。我以爲我的數學很好，結果別人也不差；我以爲我很會彈鋼琴，結果大家都會。在金華國中，似乎大家都有我不會的專長。申請高中時，我拿出了一張獎狀，別人拿出了一整本獎狀。別人考上建中，我卻被「流放」到邊疆的麗山，雖然它是我們家人都很喜歡的學校，但大家都問：「你怎麼考那麼爛？ 麗山高中在那裡？曾母暗沙嗎？」，這時我原有的自大性格就再也沒有出現了。

既然已經考上了，就「念念看」吧。原本打算這三年只是讀書背書考試直到大學，麗山還能給我甚麼？

事實上麗山有許多特點是其他學校缺乏的，例如班級的人數都在三十人以內、比多數高中自由的校風，我在麗山專題研究課程中學習到的能力更是終生受用。

這三年奇妙的歷程得從高一參加地科社說起。當年麗山地科社的活動被列爲內湖區高中生可參加的選修天文課程，所以每週社團時間都會有外校生來上課。這時我經內湖高中同學的介紹第一次接觸到「臺北濕地網」， 一個由北臺灣許多高中社團共同組成的非營利性、濕地資訊交流網路。在定期的集會中討論、報告相關的議題進而促進社團對濕地的研究、關心與環境自覺。原來只打算去一次補充公共服務時數，後來在臺北濕地網的活動中體會到了環境與我們的關係是多麼密切；我也從麗山地科社的代表成爲臺北濕地網的召集人。我在擔任召集人的這一年裡，除了協辦各次的常會並在其中報告、討論外，還參加了這生第一次的學術研討會、應邀至青輔會的座談會等場合。這些經驗和我在學校專題課中的科學訓練同時並行、

相輔相成。

麗山高中的學生在高一就有必修的研究方法課，到了高二就得選擇科目進行專題研究。當我要升高二時，母親提醒我一段小時候的故事：

我從小不敢坐飛機，不相信如此重的物體可待在空中。後來經友人講解飛機的原理後才願意嘗試坐飛機，得以赴美就學。從此我對自然現象就一直懷有興趣與好奇。可能是因爲這原因，也可能是因爲當時和物理老師較熟，所以我選了物理專題研究。麗山的學生較別的學生幸運之處就是每個人都有參與研究的機會，不像某些學校只有資優班中的菁英才有資格。老師熱情、耐心的指導，讓我們在高中就有研究生做研究的經驗。我還曾經參加校內、外的各種科展、競賽。有人會問：花這些時間做專題研究，甚至參加科展，會不會嚴重影響課業？其實，我們也不過是在別人打電動、唱歌、逛街時進行另外一種活動。 在研究過程中，讀了研究所的論文、科學期刊的文章，體悟到當所知、所學的越多時，才發現還有那麼多不會的，也就是「學得越多，知道的越少」；這使我以更謙遜的態度看待事情。 在各次的科展中，除了做研究的訓練外，也看到別人的作品，發現優秀的人才實在太多了。當時我感覺像井底之蛙剛跳出來，真正見到世面，發現自己是多麼渺小。

高中三年參加的事務眾多，難免會感受到壓力。我從小就有跟隨家人去教會做禮拜的習慣，在高中受到挫折時，除了聽音樂、彈鋼琴外，麗山學生團契中同學間的關懷成爲最好的安慰。回想起這十幾年來的經歷，就像是神把我的一生分爲三年一「幕」的戲劇，有高潮、低潮，將我從驕傲的深淵中救禳，祂爲我開的路遠超過我所求。現在我只想說一聲「謝~謝」，感謝那些曾關心、幫助、鼓勵過我的親戚、朋友；也感謝那些曾嘲笑我、欺負我的人，你們幫助磨練我成爲今天的邢本元（請注意「邢」的寫法）。

↑2003 臺北濕地網參加碧砂漁港淨灘合影；當別人在打電動、逛街時，

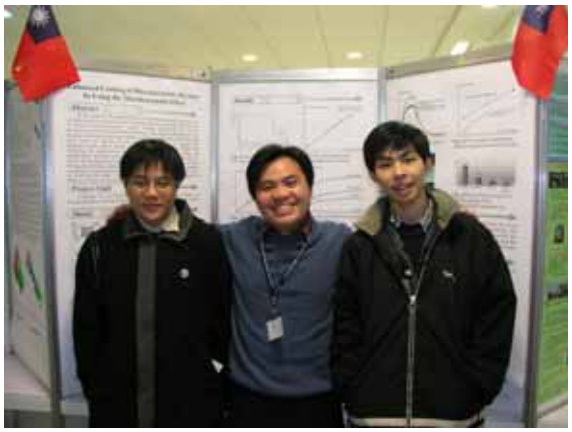

↑2005 臺灣國際科展第一名；張良肇老師和學生於國旗及英文海報前合影。(由左至右：邢本元、張良肇老

致　謝

本組希望感謝下列人員與單位在本研究過程中所提供的大量指導和協助：

國立臺灣大學應用力學研究所　李 教授 世光
國立臺灣大學應用力學研究所　鄭 學長 志強
臺北市立麗山高級中學　吳 老師 明德
臺北市立麗山高級中學　張 老師 良肇
臺北市立麗山高級中學　盛 老師 寶徵
臺北市立麗山高級中學　徐 老師 慰筠
臺北市立麗山高級中學　許 同學 曾昱
國立臺北科技大學冷凍空調技術系 黃 教授 博全
Robert W. Smith Ph.D., Graduate Program in Acoustics, Applied Research Laboratory, Pennsylvania State University.
臺北市立麗山高級中學　孫 老師 欽祥
臺北市立麗山高級中學　徐 老師 志成
臺北市立麗山高級中學　陳 老師 聲台
臺北市立麗山高級中學　陳 老師 銘志
臺北市立麗山高級中學　駱頌揚 同學
臺北市立麗山高級中學　蔣璿震 同學
臺北市立麗山高級中學　張育銘 同學
臺北市立麗山高級中學　翁正達 同學
臺北市立胡適國民小學　陳 老師 明仁
鉅威科技有限公司數位複印輸出中心
臺北市立麗山高級中學　曾昱智 同學
臺北市立麗山高級中學　郭沛群 同學

最後，本組希望對我們的家長、其他繁簇不及備載的親戚朋友們至上最深的謝意，你們的支持與鼓勵是我們最重要的動力，謝謝！

摘　　要

近年來在熱聲效應方面的研究產生了許多新發明，如冰淇淋冰箱與太空梭溫控系統等。然而，將熱能轉換成聲能的熱聲引擎，在散熱方面的效用只有被提起而從未被實際應用。本研究參考美國賓州大學「聲學雷射」裝置來研究熱聲引擎的特性，並提出一個以熱聲效應改善微電子器材散熱的裝置。它的優點是由電子裝置產生的熱即可啟動熱聲效應，而熱聲效應所加強的熱對流可降低該電子零件的溫度。實驗中發現透過熱聲效應的強烈散熱，可以大為降溫，由 200℃降為 50℃左右，這正是當代電腦內中央處理器（CPU）的工作溫度範圍。未來的研究可以針對陣列式的熱聲散熱裝置進行測試。

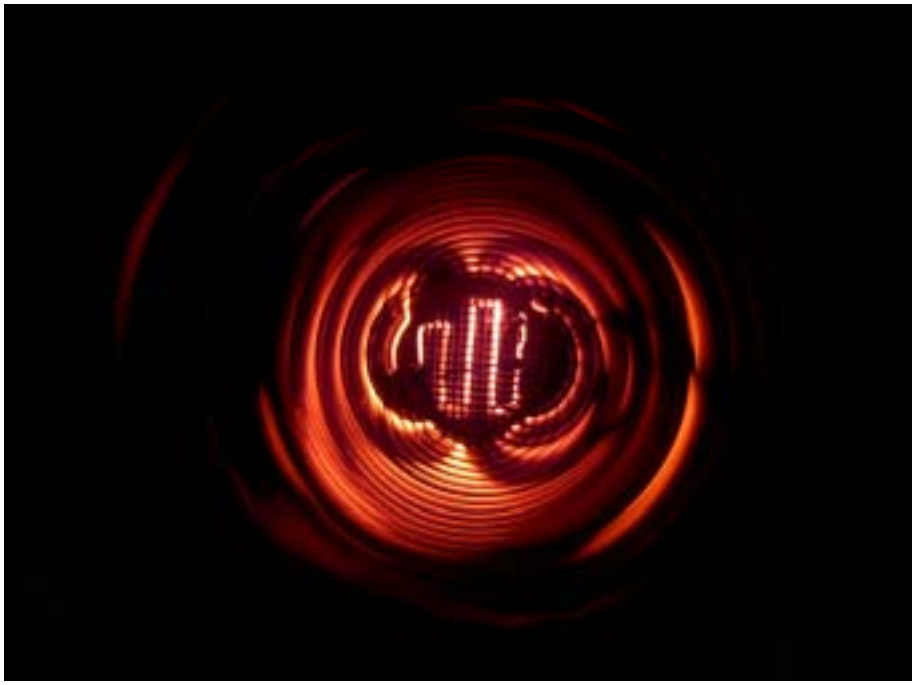

▲熱聲效應共振管中加熱中的鎳鉻絲。

Abstract

In this project, the characteristics of the thermoacoustic engine were first studied using the “Acoustic Laser” concept. A passive thermoacoustically enhanced convection engine capable of improving the cooling effect of microelectronic devices was then proposed. This design has the advantage that no additional energy input is required, a contrast to the usage of mini-fans in today’s computers. A testbed combining a heated NiCr wire with a glass tube was used to examine the overall cooling effect. In order to evaluate its performance, we measured the following parameters: radiation, convection, conduction, and acoustic radiation. We found that the heat caused by today’s microelectronic devices is sufficiently high to trigger the thermoacoustic effect. Based on this finding, we designed a new configuration to utilize this thermoacoustically enhanced convection to significantly lower the temperature. Our approach has a potential application to tackle the heat problems caused by the rapidly advancing microelectronic devices.

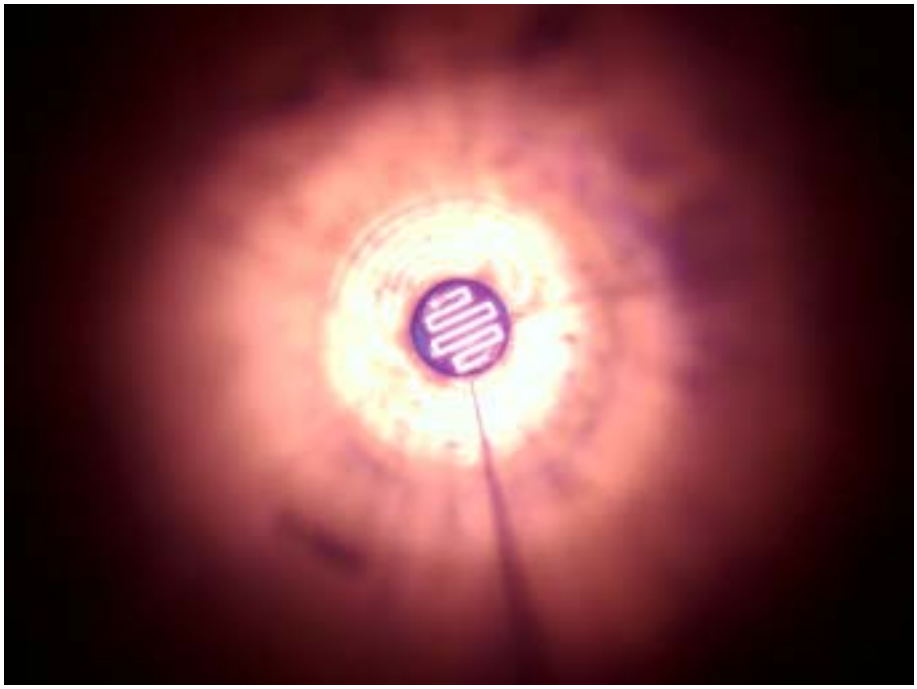

▲ The NiCr wire heating up inside the resonance tube.

目　錄

圖　次

壹、前言

一、研究動機

二十世紀初期由於冷凍機的發明，使得人類的生活便利性產生重大革命，而今冷卻技術的發展，莫不以研發更有效率、更小型化的散熱器爲主要目標。鑑於莫爾定律(Moore's Law)--半導體產業每十八個月成長一倍，積體電路工作時所產生的廢熱量也將大幅攀升，如何有效率地散熱是主宰了下一世代處理器發展的關鍵。因此，本組曾經研究熱電半導體（thermoelectric semiconductor）與圓錐套來降低溫度及增強風扇的散熱效率，但是效果並不如預期。審視現今之散熱技術，諸如散熱片、風扇、熱管(heat pipe)、熱電半導體等，從中發現一種新穎的冷卻降溫方式：熱聲效應架構--熱聲降溫（thermoacoustic refrigeration）。近年來，熱聲效應已被運用在新型的冷凍設備中，例如美國有一個冰淇淋業者已將他們的冰箱全數改爲熱聲驅動。而目前市面上的熱聲裝置皆爲大型的主動式冰箱。然而，在溫降幅度不大的散熱器的應用，如微處理器的散熱，甚至於微、奈米元件局部散熱等應用熱聲效應所伴生之局部對流以增強熱傳效率，同時以熱源本身與環境之溫度梯度驅動，並不須外加能源，此一特點與散熱架構在可攜式微電子產品的應用中，獨具優勢。

二、研究目的

(一)研討熱聲效應的二種主要應用方式：熱聲冷凍（thermoacoustic refrigeration）與熱聲引擎（thermoacoustic engine）。

(二)評估熱聲效應與其加強之對流效應對熱傳效能並與傳統散熱方式比較。

(三)根據前一項的結果設計並提出可用於電子散熱的裝置。

三、研究流程

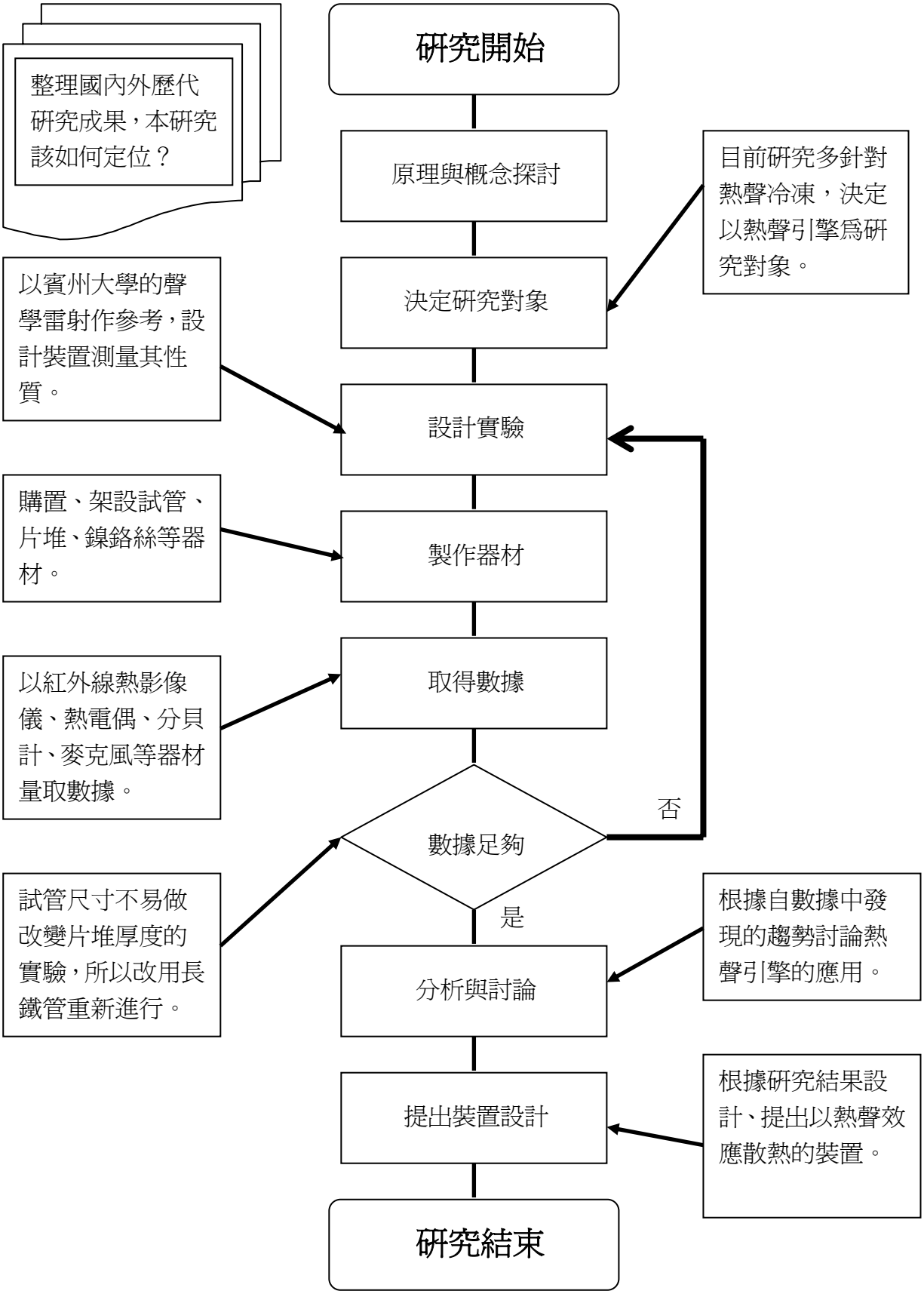
研究開始
整理國內外歷代研究成果，本研究該如何定位？
原理與概念探討
目前研究多針對熱聲冷凍，決定以熱聲引擎爲研究對象。
決定研究對象
以賓州大學的聲學雷射作參考，設計裝置測量其性質。
設計實驗
購置、架設試管、片堆、鎳鉻絲等器材。
製作器材
以紅外線熱影像儀、熱電偶、分貝計、麥克風等器材量取數據。
取得數據
數據足夠
否
是
試管尺寸不易做改變片堆厚度的實驗，所以改用長鐵管重新進行。
根據自數據中發現的趨勢討論熱聲引擎的應用。
分析與討論
提出裝置設計
根據研究結果設計、提出以熱聲效應散熱的裝置。
研究結束

貳、研究方法及過程

一、原理與概念探討

表一、國外歷年的熱聲研究與論文

年份	作者	單位	研究(論文)名稱	成果
1878	**Lord Rayleigh**	**Cavendish Laboratory, Cambridge University.**	**The Theory of Sound**	**提出 Rayleigh's Criterion 說明熱促發並維持聲波的方式。對熱聲效應進行量化的計算。**
1988	Swift, G. W.	Graduate Program in Acoustics, Penn State University.	Thermoacoustic Engines	熱聲引擎的討論。
1993	Garrett, S. L., et al.	Graduate Program in Acoustics, Penn State University.	Thermoacoustic Refrigerator for Space Applications	發明用於太空梭的熱聲冰箱。
1997	Garrett, S. L.	Graduate Program in Acoustics, Penn State Univ.	High-power Thermoacoustic Refrigerator	以熱聲效應爲原理的冰箱設計專利。
2002	Tijani, M.E.H., et al.	Department of Applied Physics, Eindhoven University of Technology.	Design of Thermoacoustic Refrigerators	探討熱聲冰箱的設計與考慮因素。
2002	Tijani, M.E.H., et al.	Department of Applied Physics, Eindhoven University of Technology.	Construction and performance of a thermoacoustic refrigerator	探討熱聲冰箱的實做過程。
2003	Qiu, T., et al.	Cryogenics Laboratory, Huazhong University of Science and Technology.	Network model approach for calculating oscillating frequency of thermoacoustic prime mover	提出計算熱聲引擎發聲頻率的方法。
2003	Qiu, T., et al.	Cryogenics Laboratory, Huazhong University of Science and Technology.	Temperature difference generated in thermo-driven thermoacoustic refrigerator	提出計算熱聲冰箱溫差的方法。
2004	**Symko, O. G., et al.**	**Deptment of Physics, University of Utah.**	**Design and development of high-frequency thermoacoustic engines for thermal management in microelectronics**	**討論熱聲冰箱與熱聲引擎應用於微電子溫控的可能性。**
2004	Sakamoto, S., et al.	Faculty of Engineering, Doshisha University, Japan.	The experimental studies of thermoacoustic cooler	製作熱聲冰箱與熱聲引擎循環作用的裝置。

表二、國內歷年的熱聲研究與論文

年份	作者	單位	研究(論文)名稱	成果
2000	陳冠勳	國立臺灣大學應力學研究所	熱驅動熱聲冷凍實驗設備之設計與性能實驗	國內最早對熱聲冰箱的研究。
2003		工業技術研究院能源與資源研究所	微型熱聲冰箱[1]	高度 9 公分的熱聲冰箱。
2004	黃博全	國立臺北科技大學冷凍空調工程學系	聲波冰箱實驗與數值模擬分析	以電腦模擬熱聲裝置。
2005	**邢本元、黃維剛、許曾昱**	**臺北市立麗山高級中學**	**以熱聲效應改善微電子裝置散熱的研究**	**(見本文)**

[1] 工業技術研究院能源與資源研究所已於 2003 年開發出系統高度 9cm 可達 10.7℃溫差的微型熱聲冷卻裝置，詳情可參閱其網站 (http://www.erl.itri.org.tw)。

自十九世紀中葉玻璃製造業著首次觀察到加熱某些玻璃容器時會發出聲音後，熱聲效應的研究就不斷進行(見表一、二)。最早被研究的是所謂的 Rijke 管[2]，在二端開口的管中放入熱源，即可聽到強大的聲響。2002 年美國 Ben & Jerry 冰淇淋公司全面改用賓夕凡尼亞州立大學聲學研究所研發出的熱聲冰箱製作冰淇淋（照片一）[3]，既環保又實惠。

照片一、賓州大學製作的聲學冰箱。左至右爲：Matt Poese、Steve Garrett **與** Robert Smith。

Garrett & Backhaus[4] 曾對熱聲效應作詳細的解釋：

> 當氣體被壓縮時，溫度會升高，反之則降低，這正是熱聲裝置利用的特性。熱聲效應裝置本質上包含一支共振管（見圖一），管中裝設一枚多孔隙的片堆（stack）。共振的聲波（通常由喇叭單體產生）帶動氣體來回通過片堆中的孔隙。起初片堆二端沒有明顯溫差，當氣體被推至一端（圖一 a）並被壓縮時，它的溫度升高並傳熱回片堆上；同樣的，氣體通到另一端（圖一 b）時壓力降低並吸熱。此過程受管內共振聲音的刺激而持續進行形成片堆二端的溫差，熱聲冰箱就是這樣運作的。

這種冰箱的好處包含：(一)不需冷煤，共振管內使用惰性氣體（通常使用氦氣或其他惰性氣體），促進環保。(二)沒有轉動零件，維修容易。(三)效率有潛力勝於熱電半導體。然而，共振管的幾何條件與密封必須製作的非常精確，目前國內雖已做出熱聲冰箱的原型機與微型冷卻裝置，但仍未被廣泛應用。

Garrett & Backhaus 進一步解釋：

---

[2] Sarpotdar, S. M., Ananthkrishnan, N., Sharma, S. D. (2003). The Rijke Tube- A Thermo-acoustic Device. *Resonance, 8*, 59-71.

[3] Ben & Jerry 冰淇淋公司的網站中有熱聲冰箱的動畫 (http://www.benjerry.com/our_company/sounds_cool/)。

[4] Garrett, S.L., Backhaus, S. (2000). The Power of Sound. *American Scientist*, *88*, 516-525.

另一方面，熱聲冷凍的逆反應即所謂的「熱聲引擎」（thermoacoustic engine）。如果片堆本身已具有溫差，熱端的氣體受壓縮時溫度仍低於片堆因而吸熱（圖一 c）；當氣體移至冷端並擴大時，它的溫度高於片堆所以放熱（圖一 d）。這樣造成的氣體振動促成並加強管內的共振聲波，達到熱能轉換成聲能的效果。

這種裝置的製作易於熱聲冰箱。賓州大學聲學研究所除了製作熱聲冰箱外，也設計了熱聲引擎的示範裝置，命名爲「聲學雷射」[5]。該裝置的片堆爲汽車中觸媒轉換器的 Cordierite 陶瓷材料做成，當電流通過纏在片堆一端的鎳鉻（NiCr）電阻時，片堆二端產生很大的溫差。此片堆位於一支 Pyrex 玻璃試管中，產生管內共振。由於其原理的概念如同光學雷射一樣：當共振管內累積足夠的能量便可從開口傳出，所以稱爲「聲學雷射」(圖二)。試管內的空氣由於聲壓加強熱對流效應改善了熱傳效應。如果啓動熱聲效應的片堆溫差可以掌握，便可利用此現象設計一個被動式熱聲效應帶動空氣對流的散熱裝置。該裝置的優勢在於，當一個物體需要散熱時，其本身的熱傳對片堆產生溫度梯度而在管中引發的聲能向外傳遞，同時所引發之空氣對流，則增強物體散熱率。當物體的溫度降低時，熱聲效應和對流減弱；反之，當物體的溫度升高時，熱聲效應和對流加強。如此只要掌握片堆溫差、對流和共振管幾何性質的關係，就可以設計針對不同散熱需求的熱聲散熱裝置。

[5] Penn State “Acoustic Laser” Kit Instructions. (2003). State College, PA: Graduate Program in Acoustics, Applied Research Laboratory, the Pennsylvania State University.

二、25~15 公分試管實驗過程

爲驗証熱聲效應加強熱傳效應，本組仿製美國賓州大學之「聲學雷射」爲作實驗基礎。該裝置包含主要材料如下：一支 20 公分 Pyrex 玻璃試管、一段鎳鉻電阻與一塊 Cordierite 陶瓷片堆（照片二）。

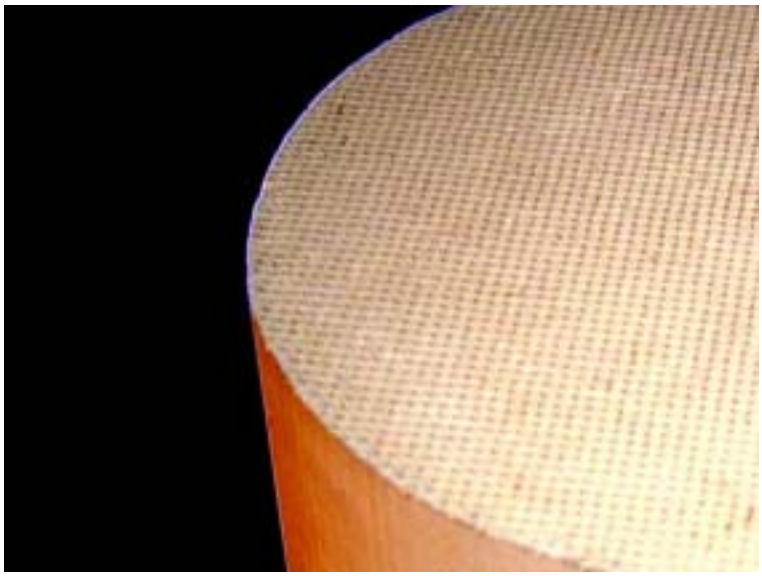

照片二、Cordierite 陶瓷。

首先將鎳鉻電阻纏繞於片堆的一邊、將它接上漆包線後再伸入試管中適當的位置（照片三），其中具有鎳鉻絲的「熱端」朝向管內、另一「冷端」朝向管口。漆包線連接上電源供應器[6]。當電源供應器開啓時，通過鎳鉻絲的電流使之發熱，進而促發熱聲效應。除了原套件外，額外添購了 15 公分、20 公分、25 公分的試管、各長度試管分別爲 1.5 公分、2 公分、2.5 公分三種管徑。共九種不同的試管（照片四）。

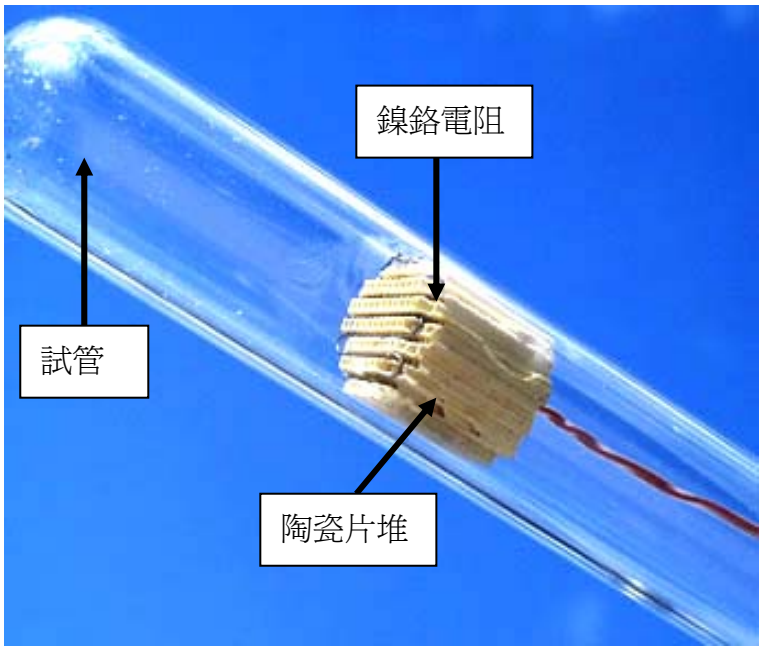

照片三、本實驗「聲學雷射」結構。

[6] ABM 9306D Dual-Tracking Power Supply.

照片四、三個長度（15,20,25cm）、三種管徑（1.5,2,2.5cm）的試管共九枚。

爲了解熱聲效應的強度與共振管的關係，進行下列研究：

(一)共振管幾何性質與發聲頻率的關係

把欲測量的試管接上電源供應器，開口朝上直立於一個麥克風[7]下。將電源供應器之供給功率調至可發出聲音；此時把麥克風接到個人電腦上以 Voice Spectrograph[8]軟體讀取頻率（圖三）。

１．管長與頻率的關係

爲方便改變管長，將三種長度的試管（15、20、25 公分）套上紙套，以伸縮紙套的方式製造出更多不同的管長（圖四）；利用這個方法在管長 35 cm 到 5 cm 間每隔 2.5 cm 取一頻率，繪製成管長與發聲頻率的關係圖。

２．管徑與頻率的關係

取 15 公分長、三種不同管徑的試管：2 cm，2.5 cm，3 cm。在這些管徑下，以相同的方法量取聲音頻率，以了解此範圍內管徑造成的影響。

(二)共振管長度以及片堆溫差的關係

由於「聲學雷射」之熱聲效應強度取決於片堆兩端的溫差，爲了測出最小啓動溫差與其他變因的關係，設計了以下的實驗：

１．片堆在試管內的最佳位置

本組分別在不同長度與口徑的試管中找出片堆放置的最佳位置。實驗步驟爲：將分貝計[9]置於「聲學雷射」的上方；啓動後，慢慢移動片堆，當移動到的位置可使分貝計恰可產生最大的數據，此位置便爲片堆的最佳爲置。如圖五所示，在 35cm 到 5cm 間的每一個管長下，同時以分貝計測量片堆在試

[7] Philips Corded Electret Microphone SBC-ME570。
[8] 取自 VoiceSync 網站(http://www.voicesync.org/)。
[9] Extech Digital Sound Level Meter 407727。

管中的最佳位置（聲音最強處，即熱聲效應最佳處；片堆位置指片堆之中點離管口之距離）。

照片六、分貝計(Extech Digital Sound Level Meter 407727)

２．不同長度試管下的片堆溫度測量

片堆長度與兩端之溫度梯度是熱聲效應的重要參數，因此對於不同的試管長度與片堆的最佳位置之關係，本組在不同長度的試管中（15 cm, 17.5 cm, 20 cm, 22.5 cm, 25 cm），在每個管長的最佳片堆位置下，發生熱聲效應所需的最小溫差。改變輸入的電流（即影響熱端溫度），以找出熱聲效應所需的最小溫度梯度。然後更換不同長度的試管，重複試驗。

由於一般溫度計無法量測本實驗中片堆兩端的溫度，主要是因爲一般溫度計不能量測太高的溫度，也無法深入試管中，所以嘗試以下兩種方式來進行溫度測量：

１．使用紅外線熱影像儀

「紅外線熱影像檢測技術是利用物體表面溫度高於絕對零度輻射出的紅外線（能量）以計算物體表面溫度分佈。此項技術具有非接觸式、測溫快速、反應靈敏及視覺直接觀測等特性...」[10]。因此，本組借用一臺國立臺灣大學應用力學研究所生醫微奈米機電系統實驗室之 Avio TVS-100 紅外線熱影像儀[11]架設於述的實驗裝置前。該影像儀的優點是，除了顯示拍攝範圍溫度的分層設色圖外，也可對影像中的每一點測量溫度。借此可以觀測整個裝置的溫度分布並針對片堆的二端量取精確的溫度。觀測方法如圖六所示。

[10] 鄭 益志 (民 91)。紅外線熱影像檢測技術應用。**工安環保，7，技術報導**。臺北市：工業技術研究院環安中心 (http://she.moeaidB.gov.tw/issue/issue7/tec7_2.htm)。

[11] Nippon Avionics Co., Ltd. Avio Handy Thermo TVS-100 Infrared Thermography.

照片七、Avio TVS-100 紅外線熱影像儀。

２．使用熱電偶[12]

雖然使用熱電偶只能得到一點的溫度，其量測範圍遠高於紅外線熱影像儀（263~1573 K）。將兩個 k-type 熱電偶分別固定於片堆冷熱兩端並測量其溫度，相減之後得其溫差（圖七）。

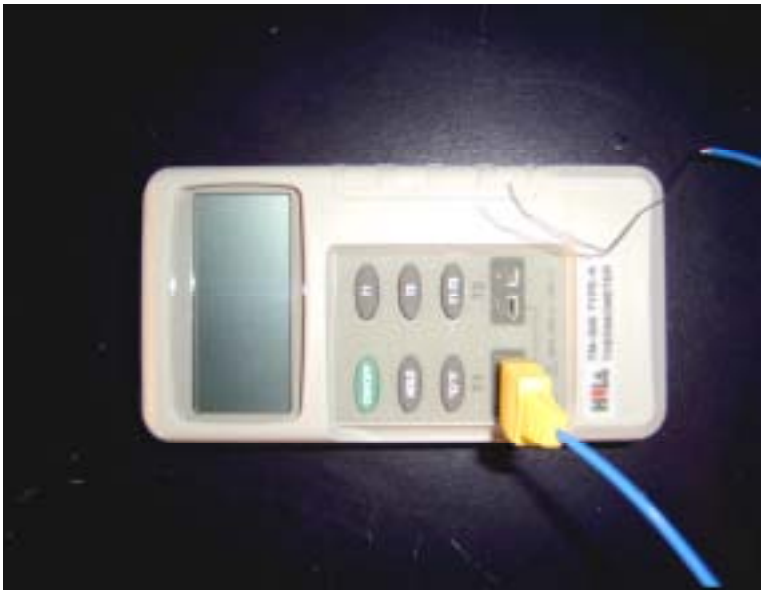

照片八、海碁 TM-906 k-type 熱電偶溫度計。

[12] 海碁 TM-906 k-type

(三)片堆溫差與熱傳導率的關係(圖八、圖九)

１．片堆溫差與熱聲效應強度的關係

爲了要測出「聲學雷射」產生的聲能，在距離管口 20 公分處擺設前述的分貝計。假設以管口爲球心有一個球面，根據散度定理，將球面上每一點所蒐集到的聲功率密度（即單位面積的聲功率）累加後，再與輸入的電功率相做比較，便可定量此「聲學雷射」的發聲效能。但由於無法一一測量球面上的每個點，所以改爲測量以管口爲圓心，從管口至管後每隔 15 度（共繞 180 度）的位置分別測量聲音的強度（圖十），並利用球面在空間中對稱的特性，由所測到的數據推算整個球面的聲功率密度（圖十一）；然後在不同的片堆溫差下進行測量，觀察溫差對熱聲效應的影響。

２．片堆溫差與熱對流強度的關係

聲功率的量值並不大，聲壓所引致的對流效應應佔整體熱傳率的最大比率。因此本組設計在不同片堆的溫差下測量熱聲效應引發的對流強度。如果量取管口的流速即可推算對流的強度。然而在初步的測試中發現以風速計、皮托管(pitot tube)或以熱線電阻絲（thermal hot wire）在本實驗架構中，都難以量出管口的空氣流量。因此本組嘗試以細線及保麗龍球在管口的位移測出管口風速，但受到氣流擾動的影響而無法量測(圖十二)；在不斷嘗試下，本組利用火焰在管口偏折的角度和酒精燈火焰在滑車上的速度與偏折角度關係(圖十三)，比較後即可得知管口的風速。

３．片堆溫差與熱傳導強度的關係

因爲本裝置的能量多以聲能與熱對流的方式散走，所以僅以試管內外測量到的溫差計算熱傳導量。

４．片堆溫差與熱輻射強度的關係

因爲本裝置的能量多以聲能與熱對流的方式散走，所以僅以試管內片堆的溫度計算熱輻射量。

三、47~29 公分鐵管實驗過程(圖十四)

除了以試管做實驗外，亦以從電風扇卸下的二支鐵管作爲共振管進行測試，它們的尺寸分別爲 47 公分與 43 公分、管徑爲 3.2 公分與 2.4 公分。使用這種大尺寸的鐵管可以對片堆厚度做較大的變化，提供觀察片堆厚度和管長的關係和以片堆厚度控制溫差時更大的便利性。因爲鐵管原爲兩端開口，所以可以比較一端開口和兩端開口(Rijke 管)的熱聲效應比較。實驗內容如下：

(一)一端閉口的量測

１．片堆在共振管中的最佳位置

最佳位置即片堆在管中能以最低的溫差帶動熱聲效應的位置。比照試管的做法，把欲測量的鐵管內的片堆接上電源供應器，開口朝上直立於一個麥克風下，另一端開口用水堵住(管長以加水的多寡來調整)。將電源供應器之提供功率調至可發出聲音，慢慢將片堆向上移動至聲音消失的位置記爲上限，再將片堆向下移動到聲音消失的位置記爲下限。「位置」指片堆熱、冷二端的平均深度，即片堆中點離管口的距離。此時取上限與下限的中點定爲該片堆在管中的最佳位置。爲了解片堆厚度是否影響最佳位置，所以對 2、4、6、8 公分四種厚度的片堆在 47、43、38、29 公分的管長下做測量。

２．片堆厚度與最低溫差、聲音相對強度的關係

首先量測了不同長度的鎳鉻電阻分別在不同電流下的溫度，繪製成圖二十八對應到片堆上的鎳鉻電阻。如此可以從提供給片堆的電流推算熱端的溫度，再用熱電偶量取冷端的溫度即可得到片堆的溫差。

將片堆放入管中的最佳位置，提供電源使鐵管發出聲音。慢慢降低電流至聲音幾乎消失，這就是在該尺寸的管長與片堆下能維持熱聲效應的最低溫差。這次也用 2、4、6、8 公分四種厚度的片堆在 47、43、38、29 公分的管長下做測量。根據得到的數據繪成圖表觀察在不同管長與管徑下最低溫差的關係。

爲了解片堆厚度對所產生聲能的影響，在相同輸入電流、不同片堆厚度下以分貝計(距管口 10 公分)紀錄了在不同溫差下聲音的相對強度製成圖表。

３．管長與頻率的關係

當加水改變管長時，量測每一個管長下的聲音頻率，與試管的實驗結果比對。

(二)二端開口的量測

對二端開口的鐵管進行相同的實驗。管長無法以加水的方式改變，所以僅以 47 公分與 43 公分長的鐵管進行，觀察數據變化的趨勢。

１．片堆在共振管中的最佳位置

尋找最佳位置的方式比照一端閉口的做法。唯本實驗僅對 2、4、6、8 公分四種厚度的片堆在 47、43 公分的管長中測量。

２．片堆厚度與最低溫差、聲音相對強度的關係

如同上述的方式控制片堆溫差，找出該尺寸的管長與片堆下能維持熱聲效應的最低溫差。這次也用 2、4、6、8 公分四種厚度的片堆在 47、43 公分的管長下做測量。根據得到的數據繪成圖表觀察在不同管長與管徑下最低溫

差的關係。並以以分貝計(距管口 10 公分)紀錄了在不同溫差下聲音的相對強度製成圖。

3．管長與頻率的關係

量測 47 與 43 公分管長下的聲音頻率，與一端閉口的共振管的發聲頻率數據比對。

最後照試管實驗中的做法，計算聲能、傳導、輻射與對流分別在輸出的能量中佔有多少比例(圖八、圖九)。

照片九、共振管測量實景。

參、研究結果與討論

一、25~15 公分試管實驗過程

(一)共振管幾何性質與發聲頻率的關係

１．管長與頻率的關係

在實驗中發現當熱聲效應啓動時，聲音的頻率會有不斷升高的現象，圖十五例舉 22 至 24 公分的試管在測量時，發聲頻率隨時間變化的數據。原因可能是鎳鉻絲持續對空氣加熱，根據公式（1）[13]：

v=331+0.6t…（1）

v：聲速 m/s；

t：溫度℃

聲速會隨空氣溫度升高而加快。然而管長（波長）固定，所以聽到的聲音頻率會隨之提高。所以加熱之初，溫度升高，而使聲速加快，聲音亦隨頻率增加而增加；當溫度穩定時，「聲學雷射」的頻率也會達到穩定狀態。因爲該時刻的空氣溫度仍爲室溫，所以統一取熱聲效應啓動時的頻率。

接著分別在管長從 32.5 公分到 8 公分的試管取得十三個點，再將管長的倒數與聲音頻率繪製成圖十六，並以電腦程式 Graph[14]取得逼近的線性函數：f(x)=8937.6*x+3.00167。利用公式（2）：

v=λf…（2）

v：聲速（m/s）

λ：波長（m）

f：頻率（Hz）

所以由試管「管長與頻率」的實驗中顯示，當管長變長時，頻率會隨之減少；亦可得知管長爲波長的四分之一。

２．管徑與頻率的關係

以下試舉在 15 公分試管下的數據爲例(表三)經由實驗，發現管徑在該尺度下與聲音的頻率關係甚微，頻率之變化量不超過 2.33%。

表三、管徑與頻率的關係

管徑	2 cm	2.5 cm	3 cm
頻率	601 Hz	580 Hz	593 Hz

[13] 林 明瑞(主編)(民 91)。**高中物質科學物理篇(下)**。臺南市：南一書局企業股份有限公司。

[14] Graph 3.3 by Ivan Johansen(http://www.padowan.dk).

(二)共振管長度以及片堆最小啓動溫差的關係

１．片堆在試管內的最佳位置

此實驗測出的數據如下（圖十七），由表四可知，片堆的最佳位置會隨管長改變而改變，管徑在 1.5 到 2.5 公分間不受管徑的影響。而且其最佳位置皆約爲伸入管中二分之一處。

表四、片堆在試管內的最佳位置

最佳位置 \ 管長 / 管徑	15.0 cm	20.0 cm	25.0 cm
1.5 cm	8.00 cm	9.75 cm	14.00 cm
2.0 cm	8.25 cm	10.50 cm	14.50 cm
2.5 cm	8.00 cm	10.50 cm	14.50 cm
平均（cm）	8.08 cm	10.25 cm	14.33 cm

2．不同長度試管下的片堆溫度測量

(1)使用紅外線熱影像儀

首先進行熱影像儀適用性的驗証，將它和溫度計同時測一杯熱水的溫度，但在過程中，發現當玻璃試管通過熱影像儀及水杯中間時，水杯所放出的輻射波並無法穿過試管到達熱影像儀。經過討論和研究後，本組認爲影像儀只有顯示出試管表面的溫度，因爲熱影像儀的觀測波段（3000~5400 nm[15]）與 Pyrex 玻璃的透光波段不符，資料如圖十八[16]所示。

另外，大尺寸的「聲學雷射」所產生的溫度會超過熱影像儀可測量溫度的上限。因此，將現有的片堆自試管取出拍攝，影像儀只顯示一塊白色的片堆，表示片堆溫度已超過其測量上限。惟降低輸入電流時，片堆的溫度才降到觀測範圍內（照片十）。

照片十、降低輸入電流時，片堆的溫度才降到觀測範圍內。
其中蛇狀纏繞的是鎳鉻電阻。

(2)使用熱電偶

將二個熱電偶插在雙輸入端的溫度計上，使用其中的「溫差」功能可以直接顯示兩個熱電偶讀數之差，及片堆的溫差。

由於紅外線熱影像儀可接收的波段與 Pyrex 玻璃的透光波段不符，而且測量溫度的上限也不足，因此改用熱電偶測量片堆兩端溫差。在不同的管長下，均有輸入電能與片堆兩端溫差成正相關，也跟輸出之聲能成正相關的現象；另外，越短的管子輸出的聲能也越強。

[15] 鄭 益志 (民 91)。紅外線熱影像檢測技術應用。**工安環保，7，技術報導**。臺北市：工業技術研究院環安中心 (http://she.moeaidB.gov.tw/issue/issue7/tec7_2.htm)。

[16] *Pyrex Properties*. Langen Busch, Iserlohn: Präzisions Glas & Optik GmbH. Retrieved 2004 from the World Wide Web: http://www.pgo-online.com/intl/jse/frameroute/genericset.html?Content=/intl/katalog/pyrex.html

(三)片堆溫差與熱傳導率的關係

１．片堆溫差與熱聲效應強度的關係

將實驗中半個圓弧所測到的數據繪制成圖十九，發現當分貝計越靠近試管後方，所測得的數據越大；這種現象可能是聲音的指向性造成的，或是由於聲音在實驗室中反射的結果，若要精密的測量此實驗，則需要在無回響環境中量測。

所測得的數據可經由公式(3)[17]：

$$\textbf{sound level}=20\text{dB}(P_{measured}/P_{reference})=20\log 1=0\text{dB}\cdots(3);$$

$P_{measured}$：量測值；

$P_{reference}$：參考壓力(0.02mPa)；

dB：分貝。

可得到每一點的聲壓，再由公式(4)：

$$I=(p_{rms}^2)/(\rho_0 c)\cdots(4);$$

I：聲強(W/m^2)；

p_{rms}：聲壓(Pa)；

ρ_0：密度(Kg/m^3)；

c：聲速(m/s)。

在經推算之後算出球面上的功率爲 0.22W，大約爲平均輸入功率的 0.6%。由於實驗環境不爲全無回響室，因此，反射波所造成的影響大約爲 20%，故而所計算出來之聲能，以 0.8 之係數作爲修正。

圖十九爲輸入電功率與聲能強度的關係，當輸入的電功率越大，輸出的聲能就越大。試管越短，聲能越強。

２．片堆溫差與熱對流強度的關係

根據圖二十一，輸入的電功率越大，內外溫差就越大。

算出火焰偏折角度(照片十一)與速度的關係後(圖二十二)，即可推算出管口風速；我們由公式(5)，可以計算熱對流的強度：

[17] Wolfe, J. (1998). *What is a decibel?* Sydney, Australia: Univ. of New South Wales. Retrieved 2004 from the World Wide Web: http://www.phys.unsw.edu.au/~jw/dB.html

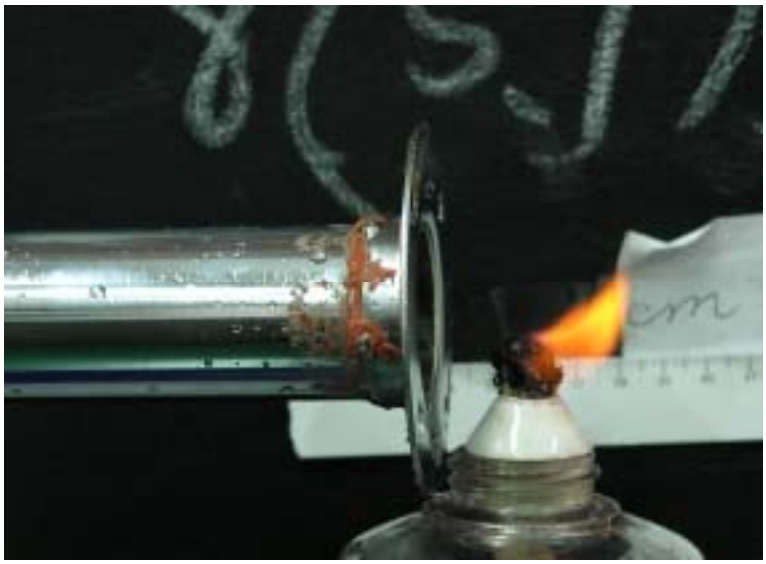

照片十一、火焰受管口對流影響而偏轉。

利用以下之公式(5)[18]，可以計算熱對流的強度：

P=ρAvS△T・4.2…(5)

P：功率(W)

ρ：空氣比重(g/cm^3)

A：面積(cm^2)

V：速度(cm/s)

S：空氣比熱(cal/g-℃)

△T：溫差(℃)

4.2：熱功當量(J/cal)

3．片堆溫差與熱傳導強度的關係：

利用以下之公式(6)，可以計算熱傳導的強度：

Q_{cond}=kA（ΔT/ΔX）.....（6）

Q_{cond}：熱傳導功率（W）。

k：熱傳導係數。

A：面積（m^2）。

ΔT：溫差（K）。

ΔX：二點間距離（m）。

4．片堆溫差與熱輻射強度的關係：

利用以下之公式（7），可以計算熱輻射的強度：

[18] Çengel, Y. A. (1998). *Heat Transfer A Practical Approach*. Hightstown, NJ: WCB/McGraw-Hill.

$$Q_{emit} = \varepsilon Ó A (T_s)^4 \text{.....（7）}$$

Q_{emit}：熱輻射功率（W）。

ε ：輻射率。

Ó：5.6703×10^{-8}（$W/m^2 \times K^4$）Stefan-Boltzmann 常數。

A：面積（m^2）。

T_s：（K）。

根據圖二十三所示，**A** 線是試管內與室溫的溫差，可以用來計算對流的強度；**B** 是管內片堆的溫差，可與量測到的聲能比較；**C** 是管內空氣溫度的變化（約在 50℃上下），而圖二十四爲裸露片堆鄰近空氣仍有 200℃左右。由此可以說明透過熱聲效應的強烈對流、散熱，可以大爲降溫，由 200℃降爲 50℃左右，這正是當代電腦內中央處理器（CPU）的工作溫度範圍。

二、47~29 公分鐵管實驗過程

(一)片堆在共振管中的最佳位置

經過計算，得到在一端閉口的管中，最佳位置對管長的的比值皆約爲 0.49，即深度爲管長的二分之一處(圖二十五)。

圖二十六爲二端開口在 2.4 與 3.2 公分管徑下，管長 47、43 公分，以 8、6、4 和 2 公分厚的片堆量出的最佳片堆位置。經過計算，得到在二端開口的管中，最佳位置對管長的的比值皆約爲 0.26，即深度爲管長的四分之一處。

(二)片堆厚度與溫差、聲音相對強度的關係

鎳鉻電阻長度與溫度隨輸入電流的關係如圖二十七所示，在 3 到 15 公分的電阻中，溫度均與輸入電流乘正比。因爲管徑 3.2、2.4 公分的片堆中電阻長度分別約爲 15 與 6 公分長，根據圖二十七的數據作成圖二十八中 15 與 6 公分電阻溫度隨輸入電流的變化。例如在 3.2 公分管徑的片堆中，熱端輸入 3 安培的電流即可根據圖二十八推算出熱端的溫度約爲攝氏 400 度。

根據圖二十八的數據當作實驗中、不同電流下片堆熱端的溫度，與用熱電偶量得的冷端的溫度相減得到溫差。

圖二十九、圖三十、圖三十一爲一端閉口粗 3.2 公分、管長 47、38、29 公分下片堆厚度與溫差、相對聲能的關係。

圖三十二、圖三十三、圖三十四爲一端閉口粗 2.4 公分、管長 43、38、29 公分下片堆厚度與溫差、相對聲能的關係。

圖三十五、圖三十六、爲二端開口粗 3.2、2.4 公分、管長 47、43 公分下片堆厚度與溫差、相對聲能的關係。

根據此三套數據觀察出當溫差在可以維持聲音的範圍內，越薄的片堆可以較小的溫差產生能量越大的聲音，即越多的能量以聲能的形式帶走。如果能克服材料上的問題、使用導熱係數更小的材質，就可以製作更薄的片堆以更低的溫差啓動熱聲效應。由於聲音在試管內的駐波爲四分之一波長，故管口即爲波腹，管底則爲波節；因爲空氣在波腹振動最大，使得此處的壓力爲最大；相反的，波節處壓力最小。由壓力的變化可以繪製成圖三十七，紅色曲線爲壓力變化，當片堆越薄時，片堆兩端所需的壓力差較小，故較容易啓動；而較厚的片堆則因爲所需的壓力差較大，所以較不易啓動。此外，片堆越靠近管口所需的壓力越高，而越靠近另一端則需要越大的壓力差，因此在將片堆置於開口端或閉口端皆不易發出聲音。爲驗證此說法，本組做了另一實驗：將片堆置於管中不同位置、測量聲強的變化，並改變供應的電流，觀察片堆在管中可發出聲音的範圍，數據如圖三十八所示。

(三)管長與頻率的關係

量測管長爲 47、43、38、29 公分下的聲音頻率，將數據加到試管數據製成的趨勢線如圖三十九所示，其中的趨勢線爲圖十六中的線性函數：
f(x)=8937.6*x+3.00167。鐵管聲音的頻率符合圖十六的趨勢，所以熱聲效應的發聲頻率與管長的倒數成正比，而且管長也是波長的四分之一。

肆、結論與應用

一、結論

(一)文獻中多以「聲熱」來研究致冷效應，本文爲**第一**個利用「熱聲」散熱的研究。

(二)一端閉口產生熱聲效應，管長爲波長的四分之一。

(三)一端閉口的熱聲裝置，片堆的最佳位置約在共振管的二分之一處。

(四)熱聲效應並非由聲能散熱，而以引發的強烈對流帶出熱能，如表五與圖四十所示。

(五)片堆相對於管長的比例越小，所需維持的溫差越小，並且放出的聲能較大，可以用此研究結果將該散熱裝置縮小至超聲波發聲範圍。

表五、聲能、傳導、輻射與對流分別在輸出的能量中佔有比例

Convection	Conduction	Radiation	Acoustic radiation
74.46%	19.78%	5.76%	0.00073%

二、應用

(一)由本研究發現的趨勢得知在小尺寸下亦可製作一個微型的熱聲散熱裝置。

(二)可製作陣列式的熱聲裝置更有效地散熱。

(三)圖四十一爲本研究所設計的 CPU 散熱裝置。

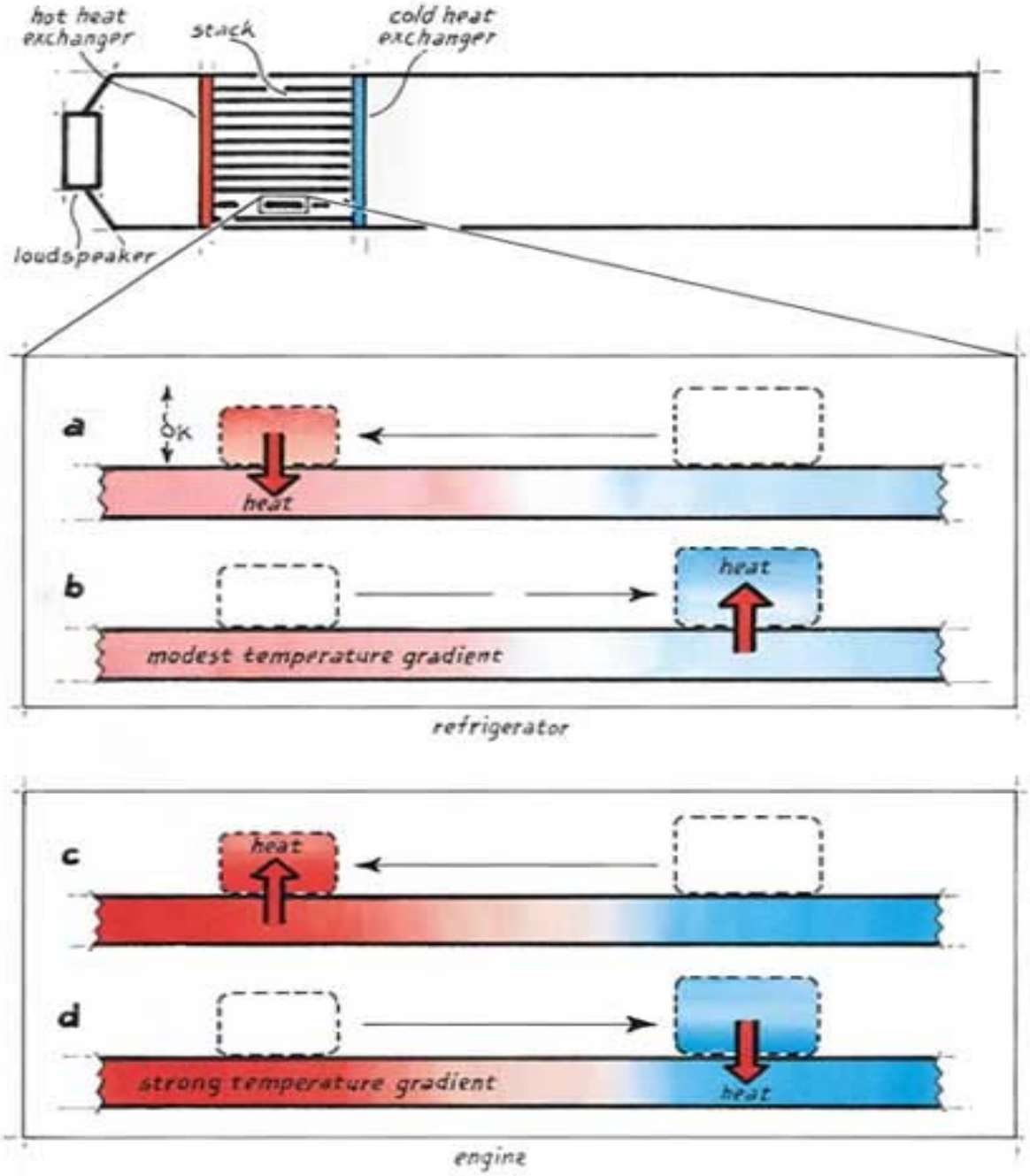

圖一、熱聲效應示意圖。**a b** 爲熱聲冷凍過程。**c d** 爲熱聲引擎。

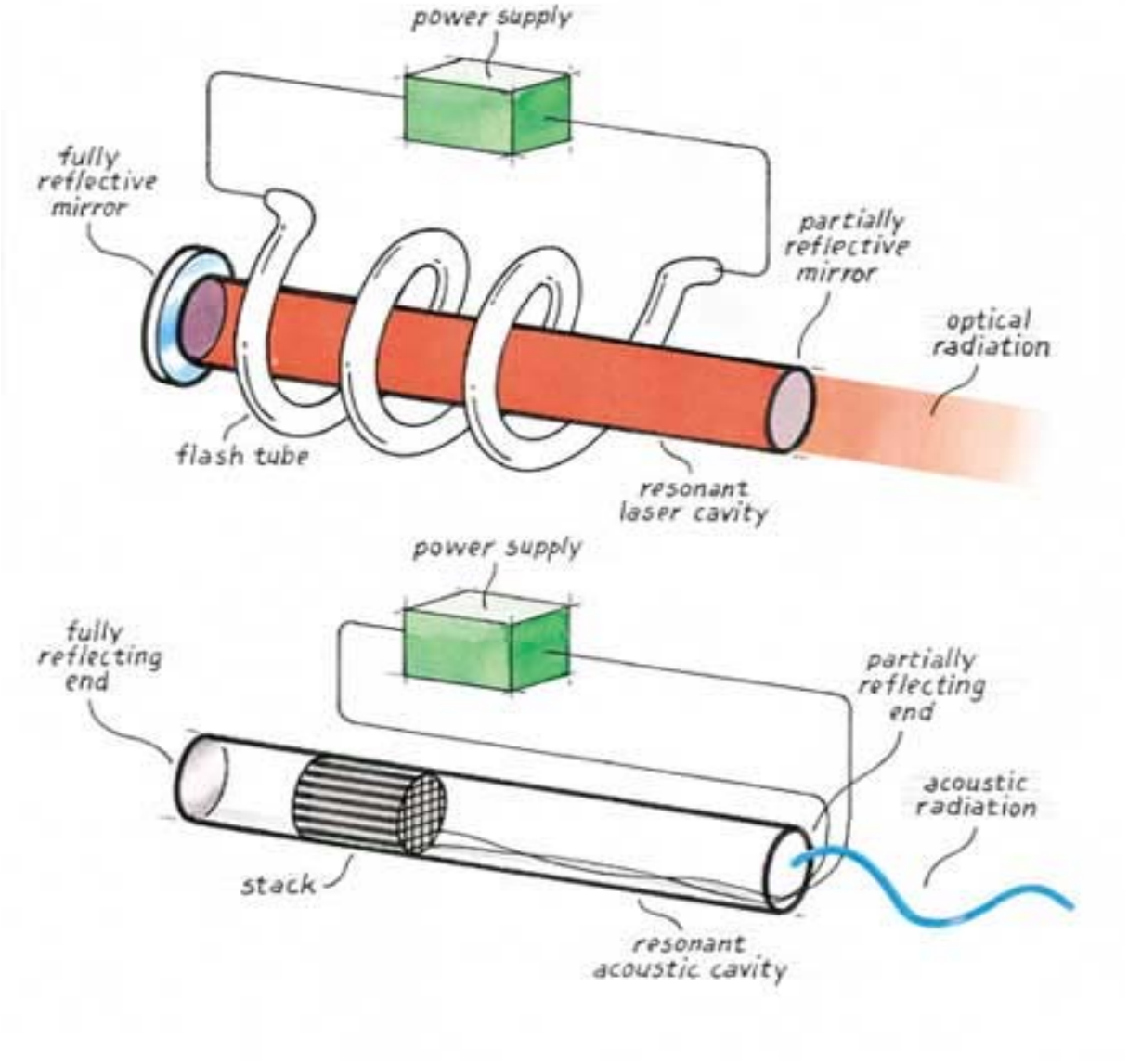

圖二、光學與聲學雷射的比較。

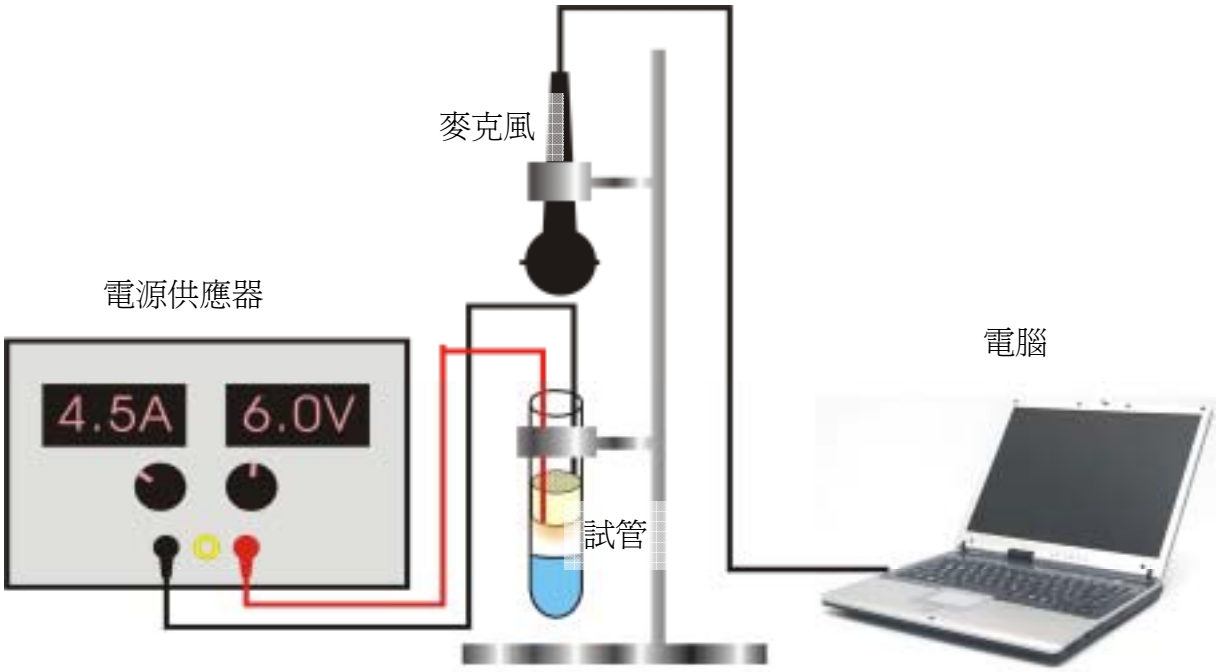

圖三、實驗使用之「聲學雷射」裝置圖。

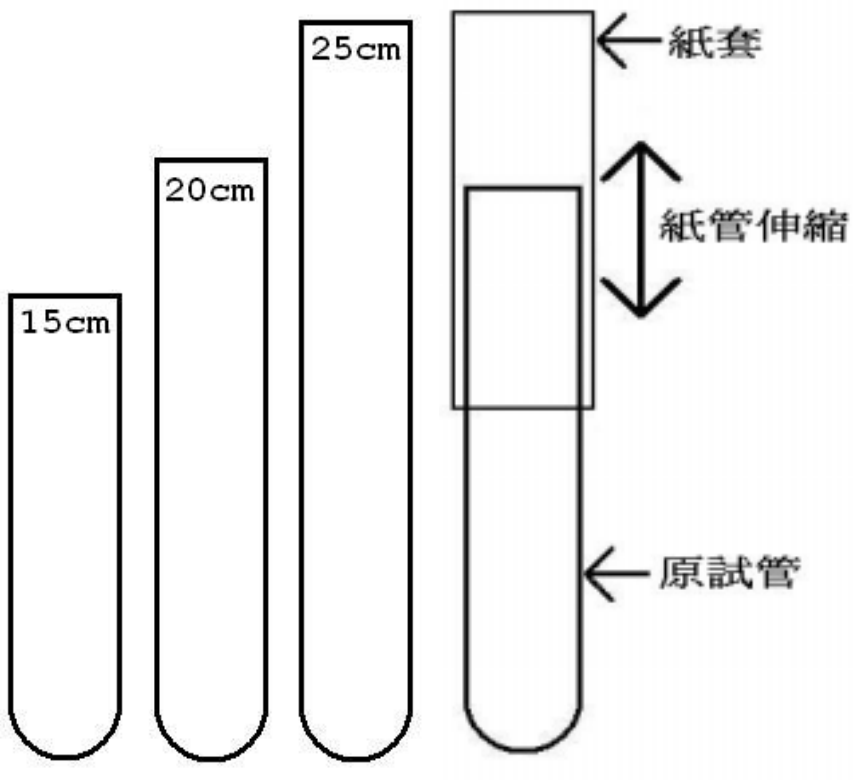

圖四、原有的三支試管，右爲加上紙套後以紙套的伸縮改變長度。

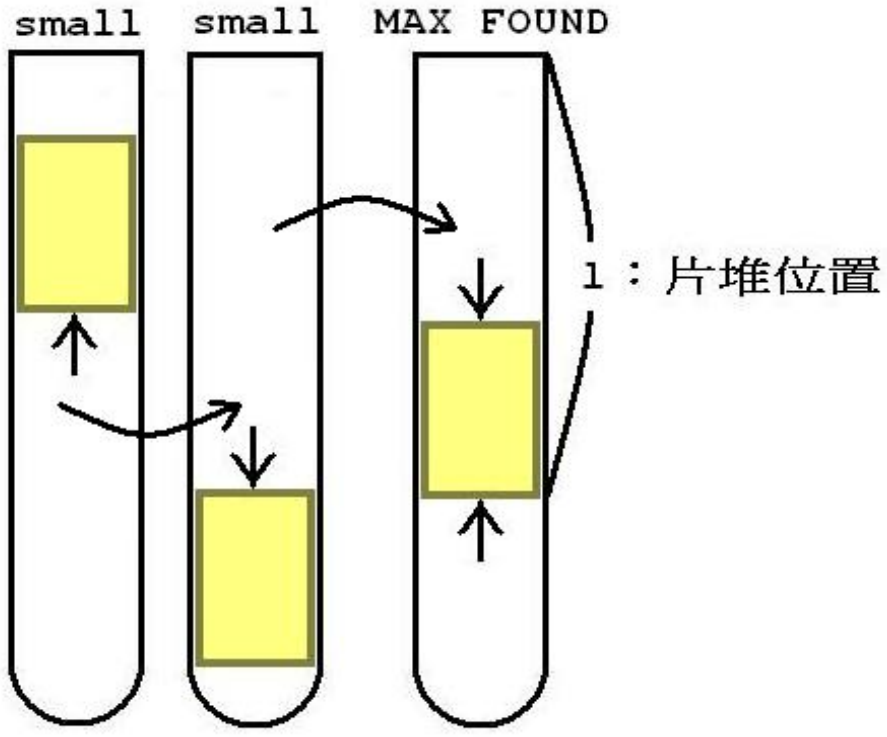

圖五、尋找最佳片堆位置。移動片堆在管中的位置到分貝計的讀數最大。

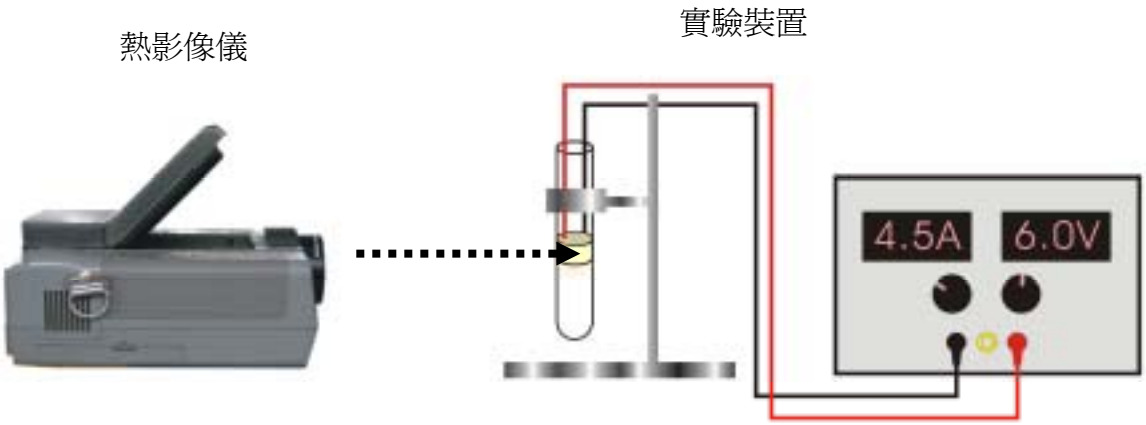

圖六、以熱影像儀測量試管中溫度變化。

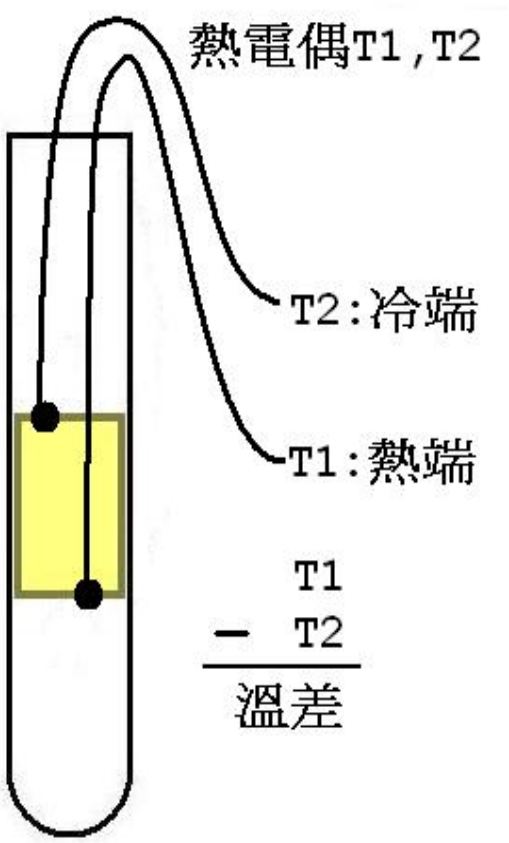

圖七、以海碁 T-103 k-type 熱電偶量測片堆之溫差。

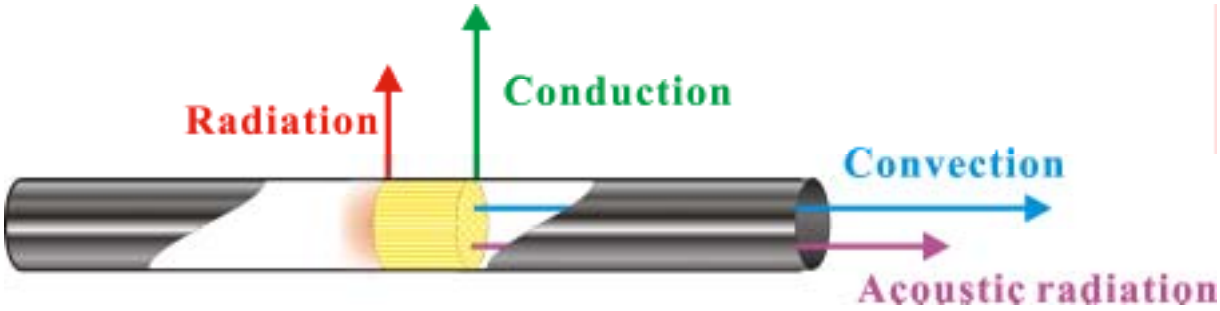

圖八、熱聲裝置在鐵管中輸出方式。

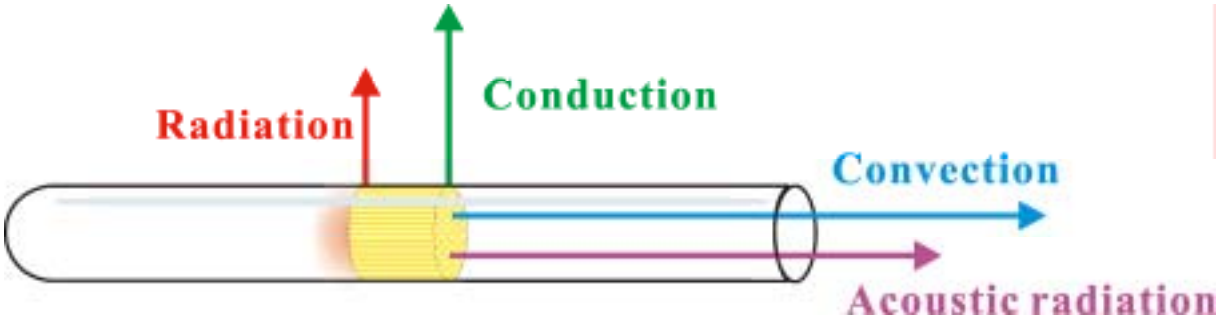

圖九、熱聲裝置在玻璃試管中輸出方式。

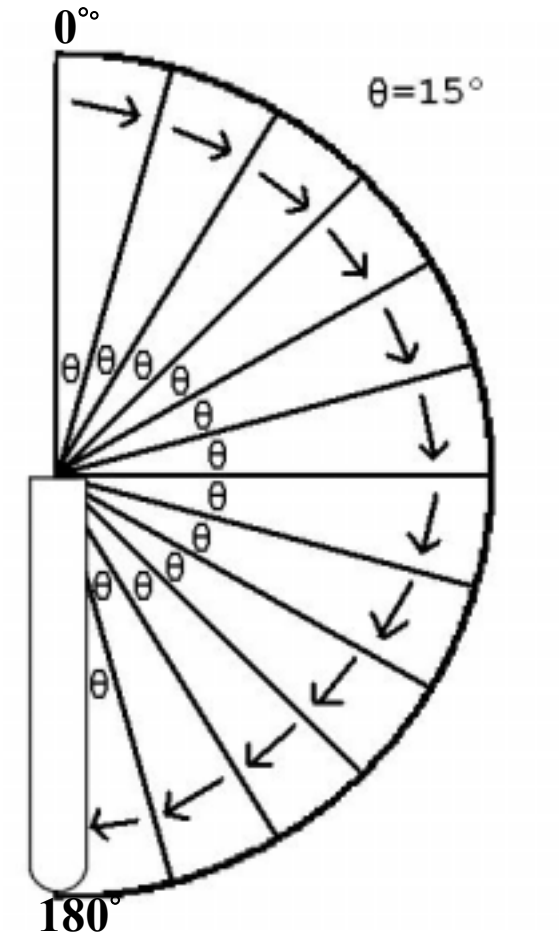

圖十、每隔 15 度（共繞 180 度）的位置分別測量聲音的強度。

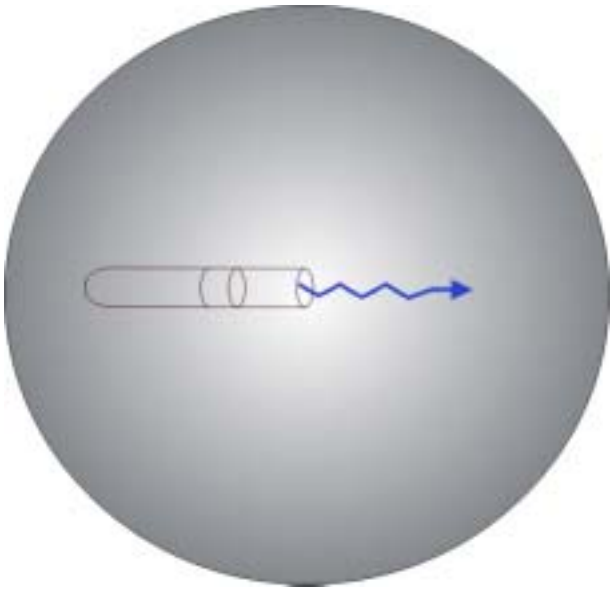

圖十一、假設聲能均勻擴散至球面。

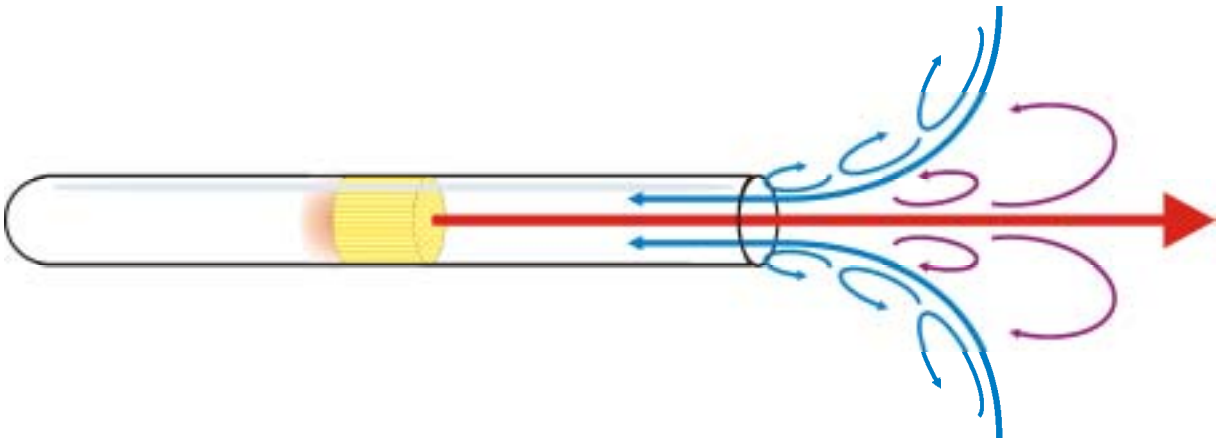

圖十二、空氣在管口形成渦流。

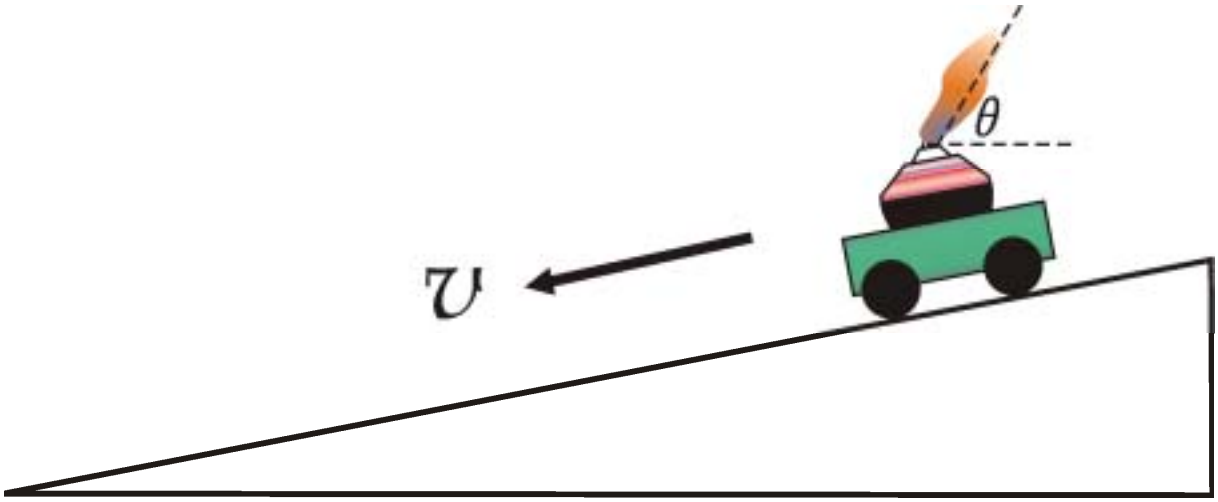

圖十三、利用滑車在不同速度下找出速度與火焰角度的關係。

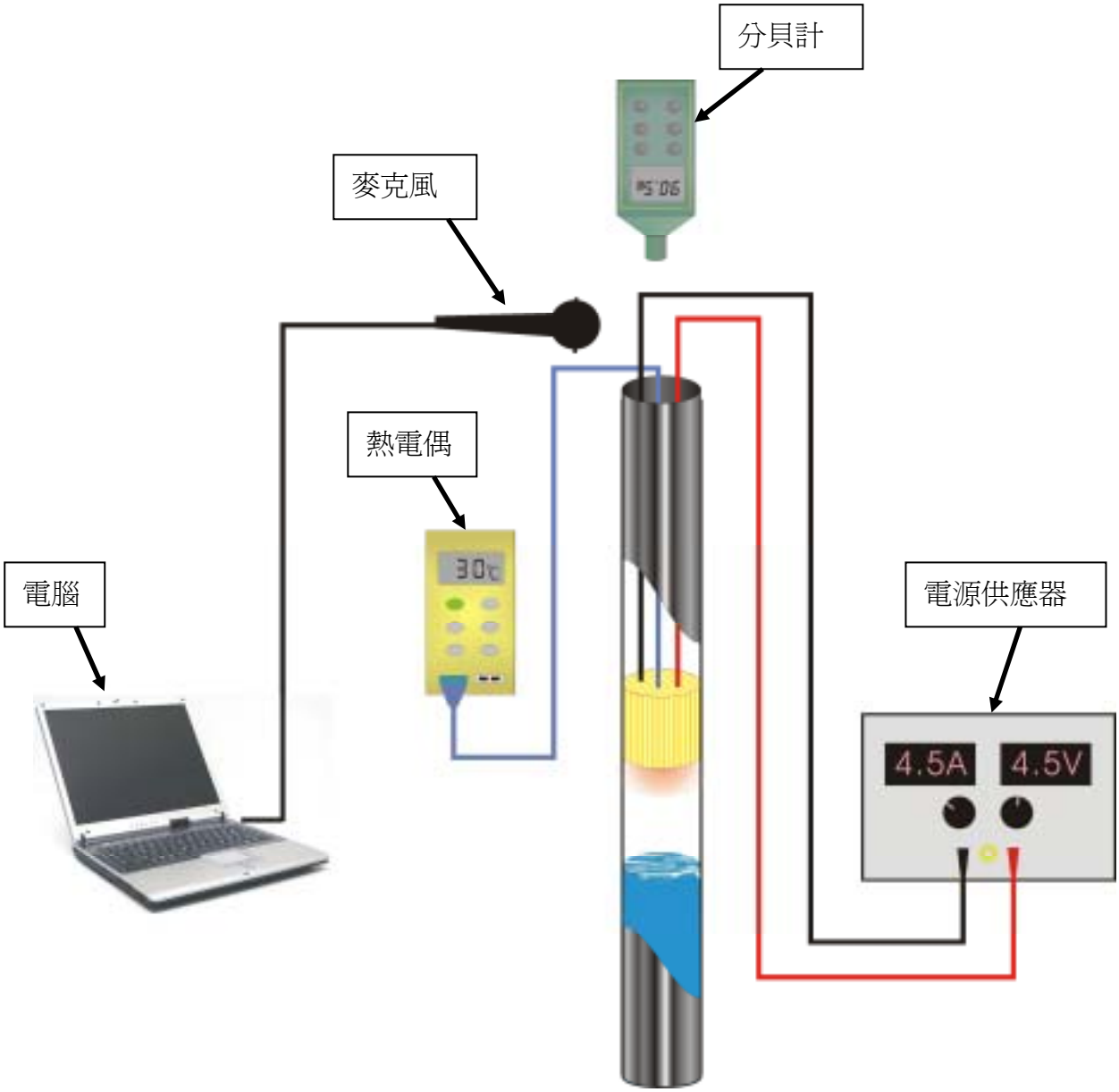

圖十四、47~29 公分鐵管實驗裝置圖。

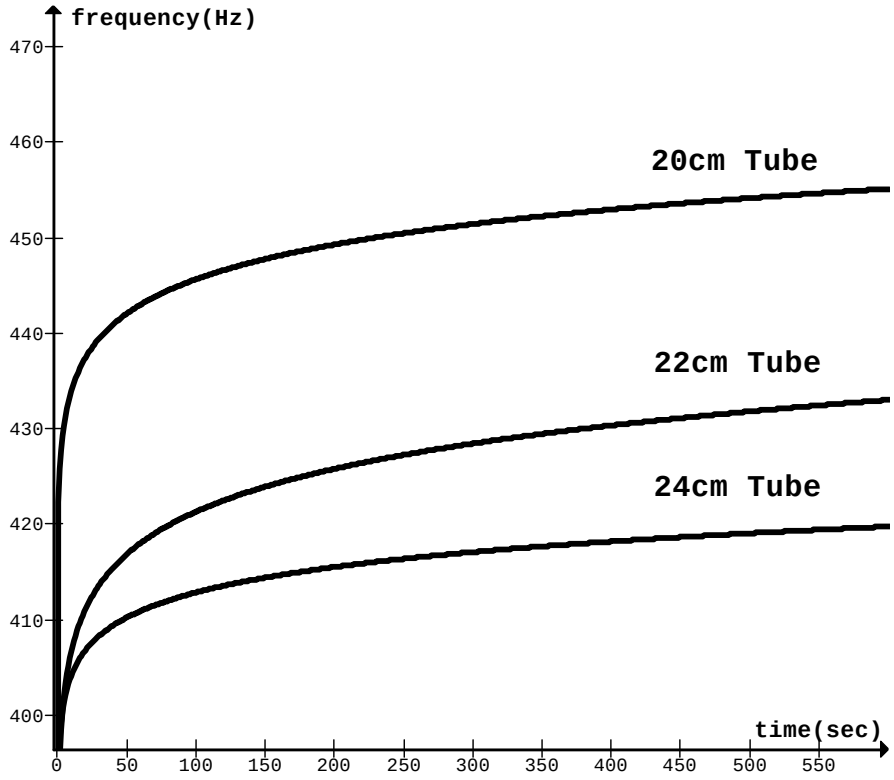

圖十五、20~24 公分試管的頻率變化。

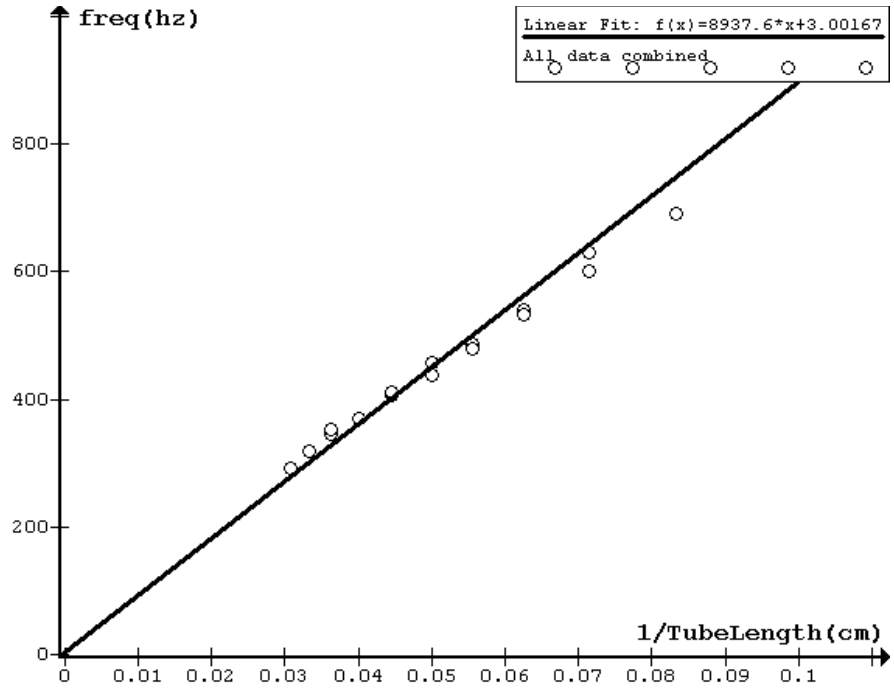

圖十六、試管實驗中發聲頻率和管長倒數之關係。

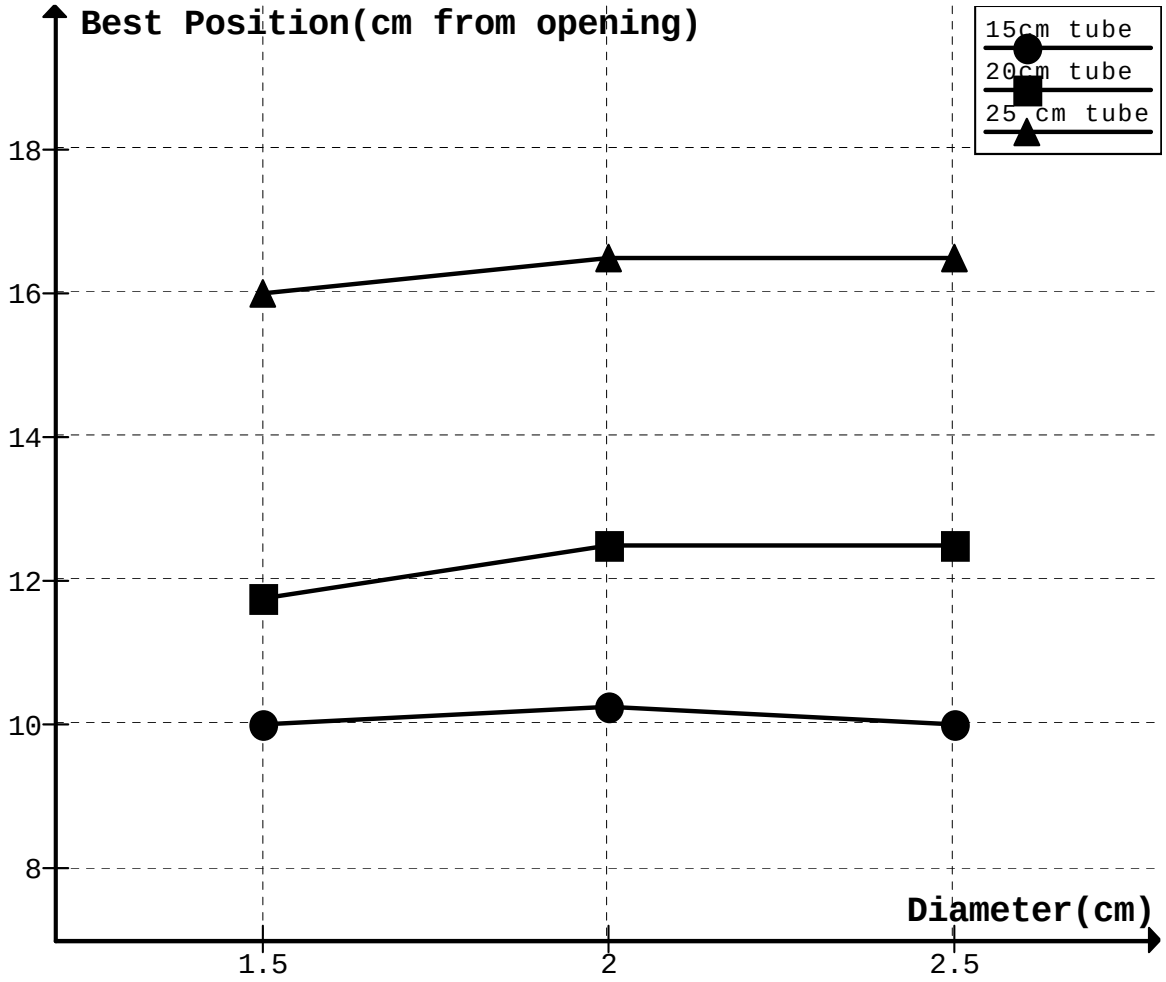

圖十七、試管中最佳位置的測量。

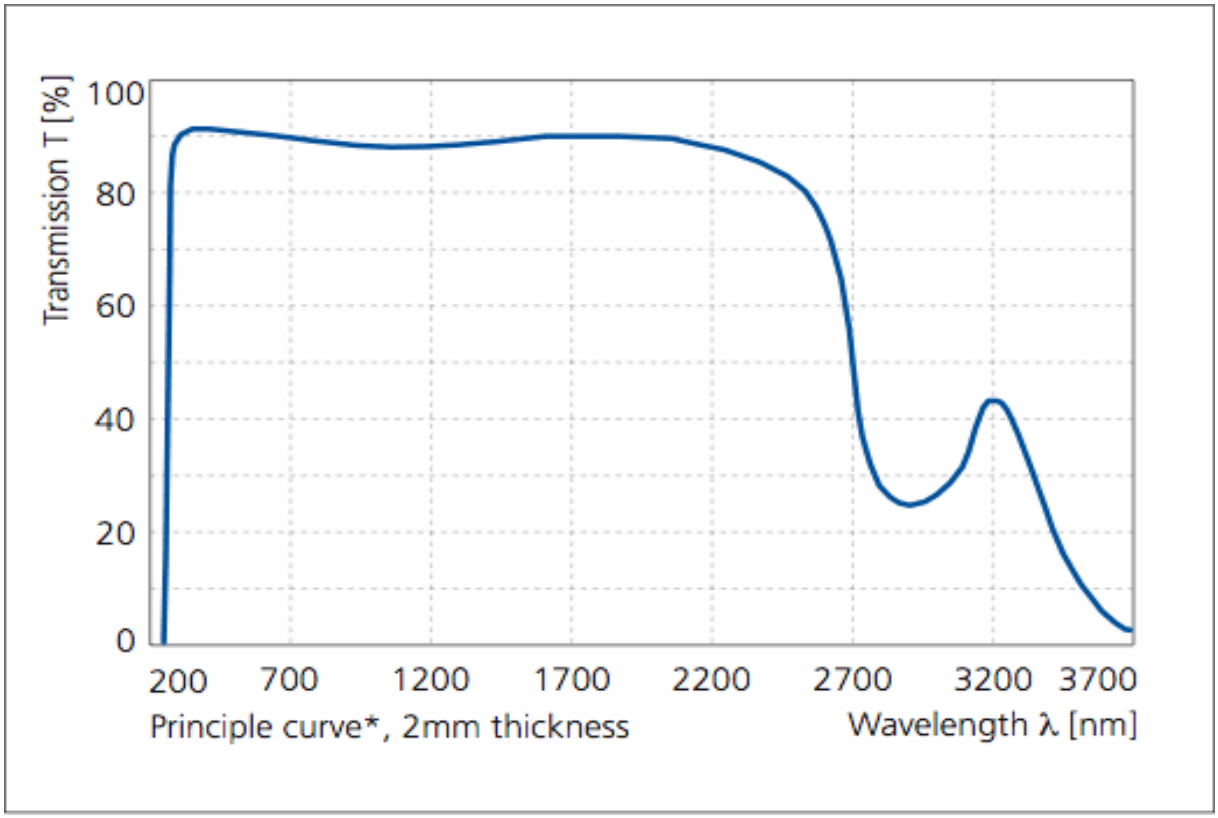

圖十八、Pyrex 玻璃之透光波段，與 TVS-100 熱影像儀的測量波段不盡相符。

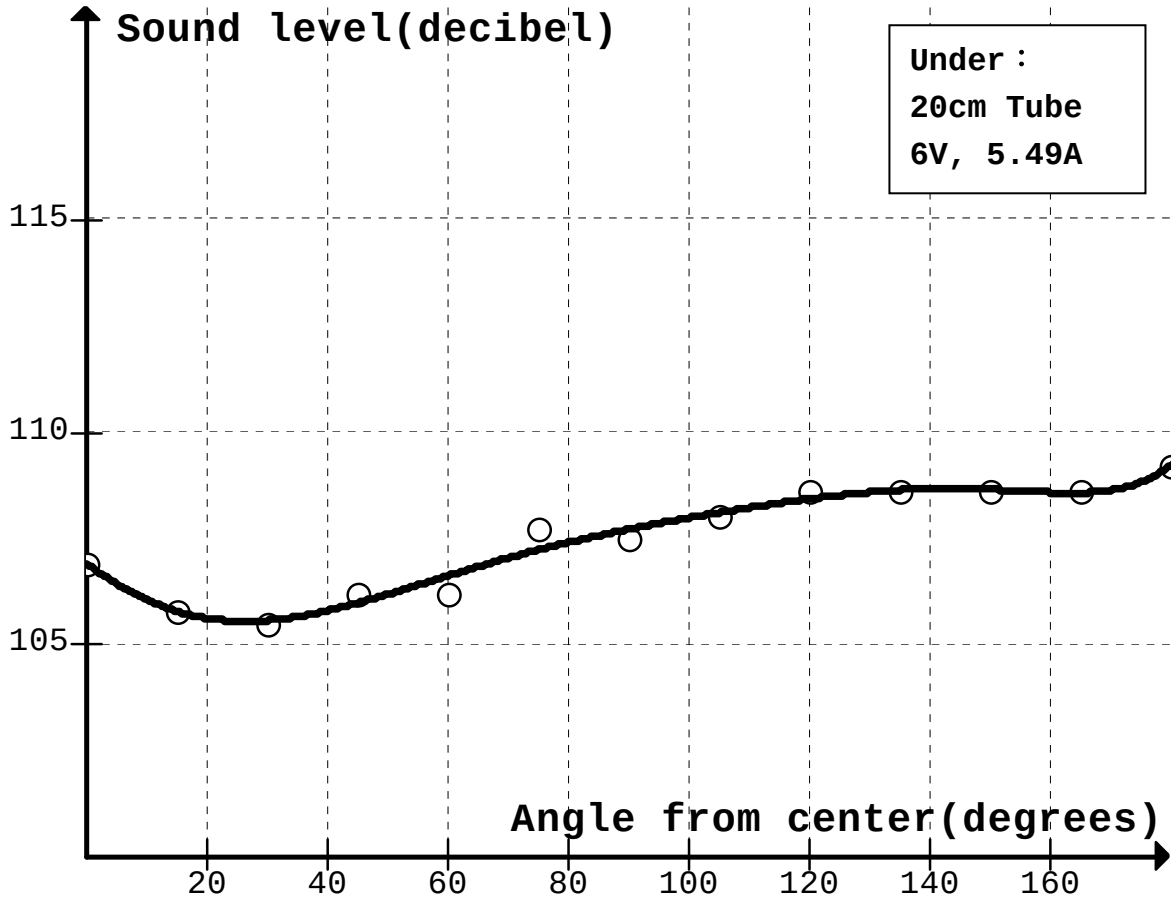

圖十九、20cm 公分試管角度與聲音強度關係圖。

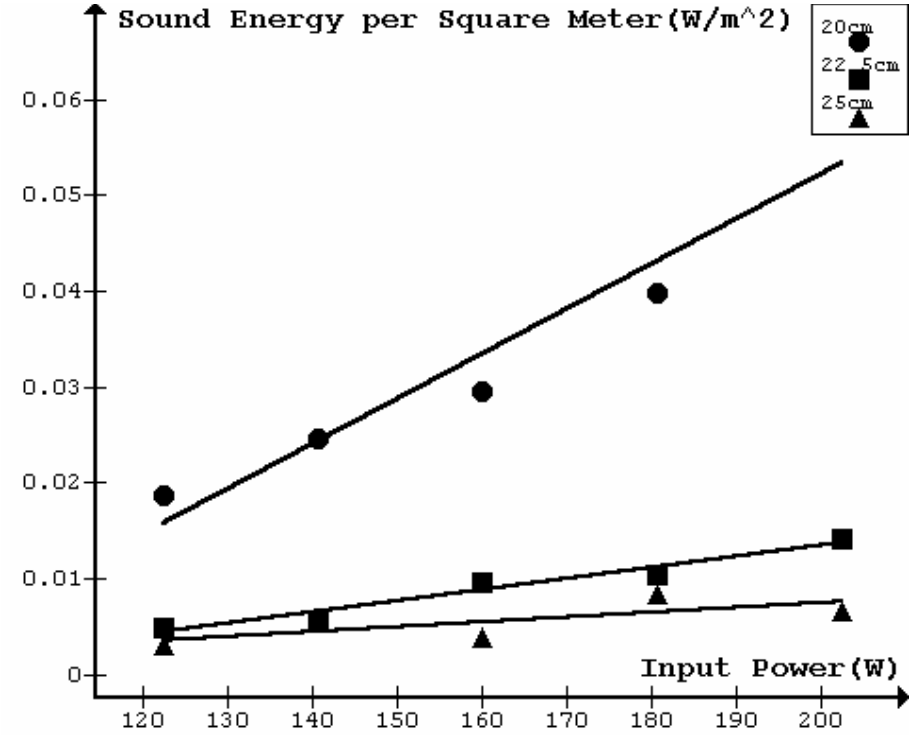

圖二十、輸入電功率與聲能強度的關係。

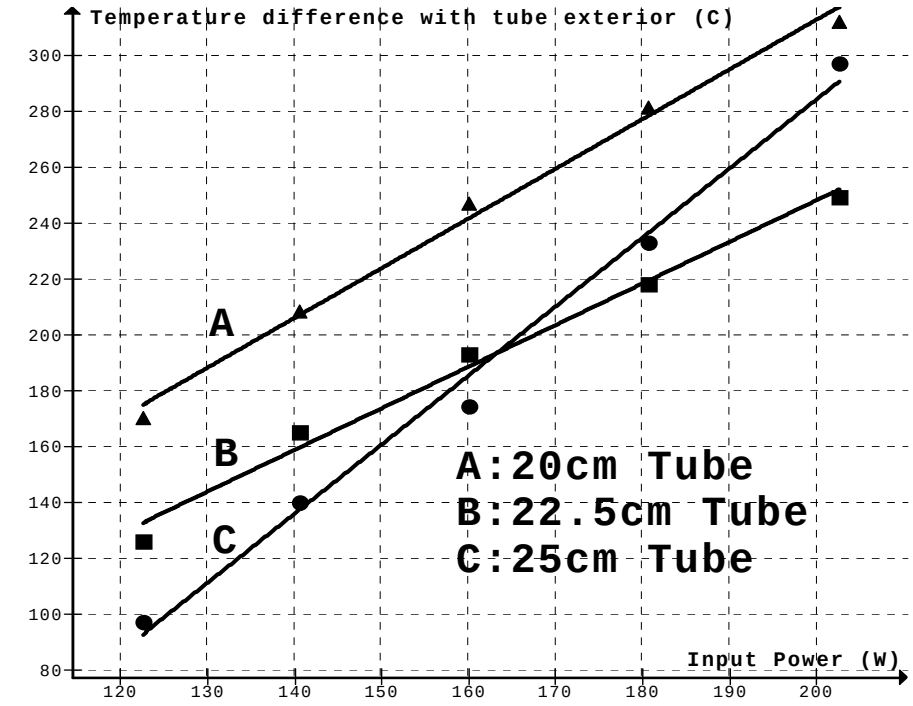

圖二十一、輸入電流與片堆、外界溫差的關係。

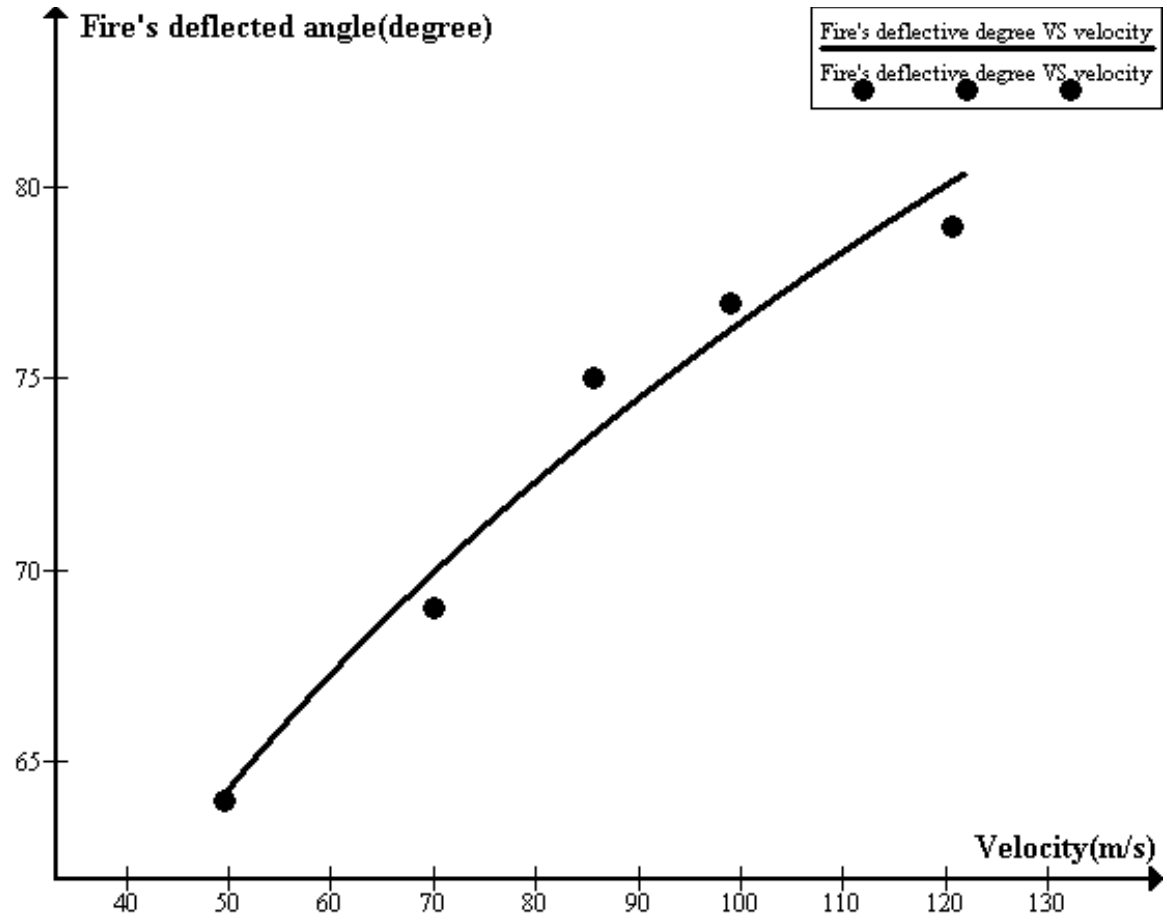

圖二十二、速度與火焰角度的關係。

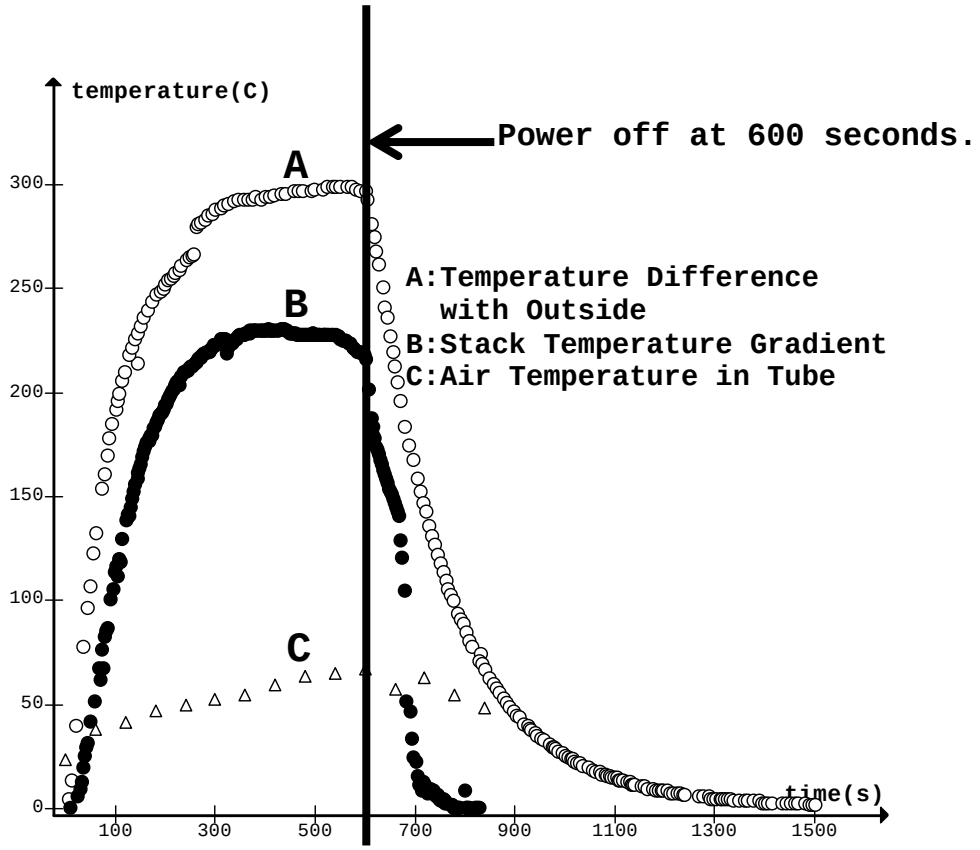

圖二十三、20 公分試管中片堆溫差、內外溫差及管內溫度變化與時間的關係。

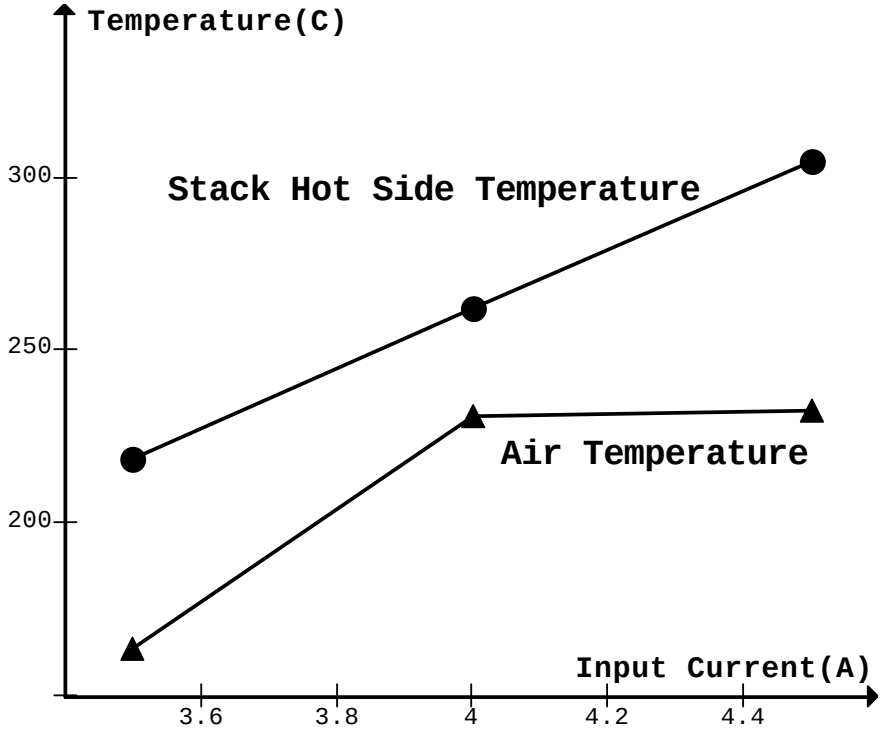

圖二十四、無試管裸露片堆，其輸入電流與熱端溫度、鄰近空氣溫度的關係。

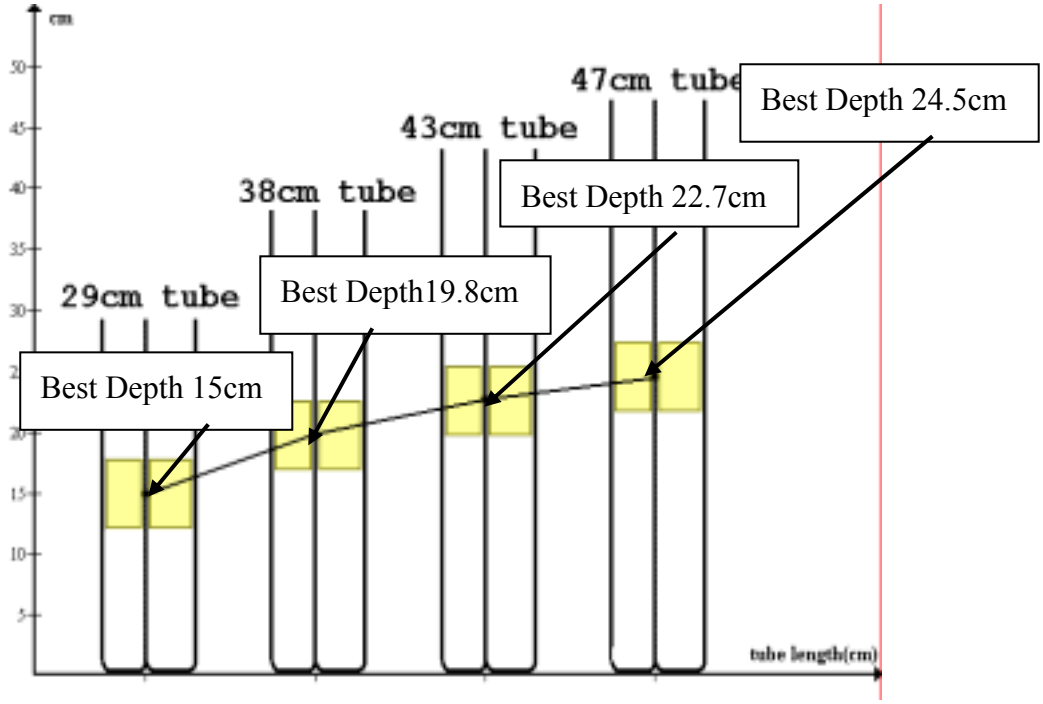

圖二十五、閉管 3.2cm 和 2.4cm 管徑下，不同管長下的最佳位置。

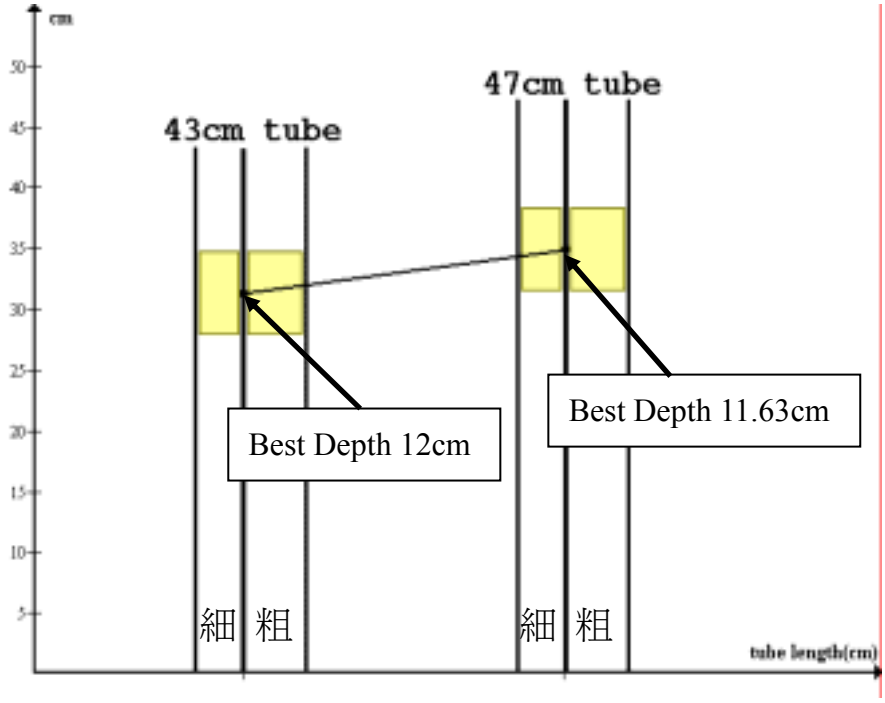

圖二十六、開管 3.2cm 和 2.4cm 管徑下，不同管長下的最佳位置。

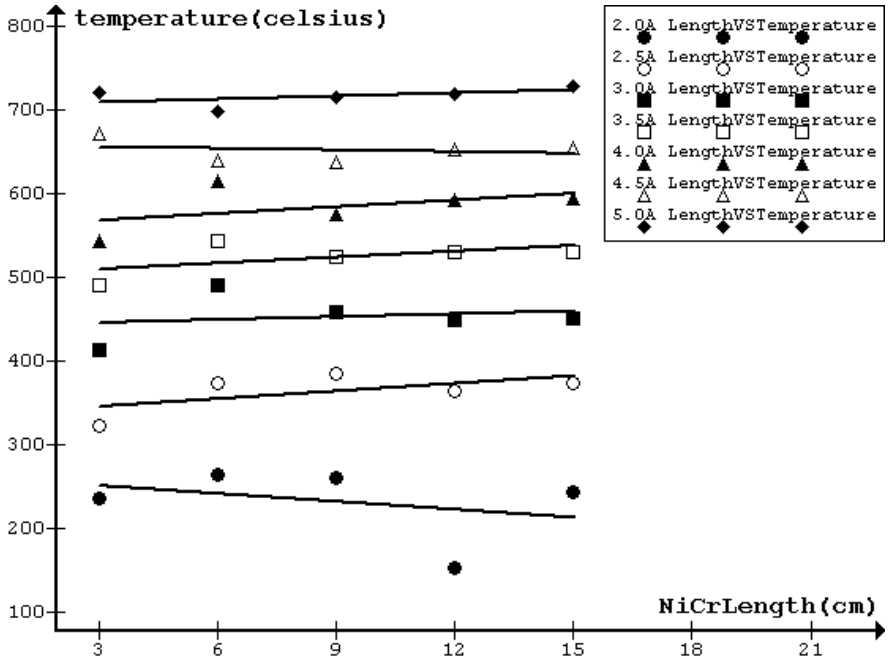

圖二十七、在不同電流下，鎳鉻電阻長度對應的熱端溫度。

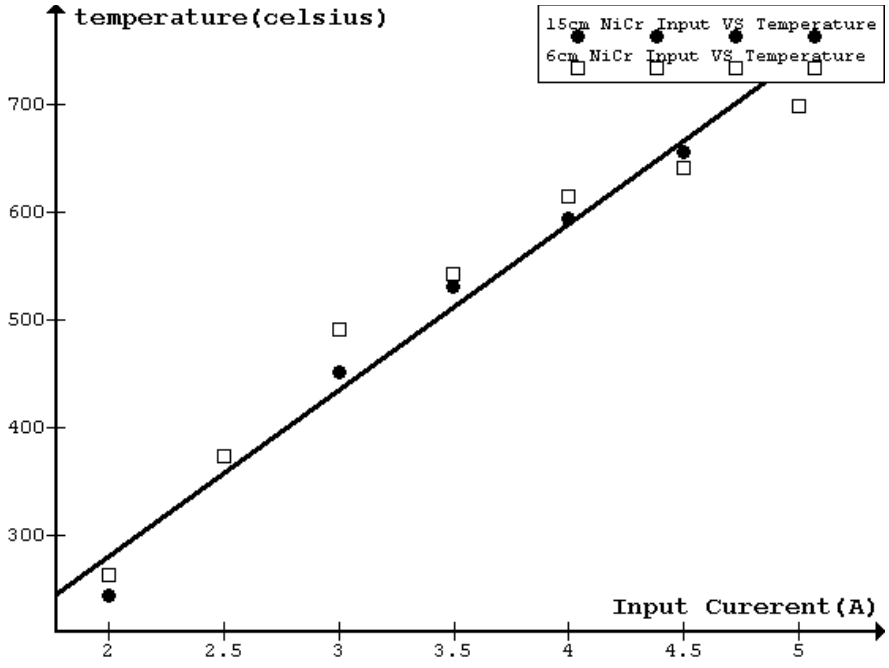

圖二十八、6cm 和 15cm 鎳鉻電阻輸入電流與熱端溫度的關係。

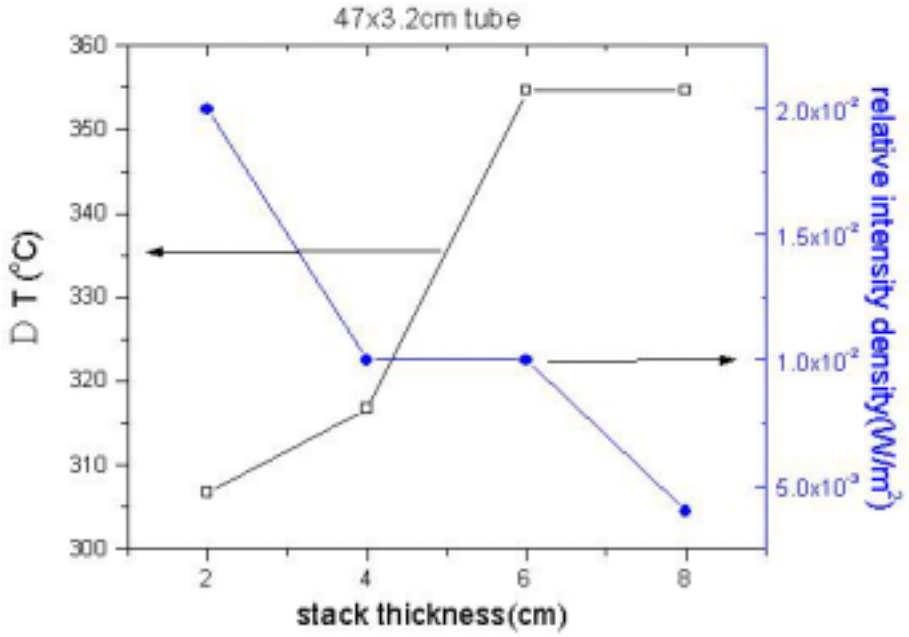

圖二十九、一端閉口管長 47cm 管徑 3.2cm 片堆厚度與溫差、聲強的關係。

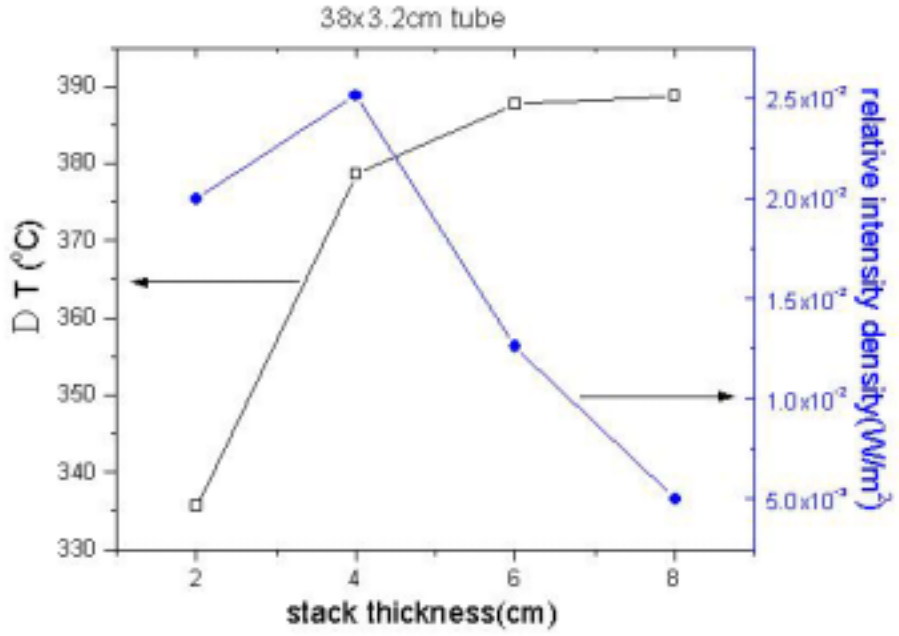

圖三十、一端閉口管長 38cm 管徑 3.2cm 片堆厚度與溫差、聲強的關係。

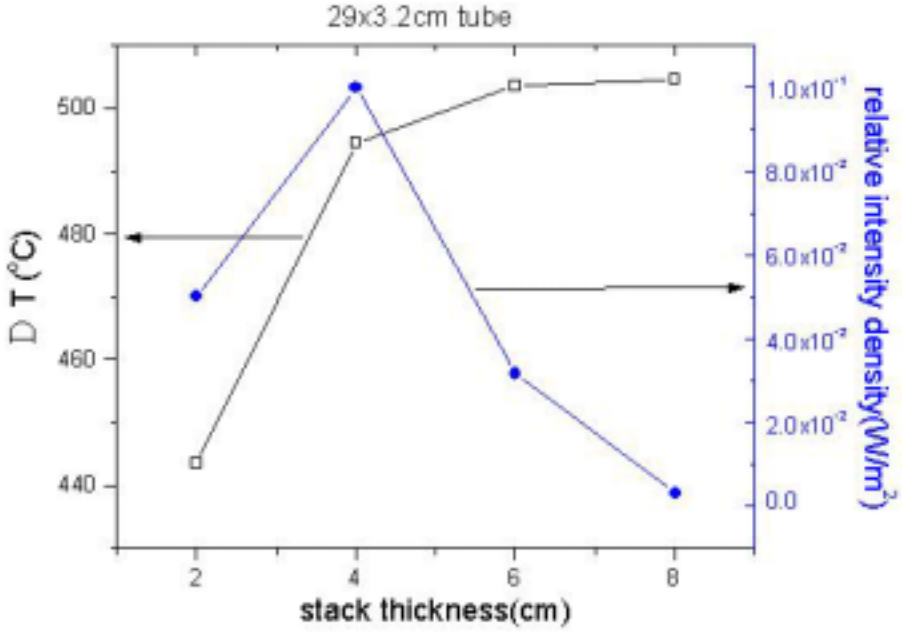

圖三十一、一端閉口管長 29cm 管徑 3.2cm 片堆厚度與溫差、聲強的關係。

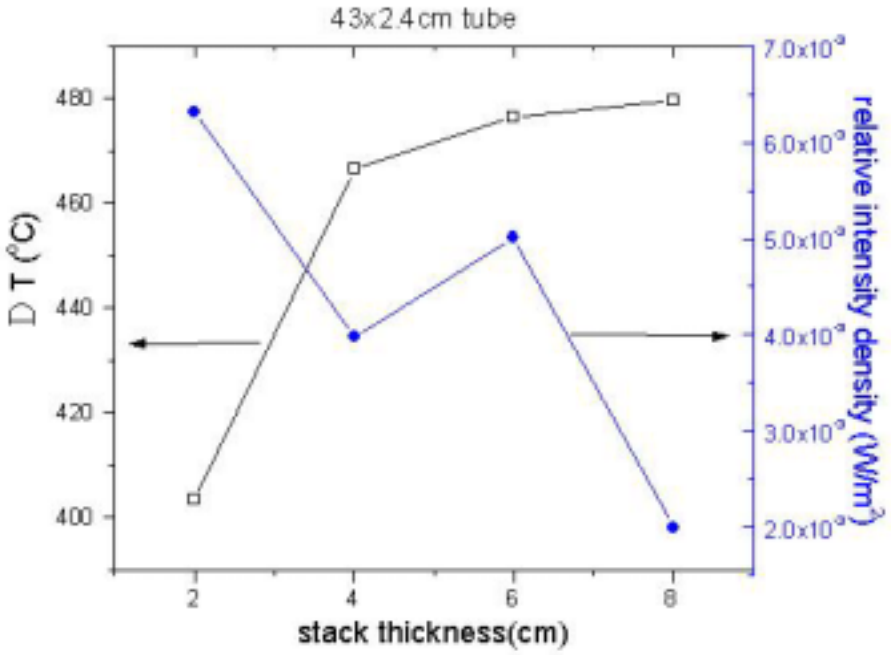

圖三十二、一端閉口管長 43cm 管徑 2.4cm 片堆厚度與溫差、聲強的關係。

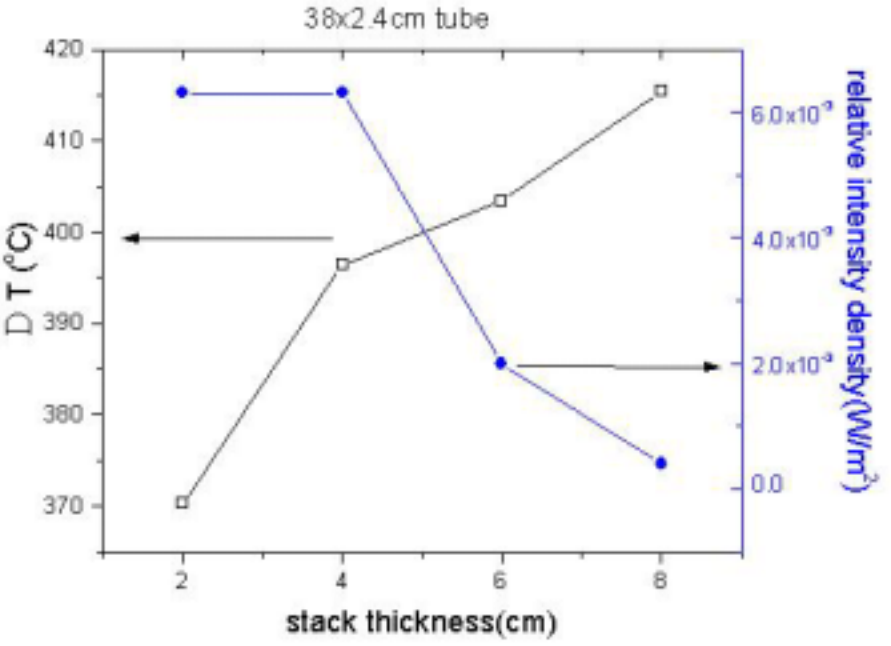

圖三十三、一端閉口管長 38cm 管徑 2.4cm 片堆厚度與溫差、聲強的關係。

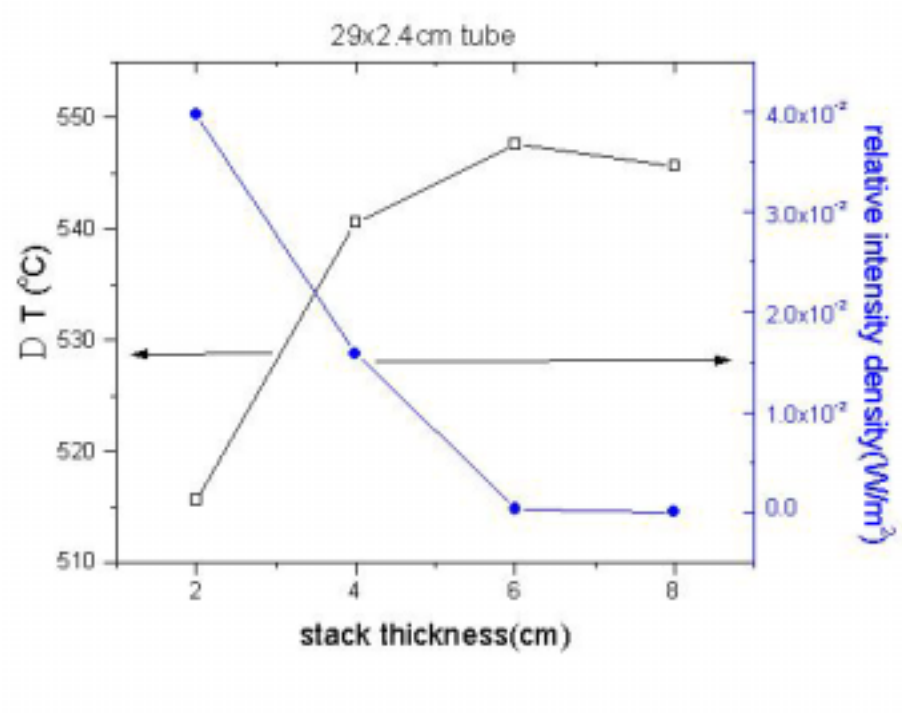

圖三十四、一端閉口管長 29cm 管徑 2.4cm 片堆厚度與溫差、聲強的關係。

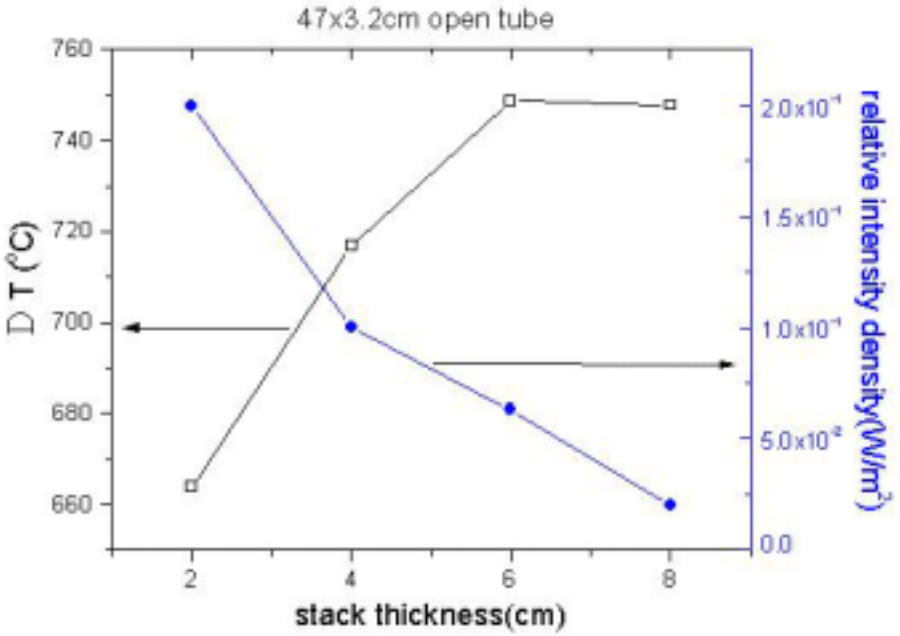

圖三十五、二端開口管長 47cm 管徑 3.2cm 片堆厚度與溫差、聲強的關係。

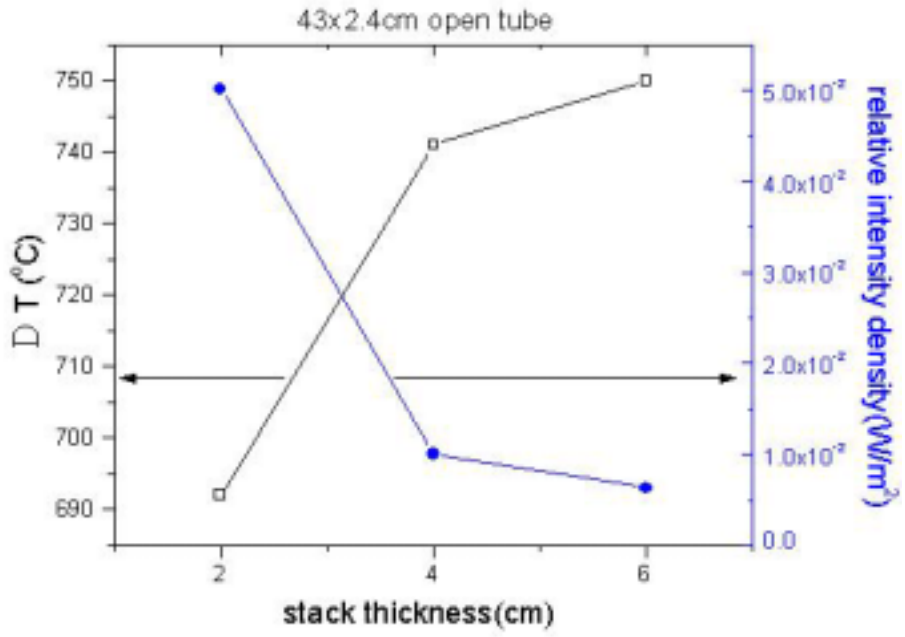

圖三十六、二端開口管徑 2.4cm 管長 43cm 片堆厚度與溫差、聲強的關係。

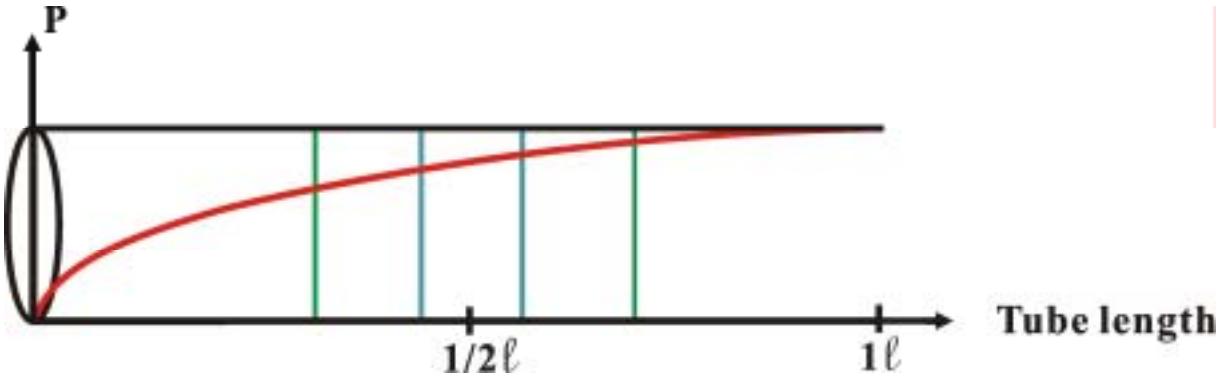

圖三十七、一端閉口管徑 2.4cm 管長 43cm 下片堆厚度與溫差、聲強的關係。

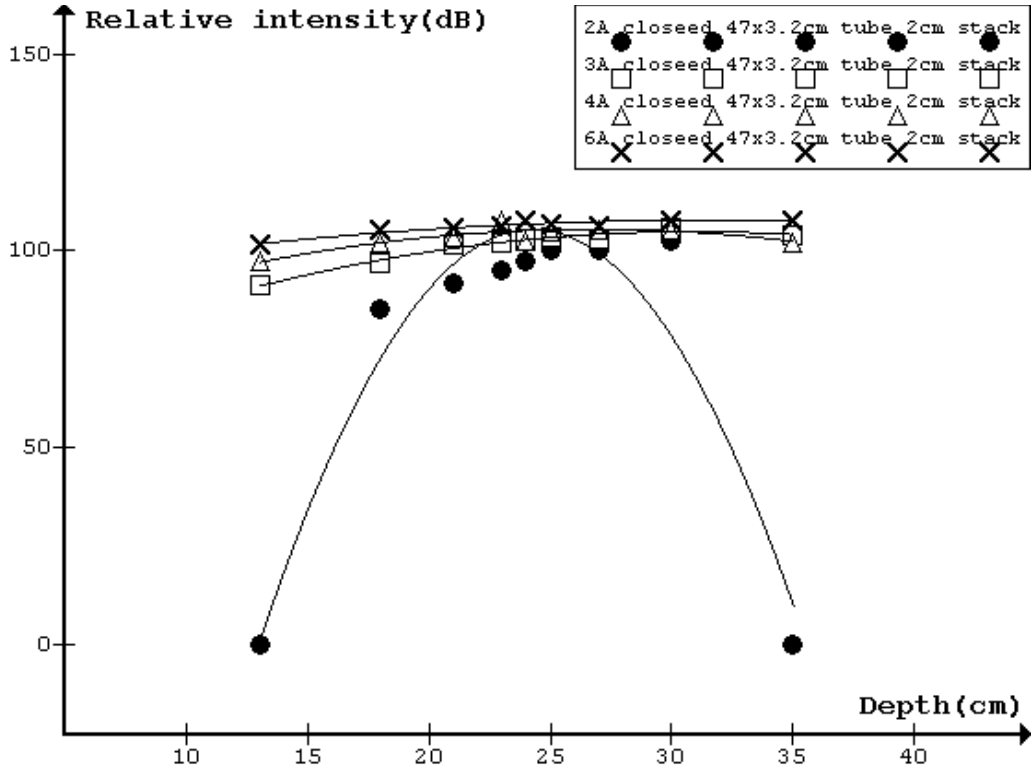

圖三十八、片堆在通過不同強度電流、不同深度下的聲強變化。

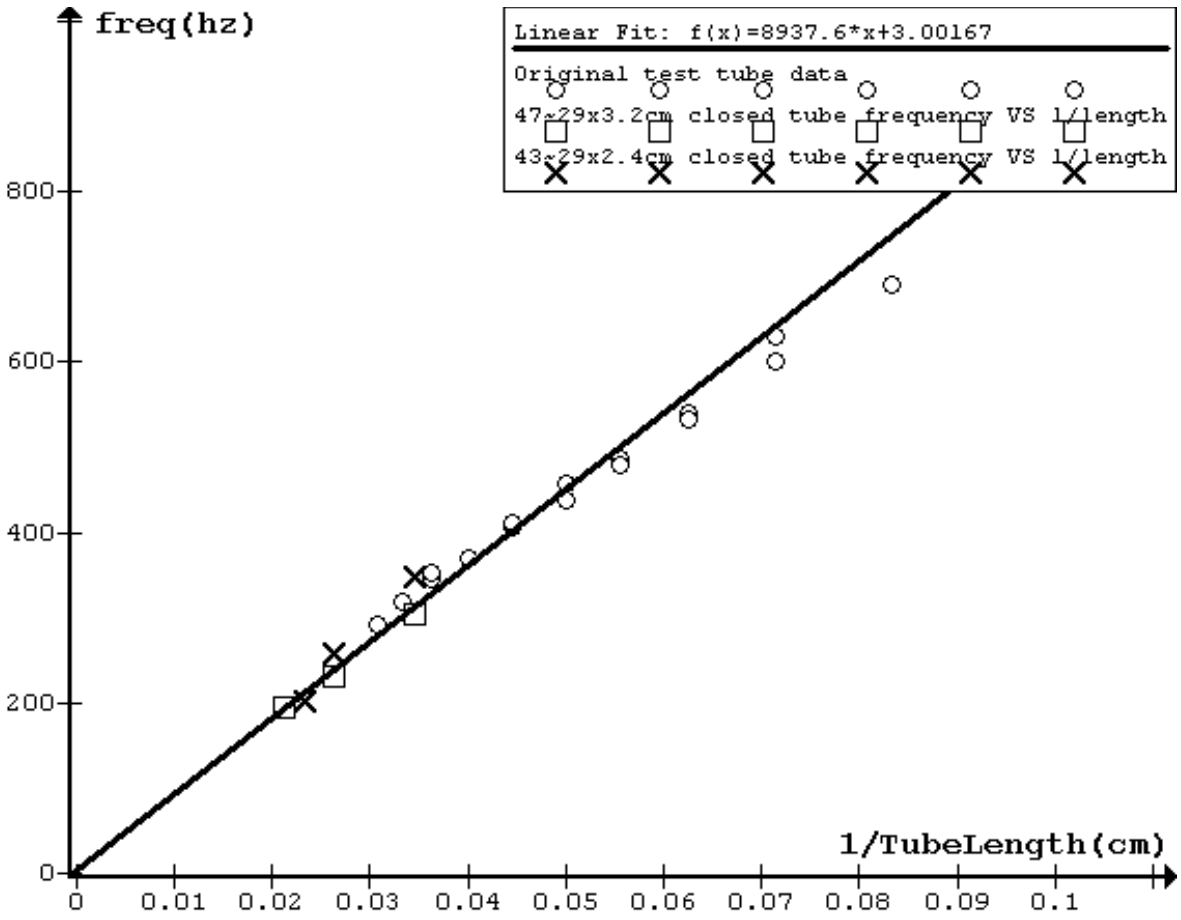

圖三十九、管長爲 47、43、38、29cm 下的聲音頻率。

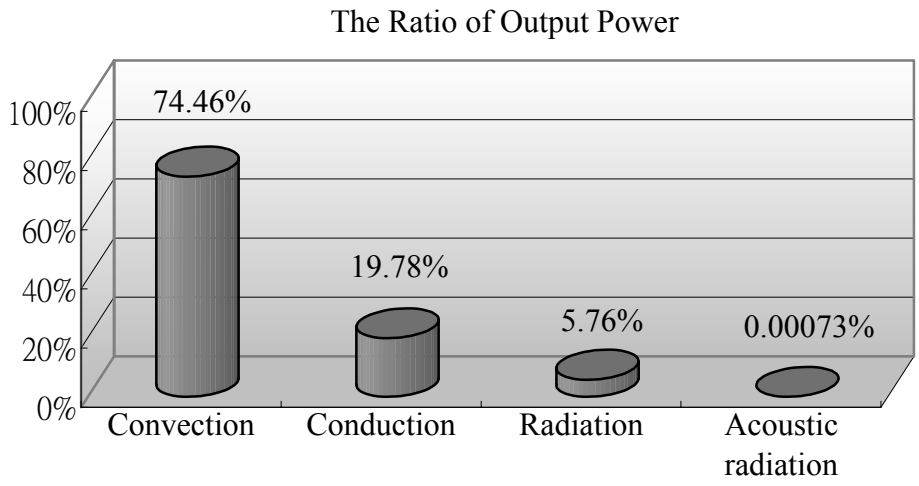

圖四十、各種輸出能量(熱對流、熱傳導、熱輻射、以及熱聲)所佔的比例。

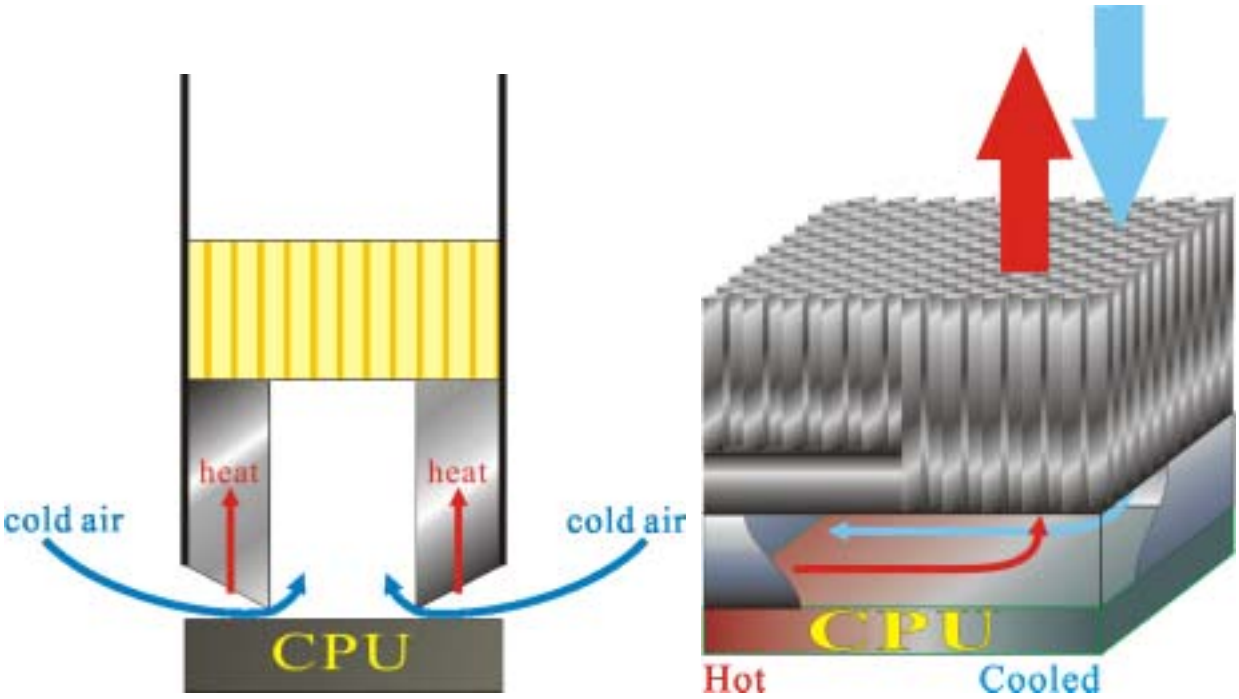

圖四十一、熱聲散熱器示意圖。

伍、參考文獻

[1]Lord Rayleigh (1945). *The Theory of Sound, Vol.II*. Dover, New York: Dover Publications.

[2]Swift, G. W. (1988). Thermoacoustic Engines. *Journal of the Acoustical Society of America*, *88*, 1145-1180.

[3]Garrett, S. L., J. A. Adeff & T. J. Hofler (1993). Thermoacoustic refrigerator for space applications. *Journal of Thermophysics and Heat Transfer*, *7*, 595-599.

[4]Garrett, S. L. (1997). *High-power thermoacoustic refrigerator*. U.S. Patent 5,647,216.

[5]Tijani, M.E.H., Zeegers, J.C.H., de Waele , A.T.A.M. (2002). Design of thermoacoustic refrigerators. *Cryogenics*, *42*, 49-57.

[6]Tijani, M.E.H., Zeegers, J.C.H., de Waele , A.T.A.M. (2002). Construction and performance of a thermoacoustic refrigerator. *Cryogenics*, *42*, 59-66.

[7]Qiu, T., Qing, L., Feng, W., Fang, Z. G. (2003). Network model approach for calculating oscillating frequency of thermoacoustic prime mover. *Cryogenics*, *43*, 351-357.

[8]Qiu, T., Qing, L., Fang, Z. G., Ji, H. W., Jun, X. L. (2003). Temperature difference generated in thermo-driven thermoacoustic refrigerator. *Cryogenics*, *43*, 515-522.

[9]Symko, O. G., Abdel-Rahman, E., Kwon, Y. S., Emmi, M., Behunin, R. (2004). Design and development of high-frequency thermoacoustic engines for thermal management in microelectronics. *Microelectronics Journal*, *35*, 185-191.

[10]Sakamoto, S., Watanabe, Y. (2004). The experimental studies of thermoacoustic cooler. *Ultrasonics*, *42*, 53-56.

[11]陳冠勳(民 89)。**熱驅動熱聲冷凍實驗設備之設計與性能實驗**。國立臺灣大學應力學研究所碩士論文，臺北市。

[12]工業技術研究院能源與資源研究網站 (http://www.erl.itri.org.tw)。

[13]黃 博全 (民 93)。**聲波冰箱實驗與數值模擬分析**。臺北市：國立臺北科技大學冷凍空調工程學系。

[14]Sarpotdar, S. M., Ananthkrishnan, N., Sharma, S. D. (2003). The Rijke Tube- A Thermo-acoustic Device. *Resonance, 8*, 59-71.

[15]Ben & Jerry 冰淇淋公司網站 (http://www.benjerry.com/our_company/sounds_cool/)。

[16]Garrett, S.L., Backhaus, S. (2000). The Power of Sound. *American Scientist*, *88*, 516-525.

[17]*Penn State "Acoustic Laser" Kit Instructions*. (2003). State College, PA: Graduate Program in Acoustics, Applied Research Laboratory, the Pennsylvania State University.

[18]鄭 益志 (民 91)。紅外線熱影像檢測技術應用。**工安環保，7，技術報導**。臺北市：工業技術研究院環安中心(http://she.moeaidB.gov.tw/issue/issue7/tec7_2.htm)。

[19]林 明瑞(主編)(民 91)。**高中物質科學物理篇(下)**。臺南市：南一書局企業股份有限公司。

[20]*Pyrex Properties*. Langen Busch, Iserlohn: Präzisions Glas & Optik GmbH. Retrieved 2004 from the World Wide Web: http://www.pgo-online.com/intl/jse/frameroute/genericset.html?Content=/intl/katalog/pyrex.html

[21]Wolfe, J. (1998). *What is a decibel?* Sydney, Australia: Univ. of New South Wales. Retrieved 2004 from the World Wide Web: http://www.phys.unsw.edu.au/~jw/dB.html

[22]Çengel, Y. A. (1998). *Heat Transfer A Practical Approach*. Hightstown, NJ: WCB/McGraw-Hill.

[23]McGlen, R. J., Jachuck, R., Lin, S. (2004). Integrated thermal management techniques for high power electronic devices. *Applied Thermal Engineering, 24*, 1143-1156.

陸、附錄

一、使用之電腦軟體

(一)Mac OS X 10.3.5 Panther, Copyright© 2003, Apple Computer, Inc.

(二)Microsoft Windows XP Professional, Copyright© 1981-2001 Microsoft Corporation.

(三)Microsoft Word 2002, Copyright© 1983-2001 Microsoft Corporation.

(四)Microsoft Excel 2002, Copyright© 1983-2001 Microsoft Corporation.

(五)Graph 3.3, Copyright© 2004 Ivan Johansen.

(六)Voice Spectrograph, http://www.voicesync.org .

(七)Microsoft 小算盤 5.1, Copyright© 1981-2001 Microsoft Corporation.

(八)Microsoft 小畫家 5.1, Copyright© 1981-2001 Microsoft Corporation.

(九)Adobe Illustrator CS 11.0.0, Copyright© 1987-2001 Adobe Systems, Inc.

(十)MSN Messenger 6.2, Copyright© 1997-2004 Microsoft Corporation.

(十一)Microsoft Internet Explorer 6.0 SP-2, Copyright© 1995-2004 Microsoft Corporation.

(十二)WinZip 9.0 SR-1 (6224), Copyright© 1991-2004 WinZip Computing, Inc.

(十三)Microsoft 記事本 5.1, Copyright© 1981-2001 Microsoft Corporation.

(十四)CorelDraw Version 10.410, Copyright© 2000 Corel Corporation.

(十五)Microcal Origin 5.0 Professional, Copyright© 1991-1997 Microcal Software, Inc.

二、使用之硬體設備

(一)Cordierite 陶瓷材料

(二)Pyrex 試管

(三)鎳鉻(NiCr)電阻

(四)銅心漆包線

(五)不鏽鋼管

(六)電源供應器 (ABM 9306D Dual-Tracking Power Supply)

(七)麥克風 (Philips Corded Electret Microphone SBC-ME570)

(八)分貝計 (Extech Digital Sound Level Meter 407727)

(九)紅外熱影像儀 (Nippon Avionics Co., Ltd. Avio Handy Thermo TVS-100 Infrared Thermography)

(十)熱電偶溫度計 海碁 TM-906 (k-type thermocouple)

(十一)數位像機 (SAMSUNG Kenox Digmax V4)

(十二)鱷魚夾

(十三)碼表

(十四)水桶 (乃勤牌 彈力水桶)

(十五)鐵架

(十六)耳罩

(十七)電腦

I. Introduction

1. Motive for Study

According to Moore's Law, which states that the number of transistors per square inch on integrated circuits doubles every year, the need to more efficiently dissipate large amounts of heat generated by microelectronic devices also increase dramatically.

Many methods were proposed, developed and applied, such as thermoelectric coolers, heat pipes and more recently, thermoacoustic (TA) coolers. Thermoacoustic refrigeration has advanced over the years into actual ice cream refrigerators. It utilizes the temperature gradient generated on a porous "stack" placed in a resonance tube when an oscillating acoustic wave is introduced.

On the other hand, when a temperature difference is generated on the stack, it would create acoustic resonance in the tube. This acoustic resonance would enhance the air convection inside the tube creating "acoustic streaming". For applications requiring less dramatic refrigeration, such as microprocessors or even devices on a nanometer scale, the temperature gradient between the heat source and the background is sufficient to trigger thermoacoustically enhanced air convection. This passive cooling method eliminates the need for extra input energy and provides a distinctive advantage when applied on mobile electronic devices. However, there is no research being done on this cooling method. Therefore, the focus of this study is to evaluate the potential of using thermoacoustic engines on the passive cooling of microelectronic devices using actual experiments and to propose an actual passive TA cooler design.

2. Thermoacoustic Theory and Previous Research

Early research regarding thermoacoustics began after a humming sound was heard by glassblowers in the 19th century (see **Tables 1** and **2** for a partial list of notable studies). An early apparatus studied was the Rijke tube[1], which produces audible sound when a heat source is introduced into a metal tube with two openings. In 2002 Ben & Jerry's Ice Cream with researchers from Penn State University developed a thermoacoustic ice cream refrigerator which literally "Sounds Cool" (see **Picture 1**)[2]. It is just as efficient as traditional refrigerators yet it is significantly more environmentally friendly.

[1] Sarpotdar, S. M., Ananthkrishnan, N., Sharma, S. D. (2003). The Rijke Tube- A Thermo-acoustic Device. *Resonance, 8*, 59-71.

[2] Ben & Jerry's Ice Cream has a Shockwave demonstration of the thermoacoustic effect: http://www.benjerry.com/our_company/sounds_cool/

Picture 1 Thermoacoustic researchers at Penn State. Left to right: Matt Poese, Steve Garrett and Robert Smith.

Garrett & Backhaus[3] have a clear explanation of the workings of a thermoacoustic refrigerator:

*Thermoacoustic device consists, in essence, of a gas-filled tube containing a "stack" ([**Fig. 1**] top), a porous solid with many open channels through which the gas can pass. Resonating sound waves (created, for example, by a loudspeaker) force gas to move back and forth through openings in the stack. If the temperature gradient along the stack is modest ([**Fig. 1**] middle), gas shifted to one side (a) will be compressed and warmed so that a parcel of gas with dimensions that are roughly equal to the thermal penetration depth (δk) releases heat to the stack. When this same gas then shifts in the other direction (b), it expands and cools enough to absorb heat. Although an individual parcel carries heat just a small distance, the many parcels making up the gas form a "bucket brigade," which transfers heat from a cold region to a warm one and thus provides refrigeration.*

Thermoacoustic refrigerators have the following advantages: (1) The resonance tube contains inert gases (for example, Helium), instead of environmentally damaging refrigerants, (2) no moving parts, which reduces maintenance costs and (3) high efficiency.

Garrett & Backhaus further explains the thermoacoustic engine:

*The same device can be turned into a thermoacoustic engine ([**Fig. 1**] bottom) if the temperature difference along the stack is made sufficiently large. In that case, sound can also compress and warm a parcel of gas (c), but it remains cooler than the stack and thus absorbs heat. When this gas shifts to the other side and expands (d), it cools but stays hotter than the stack and thus releases heat. Hence, the parcel thermally expands at high pressure and contracts at low pressure, which amplifies the pressure oscillations of the reverberating sound waves, transforming heat energy into acoustic energy.*

[3] Garrett, S.L., Backhaus, S. (2000). The Power of Sound. *American Scientist*, *88*, 516-525.

Other than developing thermoacoustic refrigerators, the thermoacoustic research group at Penn State also made a thermoacoustic engine demonstration device called the "Acoustic Laser"[4]. This device uses a porous Cordierite ceramic material as the stack, when a current passes through the NiCr (Nichrome, see **Picture 2**) wiring attached at one side, it generates a large temperature gradient which creates oscillating sound inside the Pyrex test tube in which everything is contained. It operates just like an optical laser: When sufficient acoustic energy is accumulated, it radiates out through the test tube's opening, hence the name "Acoustic Laser" (see **Fig. 2**). The oscillating sound in the test tube also enhances air convection.

When a microelectronic component is placed at one side of the stack, it would also generate the temperature difference required for acoustic resonance just like the NiCr wire, and the enhanced convection would help control the temperature of the component itself. In other words, when the microelectronic component is cool, the air convection and acoustic resonance are weak; when the microelectronic component heats up, it enhances the air convection caused by acoustic resonance and cools down again. The net effect of this arrangement can be used on the thermal control of a component which does not need cooling below ambient temperature. If the temperature gradient and geometric properties required to produce the oscillations are determined, a passive thermoacoustic cooling device can then be developed.

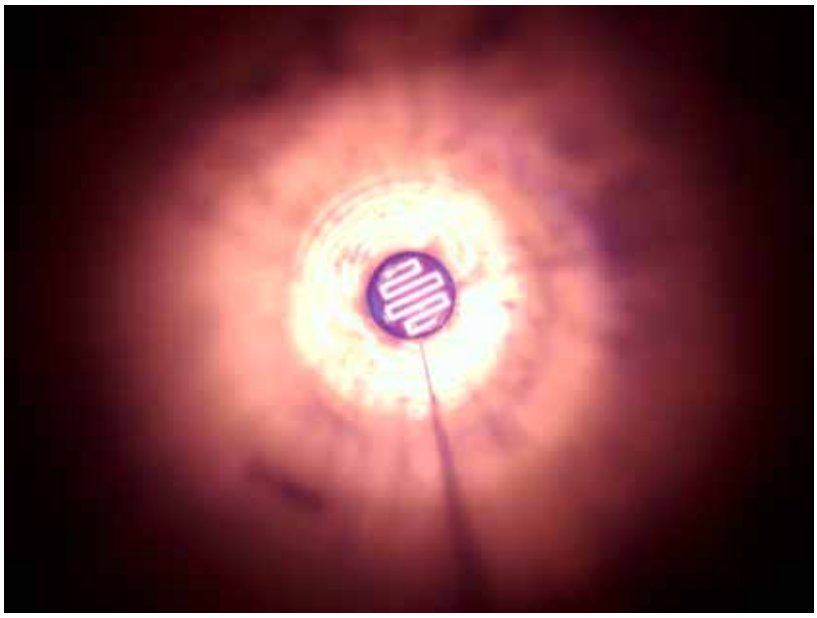

Picture 2 The NiCr wire heating up inside the resonance tube.

[4] Penn State "Acoustic Laser" Kit Instructions. (2003). State College, PA: Graduate Program in Acoustics, Applied Research Laboratory, Pennsylvania State University.

Table 1. Notable work on thermoacoustics (International)

Year	Author(s)	Institution	Title	Results
1878	**Lord Rayleigh**	**Cavendish Laboratory, Cambridge University.**	**The Theory of Sound**	**"Rayleigh's Criterion": Explains how heat triggers and maintains oscillating sound waves in a tube.**
1988	Swift, G. W.	Graduate Program in Acoustics, Penn State University.	Thermoacoustic Engines	Discussion about thermoacoustic engines.
1993	Garrett, S. L., et al.	Graduate Program in Acoustics, Penn State University.	Thermoacoustic Refrigerator for Space Applications	The development of a thermoacoustic refrigerator used on the Space Shuttle.
1997	Garrett, S. L.	Graduate Program in Acoustics, Penn State Univ.	High-power Thermoacoustic Refrigerator	Discusses a patented thermoacoustic refrigerator.
2002	Tijani, M.E.H., et al.	Department of Applied Physics, Eindhoven University of Technology.	Design of Thermoacoustic Refrigerators	Discusses the considerations for designing a thermoacoustic refrigerator.
2002	Tijani, M.E.H., et al.	Department of Applied Physics, Eindhoven University of Technology.	Construction and performance of a thermoacoustic refrigerator	A study of the construction process of a thermoacoustic refrigerator.
2003	Qiu, T., et al.	Cryogenics Laboratory, Huazhong University of Science and Technology.	Network model approach for calculating oscillating frequency of thermoacoustic prime mover	A novel method for the calculation of a thermoacoustic device's resonance frequency.
2003	Qiu, T., et al.	Cryogenics Laboratory, Huazhong University of Science and Technology.	Temperature difference generated in thermo-driven thermoacoustic refrigerator	A novel method for the calculation of a thermoacoustic device's generated temperature gradient.
2004	**Symko, O. G., et al.**	**Deptment of Physics, University of Utah.**	**Design and development of high-frequency thermoacoustic engines for thermal management in microelectronics**	**Proposes the possibility of using thermoacoustic cooling on microelectronic devices.**
2004	Sakamoto, S., et al.	Faculty of Engineering, Doshisha University, Japan.	The experimental studies of thermoacoustic cooler	Thermoacoustic research using a loop-tube apparatus.

Table 2. Notable work on thermoacoustics (Taiwan)

Year	Author(s)	Institution	Title	Results
2000	Chen, G.H.	Inst. Of Applied Mechs., National Taiwan University	Design and Experiment of a thermoacoustic refrigerator	One of the earliest studies conducted on thermoacoustic refrigeration in Taiwan.
2003		Energy & Resources Labs, Industrial Tech. Research Inst.	Micro thermoacoustic refrigerator	A 9 cm thermoacoustic refrigerator.
2004	Huang, P.C.	Dept. of Refrigeration and Air Conditioning Engineering, Nat'l Taipei University of Technology	Experimentation and Numerical Simulation of a Sonic Refrigerator	A computer simulation of a thermoacoustic refrigerator.
2005	**Hsing, P.Y., Huang, W.K., Tsu-Zheng, Y.**	**Taipei Municipal Lishan Senior High School**	**Enhanced cooling of microelectronic devices by using the thermoacoustic effect**	**The first study on passive thermoacoustic cooling.**

3. Project Goals

(1) Attempt to alleviate two major conflicting goals in engineering: efficient cooling versus low power consumption.

(2) Considering the physical properties of thermoacoustics, try to either propose a new configuration or introduce a new physical property.

(3) Evaluate using thermoacoustically enhanced air convection on passive cooling with actual experimentation.

(4) Propose a new cooler design based on experimental results.

4. Research Flow

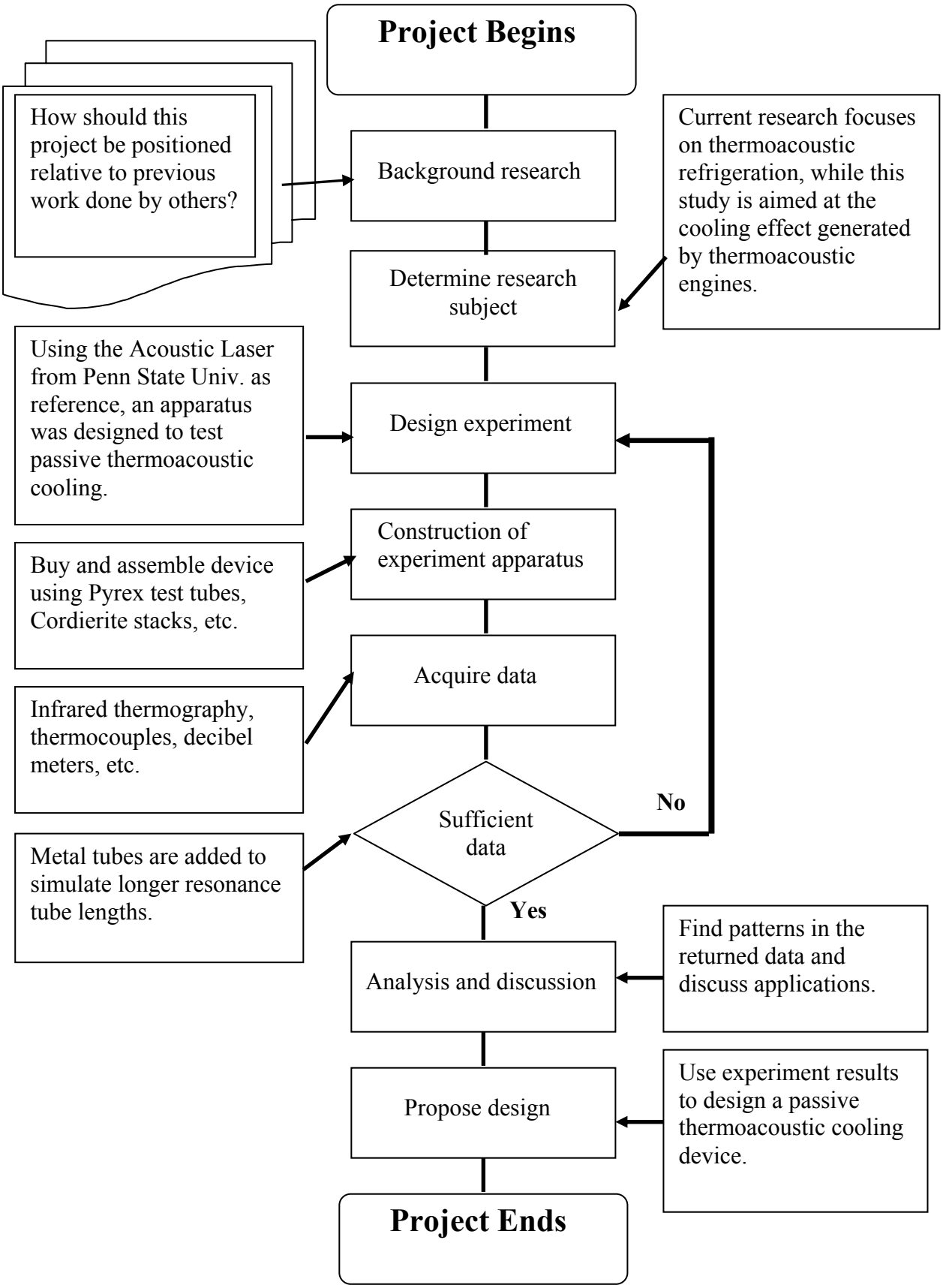

II. Materials and Methods

1. Experimental Setup

The Acoustic Laser was used as a testbed for measuring fundamental variables affecting the performance of a thermoacoustic device. A typical kit from Penn State primarily comprises of: a 20cm Pyrex glass test tube, a length of NiCr (Nichrome) wiring, and a porous Cordierite ceramic stack (see **Picture 3**).

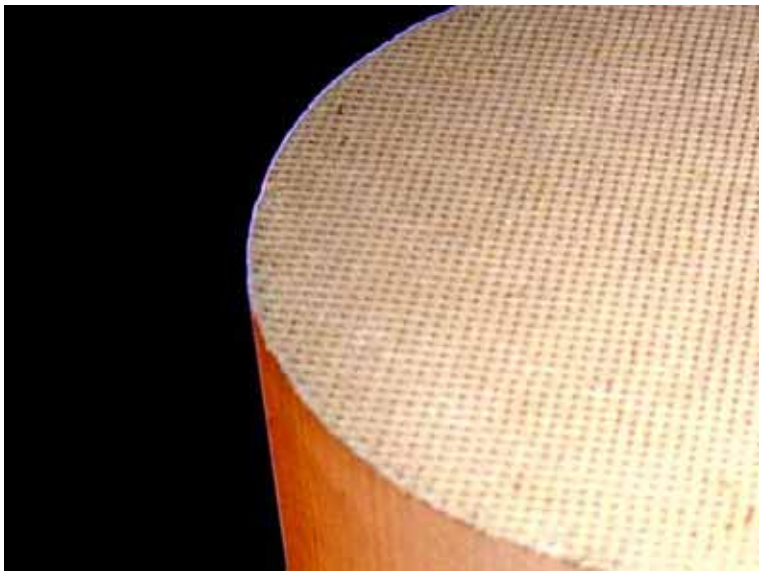

Picture 3 Porous Cordierite ceramic material used in the stack.

The Nichrome wiring was first wrapped onto one side (the "hot" side) of the ceramic stack, additional copper wires were used to connect it to an electric power supply[5] (see **Picture 4**). The stack is placed at about the center of the test tube with the cold side (without NiCr wires) facing the opening. As the power supply is turned on, electric current passes through the NiCr wiring and heats up the hot side of the stack, creates a temperature gradient, and an loud hum is produced. In addition to the original 20cm test tube, tubes with lengths of 15, 20, 25cm, and diameters of 1.5, 2, 2.5cm (a total of nine Pyrex tubes) were purchased to conduct tests (see **Picture 5**). Also, 47cm and 43cm steel tubes with diameter of 2.4 and 3.2cm were employed to augment the test tubes, and measurements made with these tubes will be noted.

[5] ABM 9306D Dual-Tracking Power Supply.

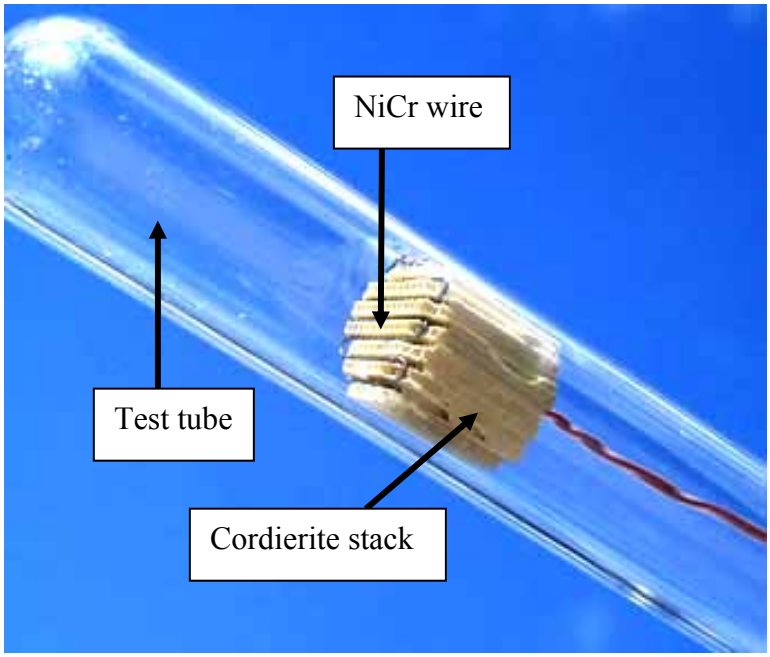

Picture 4 Components of the "Acoustic Laser".

Picture 5 Nine Pyrex test tubes with lengths of 15, 20, 25cm, and diameters of 1.5, 2, 2.5cm.

The fundamental relationships of the thermoacoustic engine were examined with the following experiments:

1.1 Tube Dimensions and Resonance Frequency

The apparatus consists of an assembled thermoacoustic engine mounted vertically under a microphone[6] connected to a computer. When the power supply is turned on, the computer records the frequency of the sound produced using the software Voice Spectrograph[7] (see **Fig. 3**). The goal of these experiments is to see if the thermoacoustic cooling device can be made to produce sound in the ultrasonic range, eliminating excess audible noise.

1.1.1 Tube Length and Resonance Frequency

In order to produce tubes of different lengths, paper extensions were added to the 15, 20 and 25cm test tubes; the length was controlled by how much the paper extended from the opening (see **Fig. 4**). Tube lengths from 35cm to 5cm were simulated in this fashion at 2.5cm intervals. For the steel tube, duct tape was used to seal one end and water was added to change the length of the resonance cavity inside, making lengths of 47, 43, 38 and 29cm. The resonance frequencies were recorded and plotted against the reciprocal of their respective tube lengths.

1.1.2 Tube Diameter and Resonance Frequency

The oscillating frequencies of 15cm test tubes acquired with diameters of 2cm, 2.5cm and 3cm were recorded and compared to see if tube diameters in this range would have a significant impact on frequency.

1.2 Stack and Tube Relationship

1.2.1 Best Position of Stack

The position of a stack inside a resonance tube where the produced sound intensity is greatest was defined as the "best" position of the stack. The "position" was defined as the distance between the center of the stack and the test tube's opening. A stack's best positions within tubes of varying lengths were determined with the following procedure: A sound intensity meter[8] (see **Picture 6**) was placed 10cm over the opening of the test tube to measure sound intensity; after activation of the Acoustic Laser, the stack was slowly moved to a point in the tube that produced the highest reading in the decibel meter, this was recorded as the "best" position of the stack (see **Fig. 5**). Measurements were conducted using 47, 38, 29, 20, 15cm test tubes.

[6] Philips Corded Electret Microphone SBC-ME570.
[7] Obtained from the VoiceSync website: http://www.voicesync.org/
[8] Extech Digital Sound Level Meter 407727.

Additionally, the best positions of stacks were also tested under 25, 20 and 15cm tubes with diameters of 1.5, 2 and 2.5cm.

Picture 6 Extech Digital Sound Level Meter 407727

1.2.2 Onset Stack Temperature Difference for TA effect

When a stack is placed at the best position in a test tube, the input electrical current was slowly reduced to an onset point just above the minimum required to maintain acoustic oscillations. The stack temperature difference and sound intensity at that point were recorded. These measurements were also carried out with stack thicknesses ranging from 8cm to 2cm. Infrared thermography[9] was attempted to visualize the interior and exterior temperature distribution of the Pyrex tube and the steel tube apparatus, respectively, while the interior temperatures of the steel tubes were measured with a K-type thermocouple[10] (See **Picture 7**).

Picture 7 Left: Avio Handy Thermo TVS-100 Infrared Thermography. Right: Hola TM-906 K-type thermocouple.

[9] Nippon Avionics Co., Ltd. Avio Handy Thermo TVS-100 Infrared Thermography.
[10] Hola TM-906 K-type thermocouple.

1.3 Heat Transfer in TA Device

In order to grasp the ratio between the four types of energy (heat) dissipation methods in a thermoacoustic engine, air convection, conduction radiation, and acoustic radiation, the following measurements were carried out using the 47cm steel tube:

1.3.1 Convection

Originally, the flow velocity at the resonance tube's opening was determined from the deflection angle of a stable flame placed at the opening of the tube. However, the data acquired proved to be highly inaccurate. Eventually, a velocity meter[11] with a spherical sensor of 2.5mm was placed at the same location to measure the mean velocity profile. This value was then used in conjunction with stack and ambient air temperature to calculate the amount of convection in the thermoacoustic engine.

1.3.2 Conduction

The amount of heat transported by conduction was calculated taking into account the heat conduction coefficient of the resonance tube material and the temperature at the hot side of the stack.

1.3.3 Radiation

Heat radiation was calculated from the mean temperature of the entire thermoacoustic engine apparatus.

1.3.4 Acoustic Radiation

The relative acoustic intensity (dB) was measured 10cm from the opening of the tube. Assuming spherical expansion, the total amount of energy dissipated via acoustic radiation was then calculated.

After having completed all of the above, an actual test was conducted by activating a 47cm steel tube thermoacoustic engine apparatus for 5 minutes while continuously recording the temperature on the hot side of the stack for the entire duration of the experiment. The test was done a second time but with the stack placed so that thermoacoustic oscillations would not occur. The results were then graphed and compared to find out the practicality of passive thermoacoustic cooling.

[11] Testo 490 anemometer.

III. Results and Discussion

1. Experimental Results

1.1 Tube Dimensions and Resonance Frequency

1.1.1 Tube Length and Resonance Frequency

26 resonance frequencies from tubes of 47 to 8cm were recorded and plotted against the reciprocal of their corresponding tube lengths (see **Fig. 6**). The data points were fitted with a first order polynomial and the resulting line showed that resonance tubes shorter than 0.5cm produce sounds above 20,000Hz, which is beyond hearing range, while previous studies indicate ultrasonic operation can be achieved with 2cm tubes. A cooling device this small can also be easily integrated into existing microelectronic devices.

The tube lengths and oscillating frequencies were calculated with :

$$v=\lambda f \qquad (1)$$

v: Velocity (m/s);
λ: Wavelength (m);
f: Frequency (Hz);

Results from the calculations showed that the tube length was always one-fourth the wavelength of the oscillating sound produced.

Another unexpected finding was the frequency of sound produced by the experiment apparatus would show an approximately 10 percent increase. The increase in pitch would gradually occur over a period of 10 minutes after onset of thermoacoustic oscillations (see **Fig. 7**). According to:

$$v=331+0.6t \qquad (2)$$

v: Sound velocity (m/s);
t: Air temperature (℃);

Sound velocity is directly proportional to the air temperature. Because tube length remains the same, the resonance frequency would also be proportional to the air temperature. Therefore, as the stack continues to heat up the air inside the resonance tube, the oscillating frequency was also elevated. In an actual thermoacoustic engine cooling device, the temperatures would not rise as high as the ones recorded in the experiments, so the frequency differences would be smaller. Also, since the actual operating frequency is already in the ultrasonic range, an increase in pitch would still be undetectable to an unaided ear.

1.1.2 Tube Diameter and Resonance Frequency

Results indicate that resonance frequency difference under the three different tube diameters of 2, 2.5, 3cm does not exceed 3% (15cm tube length) (see **Table 3**).

Table 3. Resonance frequency under three tube diameters

Diameter	2 cm	2.5 cm	3 cm
Frequency	601 Hz	580 Hz	593 Hz

Using only three tube diameters was insufficient to determine whether larger differences would significantly affect resonance frequency, this will be a focus for future studies.

1.2 Stack and Tube Relationship

1.2.1 Best Position of Stack

The best positions of stacks were measured as previously stated and graphed into **Fig. 8**. The data shows that the "best position" for a stack in a thermoacoustic resonance tube would be about 50% of its length, in other words, the center of the tube.

In 15cm tubes with diameters of 1.5, 2, 2.5cm, the amount of change in best positions are presented in **Table 4**. When the diameter is in the range of 1.5 to 2.5cm, the effect on a stacks best position in the tube would appear to be limited.

Table 4. Best stack positions under different tube diameters

Best Position / Length / Diameter	15.0 cm	20.0 cm	25.0 cm
1.5 cm	8.00 cm	9.75 cm	14.00 cm
2.0 cm	8.25 cm	10.50 cm	14.50 cm
2.5 cm	8.00 cm	10.50 cm	14.50 cm
Average (cm)	8.08 cm	10.25 cm	14.33 cm

1.2.2 Onset Stack Temperature Difference for TA effect

Originally, measurements were to be conducted on the Pyrex test tubes using infrared thermography. However, the Avio Handy Thermo TVS-100 unit's operating wavelength (3000 to 5400nm[12]) does not match the optical transmission wavelength of Pyrex glass (see **Fig. 9**[13]). As a result, the temperature observed with the infrared thermography

[12] Cheng, Y.Z. (2002). Applications of Infrared Thermography. *Safety, Health and Environment*, 7. Retrieved September 17th, 2004, from the Industrial Development Bureau, Ministry of Economic Affairs website: http://she.moeaidB.gov.tw/issue/issue7/tec7_2.htm

[13] *Pyrex Properties*. (n.d.). Retrieved September 19th, 2004, from the Präzisions Glas & Optik GmbH website: http://www.pgo-online.com/intl/jse/frameroute/genericset.html?Content=/intl/katalog/pyrex.html

unit is the temperature on the outer surface of the test tube, preventing the temperature inside it from being measured. Ultimately, two steel tubes with diameters of 3.2 and 2.4cm were chosen as the testbeds for experimentation using a K-type thermocouple to measure their interior temperatures. Infrared thermography was still conducted to visualize the temperature on the outer surface of the tubes (see **Fig. 10**). The data acquired was used to calculate the amount of conduction and radiation emitted from the apparatus.

If the problems preventing the use of infrared thermography inside the resonance tube could be alleviated, temperature measurements in the thermoacoustic engine can become much more accurate. Infrared thermography can also provide an entire view of the distribution of heat inside the resonance tube. A solution to this problem would also be an important point in future research.

Fig. 11, **Fig. 12** and **Fig. 13** were done using the steel tube with a diameter of 3.2cm under 47, 38 and 29cm resonance cavities.

Fig. 14, **Fig. 15** and **Fig. 16** were done using the steel tube with a diameter of 2.4cm under 43, 38 and 29cm resonance cavities.

Under input electric currents of 2, 3, 4 and 6A, a 2cm stack was gradually moved away from the best position in the resonance tube, the drop in acoustic intensity was recorded (see **Fig. 17**).

From these sets of data, it can be observed that under the same tube length, stack thickness is proportional to the required temperature difference to induce and maintain thermoacoustic oscillations. The produced sound intensity also drops as the stack becomes thicker. Therefore, finding a suitable material and fabrication solution for thinner stacks that can still maintain a sufficiently large temperature difference is an important goal in future research.

One explanation of the above-mentioned phenomena is the analogy between the moving air in the resonance tube and a pendulum. It is already known that the resonance tube's length is one-fourth that of the wavelength of the oscillating sound.

According to Professor Robert Smith from Penn State University (adapted from e-mail correspondence): Air at the closed end of the tube has the highest pressure with the smallest velocity, similar to the highest point of a pendulum with zero velocity yet the greatest potential. On the other hand, air at the opening of the tube has the smallest pressure at maximum velocity, which is like the pendulum at its lowest point. Under these circumstances, power produced near the closed end decreases, air near the open end flows faster but the energy would be more easily reduced by friction. A stack placed at the center would strike the best balance between the two problems.

1.3 Heat Transfer in TA Device

1.3.1 Convection

Using the data produced by anemometry at the opening of a 47cm steel resonance tube (see **Picture 8** and **Fig. 18**) the amount of convection was calculated with the equations below.

It is known that the amount of heat transferred is given by:

$$\triangle H = ms\triangle T \qquad (3)$$

△H: Heat difference (cal);
m: Mass (kg);
s: Specific heat (W/kgK);
△T: Temperature difference (K)

Considering the tube environment in which the TA effect takes place, the mass of air would be the product of tube length, cross-section area and the specific weight of air. **(3)** can then be rewritten as:

$$\triangle H = \rho Als\triangle T \qquad (4)$$

ρ: Air specific weight (kg/m^3);
A: Cross-section area (m^2);
l: Tube length (m)

Now divide **(4)** by **△t** (time difference) and convert the product to joules by multiplying the equation by 4.18 to yield **(5)**:

$$P = \rho Avs\triangle T \cdot 4.18 \qquad (5)$$

P: Convection rate (W);
V: Velocity (m/s);

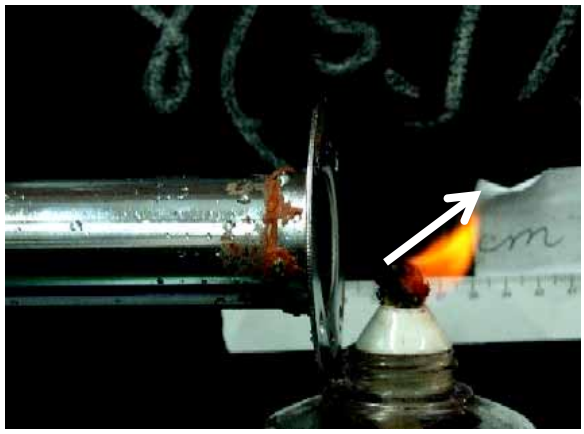

Picture 8 A flame deflected by the acoustic streaming of air.

1.3.2 Conduction

The amount of heat transported by conduction was calculated using **(6)**, taking into account the heat conduction coefficient of the resonance tube material and the temperature at the hot side of the stack.

$$\mathbf{Q_{cond}=kA(\Delta T/\Delta X)} \quad \textbf{(6)}$$

$\mathbf{Q_{cond}}$: Conduction rate (W);
k: Heat conduction coefficient;
A: Area (m^2);
ΔT: Temperature difference (K);
ΔX: Distance (m);

Also, with **(7)**, natural convection on the entire surface of the resonance tube was taken into consideration.

$$\mathbf{Q_{surface}=hA(T_h-T_w)} \quad \textbf{(7)}$$

$\mathbf{Q_{surface}}$: Resonance tube surface convection (W);
h: 10 (W/m^2K) Natural convection constant;
A: Resonance tube surface area (m^2);
$\mathbf{T_h}$: Mean surface temperature (K);
$\mathbf{T_w}$: Mean air temperature (K);

1.3.3 Radiation

Heat radiation was calculated from the mean temperature of the entire thermoacoustic engine apparatus by:

$$\mathbf{Q_{emit}= \varepsilon \acute{O} A (T_s)^4} \quad \textbf{(8)}$$

$\mathbf{Q_{emit}}$: Radiation rate (W);
ε : Radiation rate constant;
Ó: 5.6703×10^{-8} （W/m^2K^4） Stefan-Boltzmann Constant;
A: Surface area (m^2);
$\mathbf{T_s}$: Surface temperature (K);

1.3.4 Acoustic Radiation

It is already known that the basic equation for comparing sound intensity is given by the following:

$$\mathbf{dB=10\log(I/I_0)} \quad \textbf{(9)}$$

dB: Relative sound intensity;
I: Measured value;
$\mathbf{I_0}$: Weakest audible sound;

The relative acoustic intensity (dB) was measured 10cm from the opening of the tube. Using:

$$\textbf{sound level} = 20\text{dB}\left(P_{measured}/P_{reference}\right) \quad (10)$$

$P_{measured}$: Measured value (mPa);
$P_{reference}$: Reference pressure (0.02mPa);
dB: Sound intensity;

The approximate sound pressure at that point was determined. Assuming spherical expansion, the total amount of energy dissipated in the form of sound was then calculated with:

$$I = \left(p_{rms}^2\right)/\left(\rho_0 V\right) \quad (11)$$

I: Sound intensity (W/m^2);
p_{rms}: Sound pressure (Pa);
ρ_0: Density (Kg/m^3);
V: Sound velocity (m/s);

The data from the above calculations were graphed and compared side-by-side (see **Fig. 18**). Although the contribution to cooling by acoustic radiation is small, the acoustic oscillations are vital for enhancing air convection by as much as 80 times.

Finally, an actual test was conducted with the 47cm steel tube thermoacoustic engine apparatus. A significant temperature drop of about 80°C (30%, numerically speaking) caused by the enhanced convection was observed (**Fig. 19**), which can be very useful in a real cooling device. This result justified the attempt on constructing a real prototype of the passive thermoacoustic engine cooling device.

2. Prototype Design and Construction

An actual passive thermoacoustic cooling device was designed using experimental results. Dimensions were decided according to the length of the resonance tube that can oscillate in the ultrasonic range to avoid audible noise, stack position and thickness were also determined in a similar fashion.

Two Mark I prototypes were fabricated, with 7 resonance cavities of 9 cm and 20 cm long placed in an array. Each unit is composed of a stack sandwiched between a copper (hot side) cap and an aluminum (cold side) cap. The bottom of the copper cap is placed in contact with the heat source to conduct heat to the hot side of the stack (See **Picture 9**).

Picture 9 Passive TA cooler prototype (Mark I). Left: Components of prototype, copper and aluminum caps and ceramic stack. Right: Assembled device.

Two more Mark II prototypes (5cm diameter) were built to fit on a real computer's CPU, with an array of resonance tubes of 2 and 4cm long (0.3cm diameter). The resonance tubes were carved in using a 3mm drill. This time, the bottom cap was made of aluminum to conduct heat to the stack, which was integrated on one side of the top acrylic cap (See **Picture 10**). This has the advantage of further simplifying construction.

Picture 10 Passive TA cooler prototype (Mark II). The stack is integrated in the acrylic cap bringing the total components down to two, further simplifying fabrication.

3. Discussion

3.1 Project Thought Process

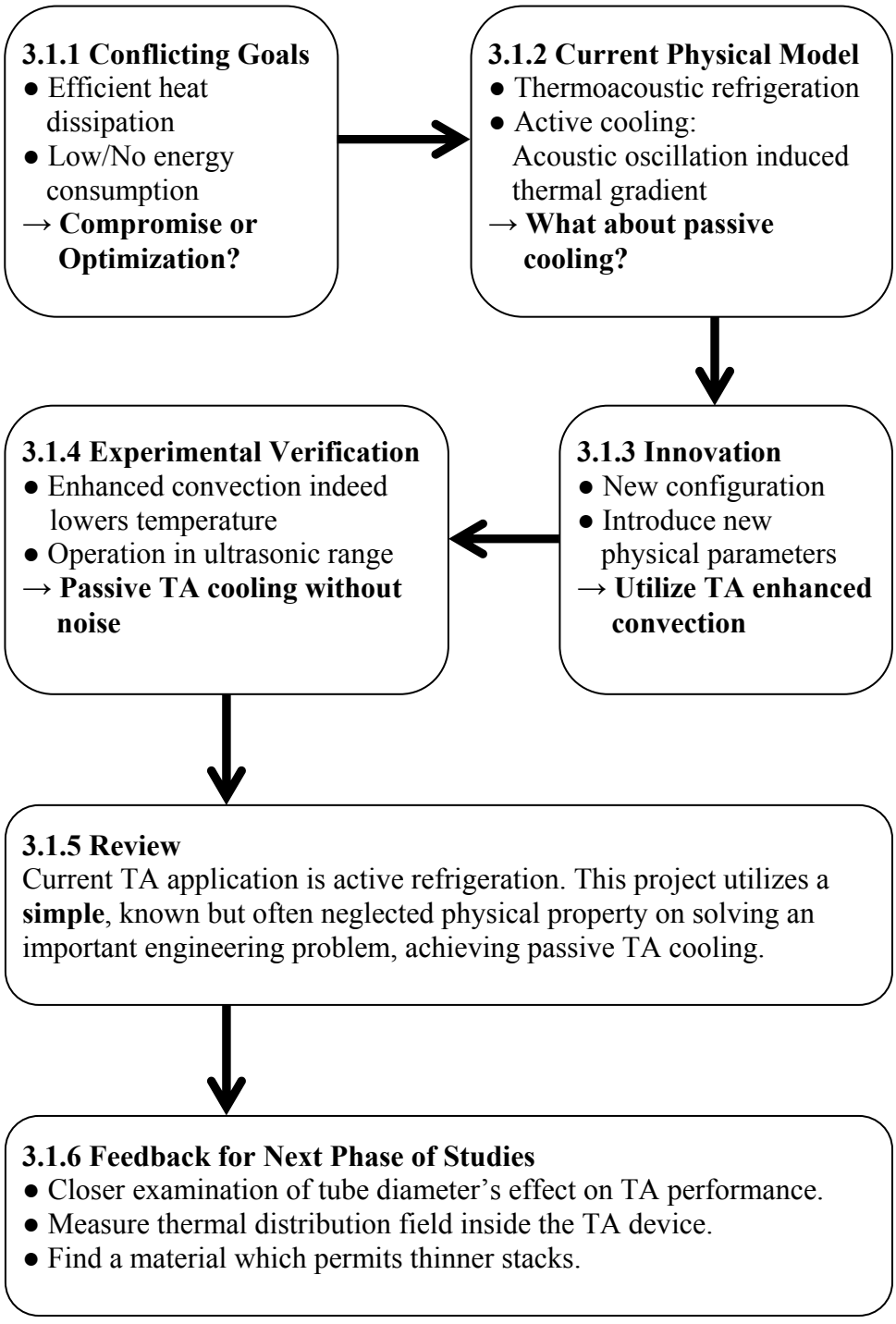

3.2 Reflection

Two major conflicting goals in engineering have always been achieving the most efficient cooling effect while consuming the least amount of energy. Most of today's solutions utilize electric fans as the primary means of heat dissipation, or more recently, thermoacoustic refrigeration. However, this kind of active cooling has the disadvantages of input energy requirements and heat buildup that compounds the original problem.

Considering the primary means of TA refrigeration today, this project introduced a known but often neglected physical property, which is the enhanced air convection in a TA engine. Starting with this knowledge, research was conducted to evaluate the effectiveness of passive thermoacoustic cooling.

Actual tests verified that enhanced convection induced by acoustic resonance is indeed capable of lowering the hot side temperature of the stack inside the experimental TA apparatus by 80°C (30%). When the NiCr simulated heat source is replaced with the to-be-cooled device, passive cooling can then be achieved. Additionally, experimental results indicate that the resonance tube of a thermoacoustic engine can be reduced to a size enabling operation in the ultrasonic range. Prototypes were then built and tested.

Today's thermoacoustic refrigeration techniques, such as navy radar coolers and Space Shuttle thermal control systems, even Ben & Jerry's ice cream refrigerators have never become widespread. The solution presented in this project has the potential application in not only microelectronic cooling but also any field requiring effective temperature control without refrigeration below ambient temperature.

This research is an important step toward improving the major heat problems posed by present and future microelectronic devices, and it can eventually help expand thermoacoustics from a relatively obscure niche market into the mainstream market of passive cooling. Two points important in future research are the resonance tube diameter's impact on TA performance and material research to enable thinner stacks.

IV. Conclusion

1. Experimental Results Summary

(1)Resonance tube length is one-fourth the wavelength of oscillating sound.

(2)Best position for stack would be 50% inside resonance tube.

(3)Resonance tubes shorter than 0.5cm can operate in ultrasonic range.

(4)Passive thermoacoustic cooling does not depend on acoustic radiation. It instead utilizes the acoustically enhanced air convection.

(5)Enhanced air convection induced by the thermoacoustic effect can lower the temperature by as much as 30%.

(6)Under the same tube length, stack thickness is inversely proportional to required temperature difference for acoustic resonance. Thinning the stack would be an important engineering goal.

2. Summarized Conclusion

This project successfully developed a new innovative solution to alleviating two major conflicting goals in engineering: efficient cooling and low power consumption. Experimental data shows enhanced air convection in the thermoacoustic engine can be used to achieve passive cooling without additional input power. Using this known, simple but often neglected physical property to solve an important engineering problem makes this research stand out on the way toward expanding thermoacoustics from a niche market to the mainstream market of passive cooling.

V. Figures and Diagrams

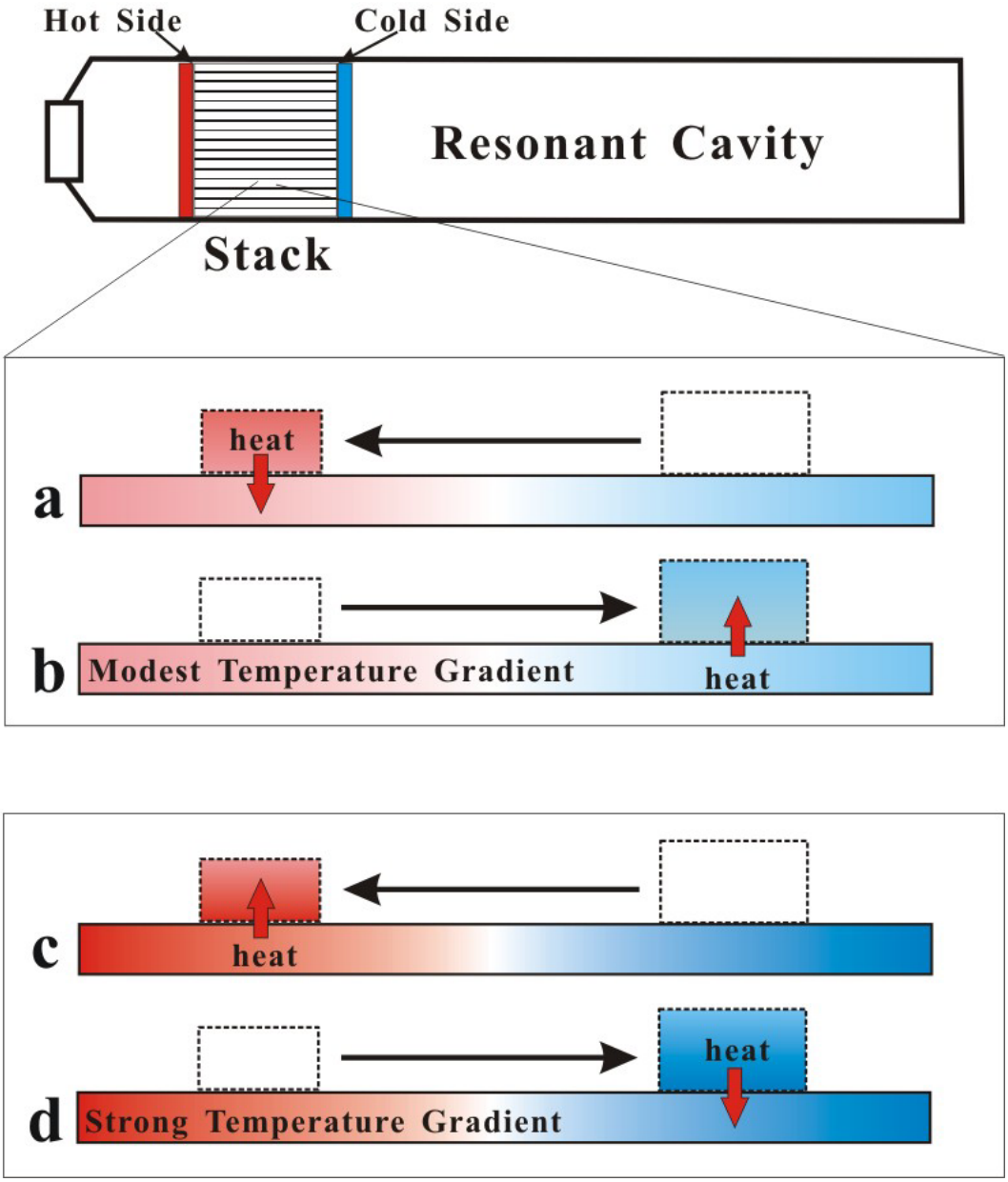

Fig. 1 **a**, **b**: Thermoacoustic refrigerator. **c**, **d**: Thermoacoustic engine.

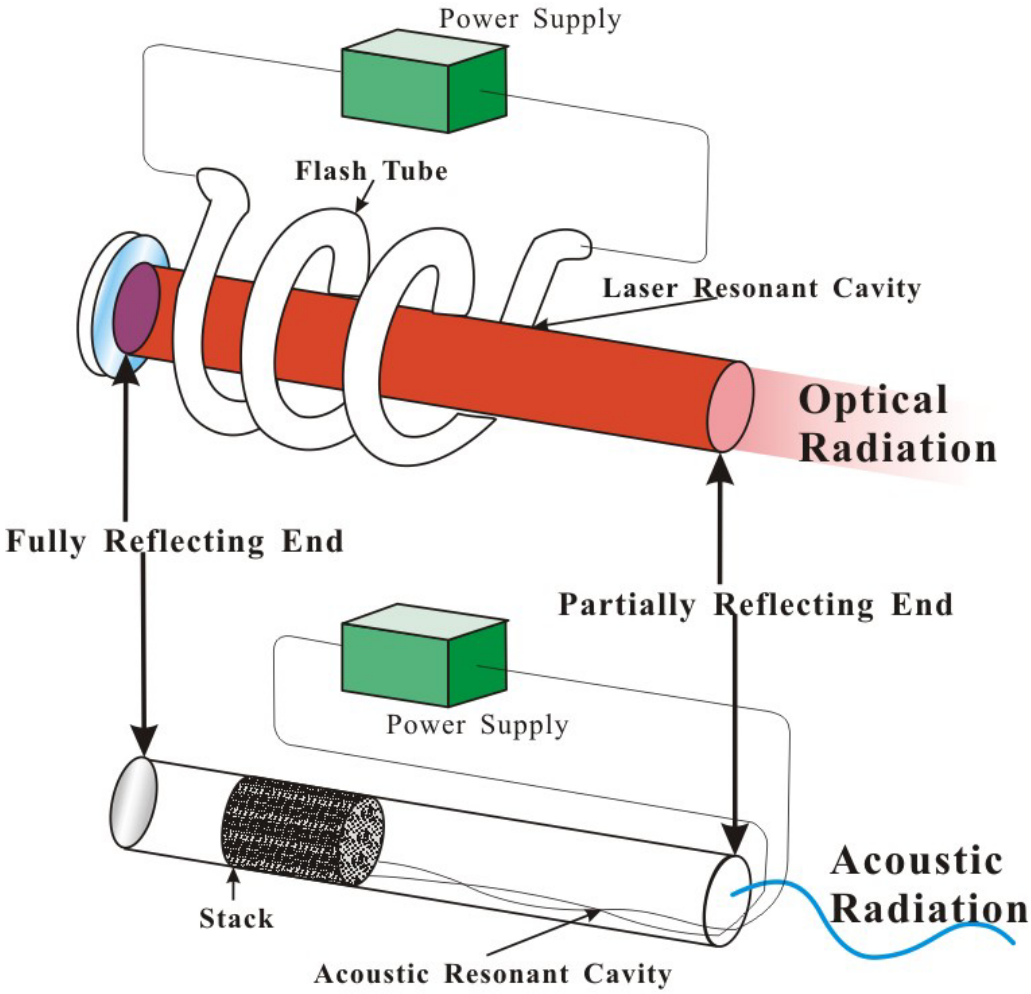

Fig. 2 Analogy between an optical laser and an acoustic laser.

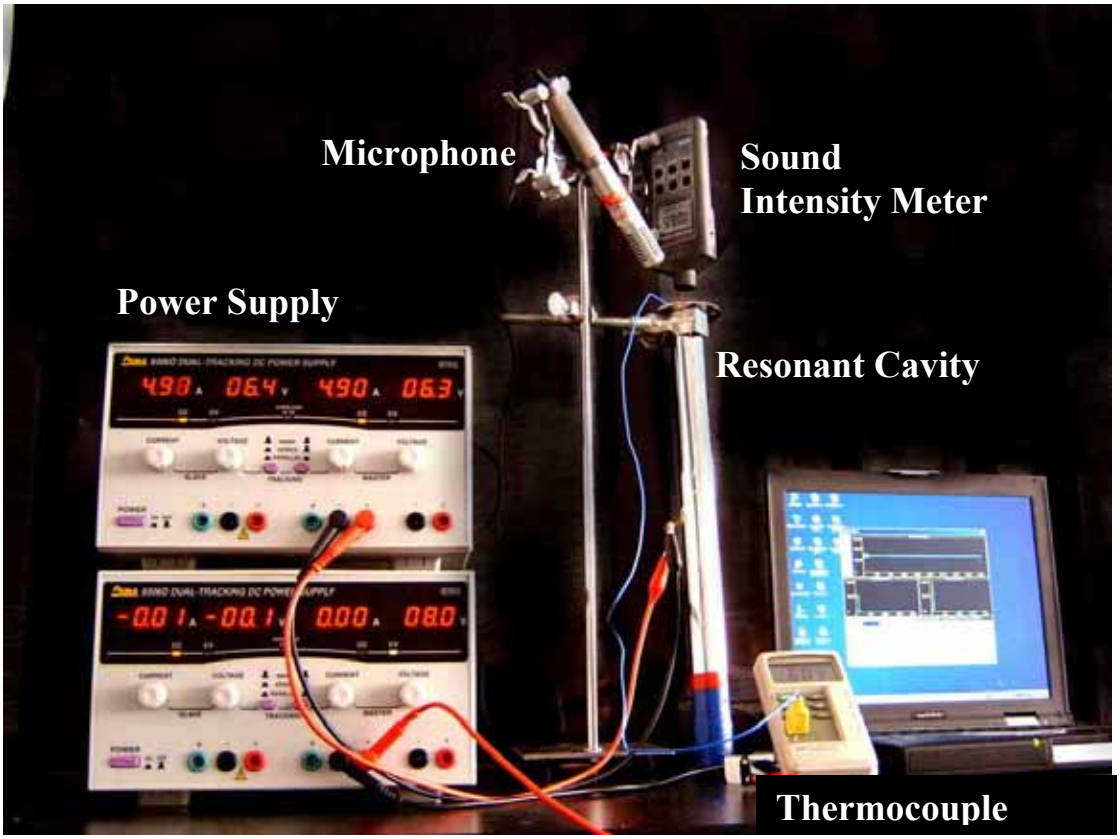

Fig. 3 Thermoacoustic engine measurement configuration.

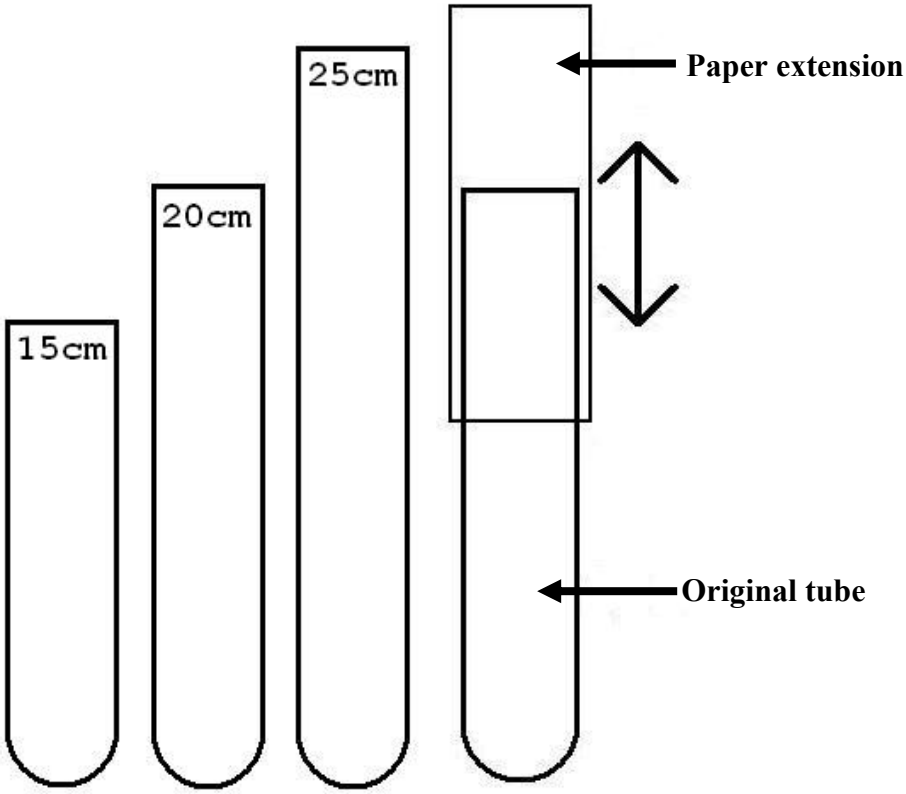

Fig. 4 Left: The three original test tubes. Right: A test tube with paper extension.

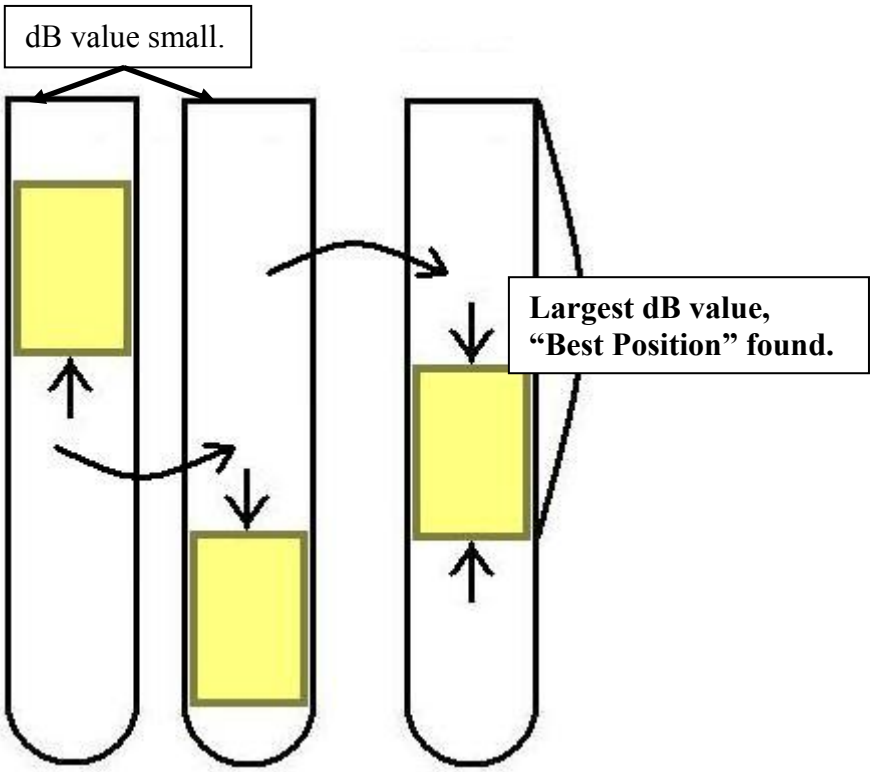

Fig. 5 Finding the "Best Position" of a stack.

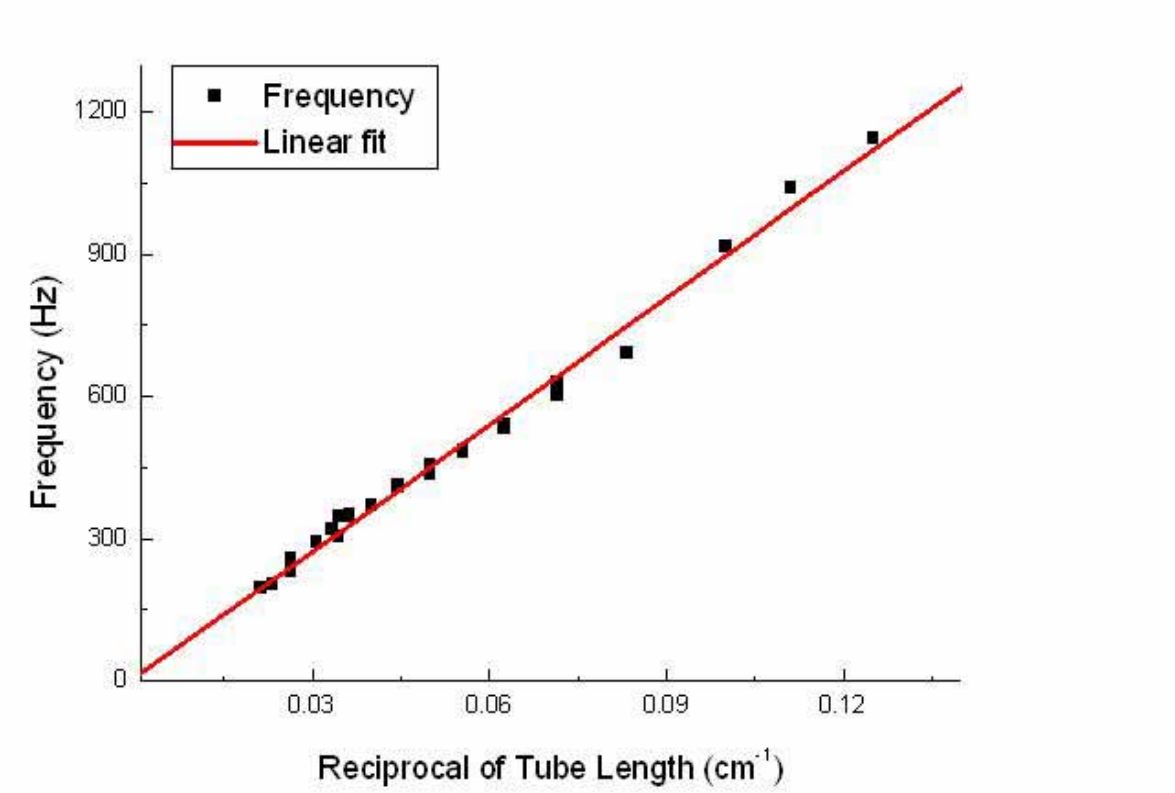

Fig. 6 Resonance frequency plotted against reciprocal of respective tube lengths.

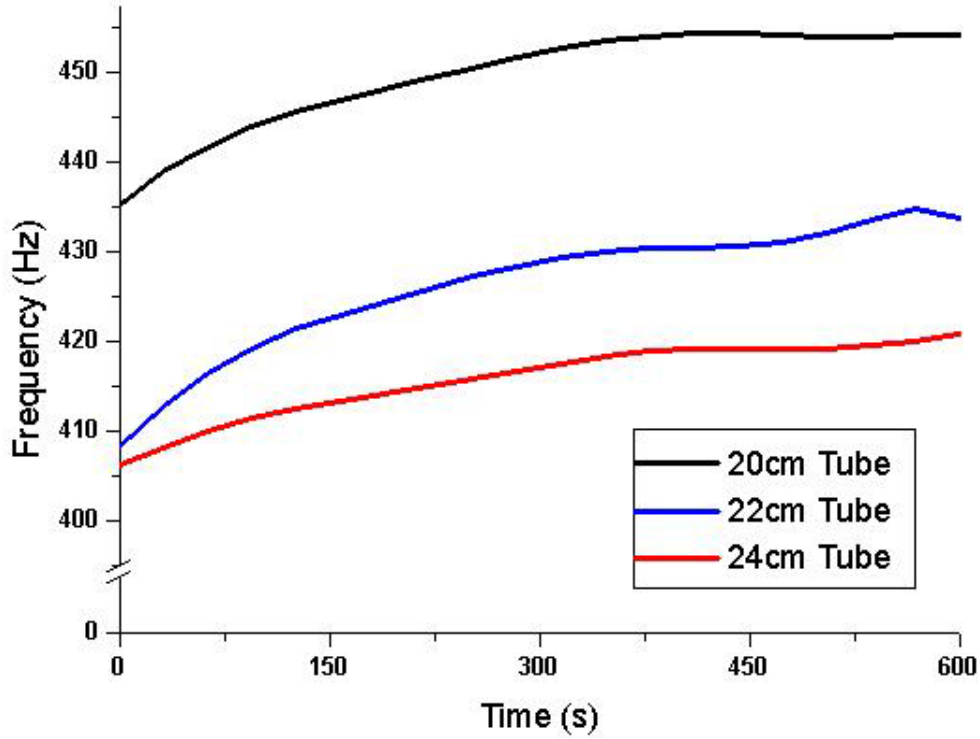

Fig. 7 Frequency increase in resonance tube over a 10 minute period.

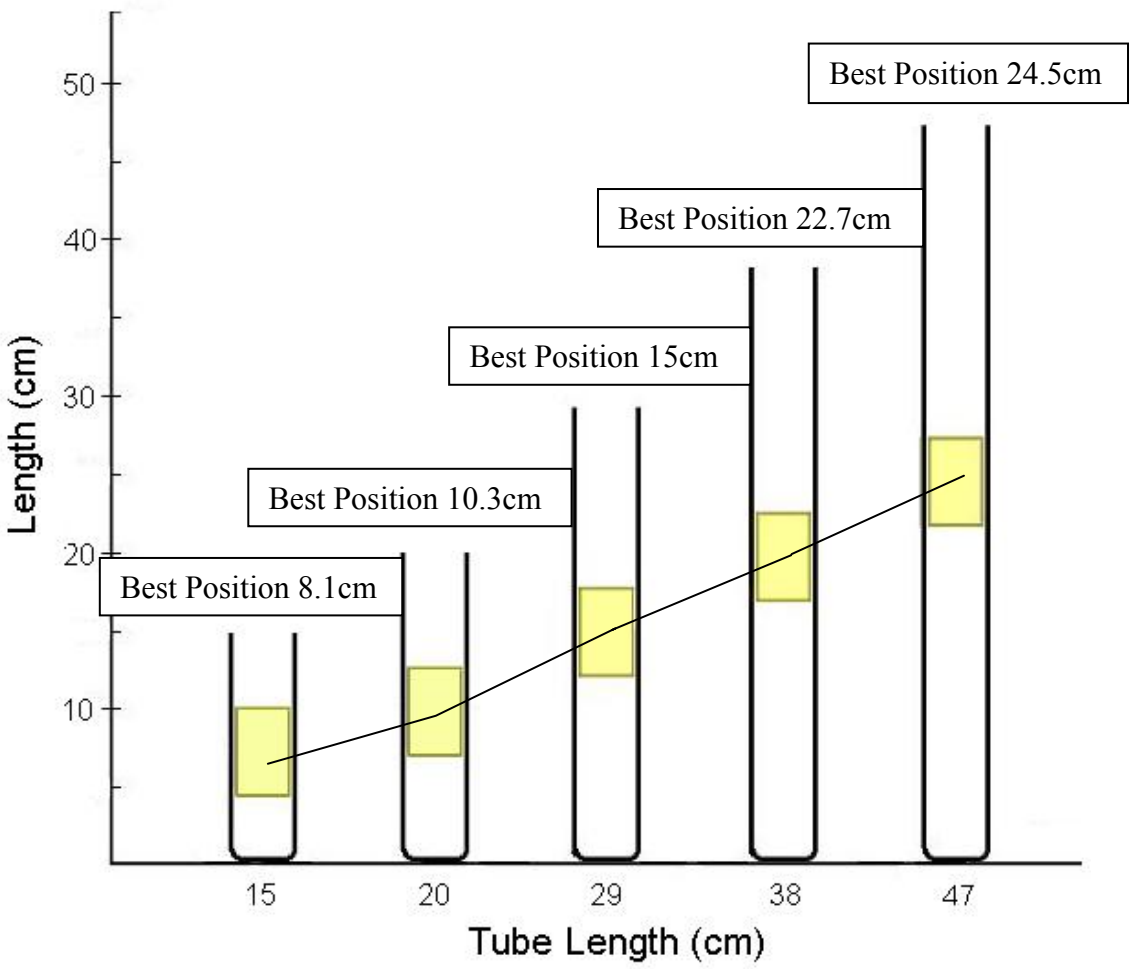

Fig. 8 Best positions of stacks are about 50% tube length.

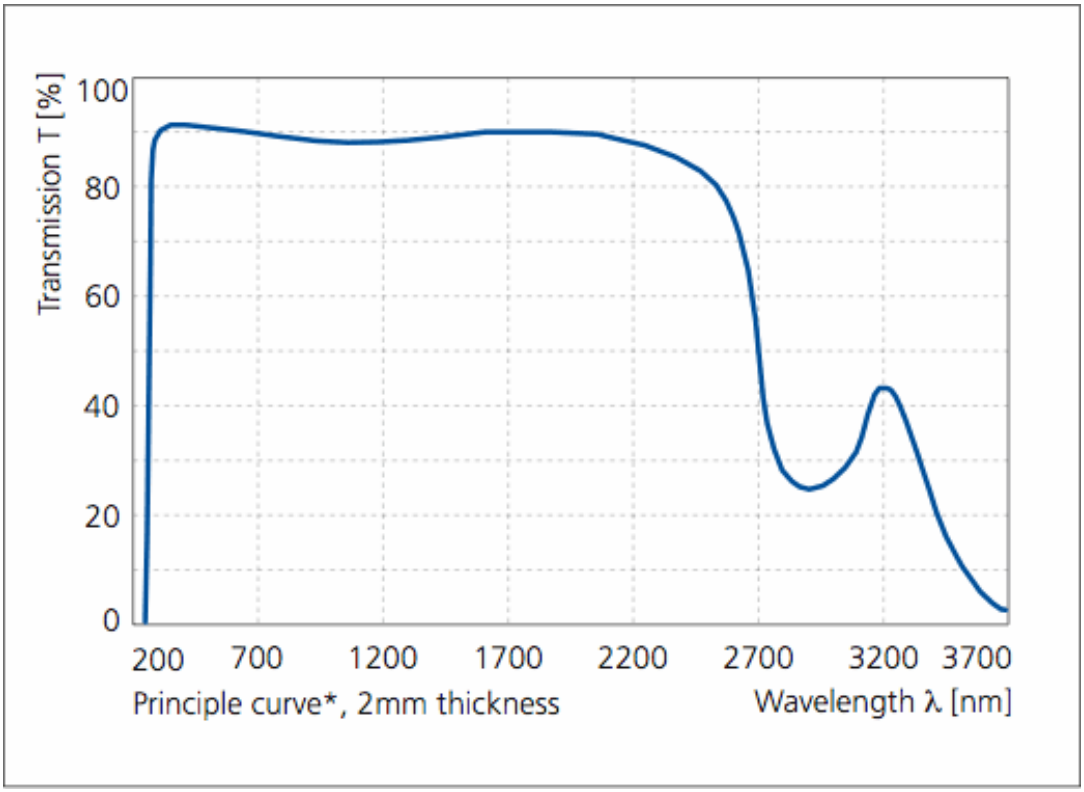

Fig. 9 Transmission wavelength of Pyrex glass.

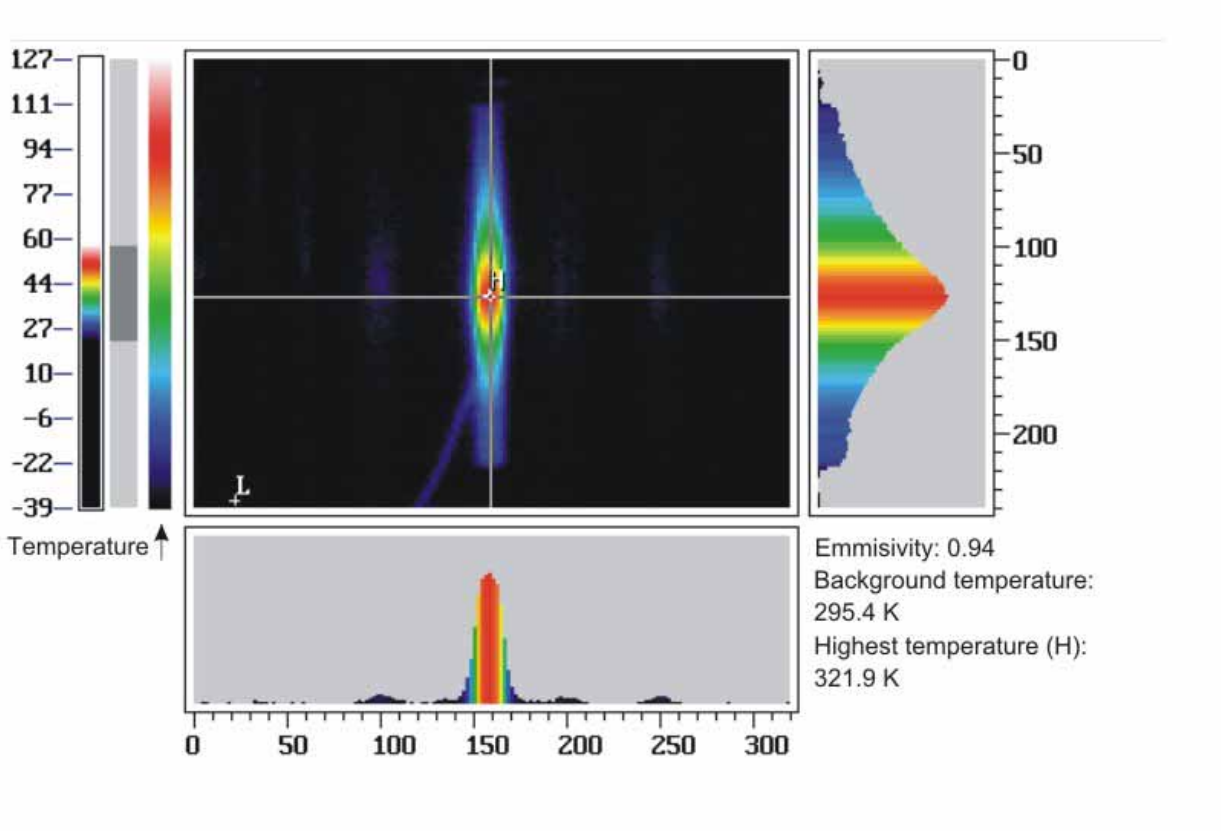

Fig. 10 Thermograph of 47cm steel resonance tube's surface, used to calculate heat conduction and radiation from the apparatus.

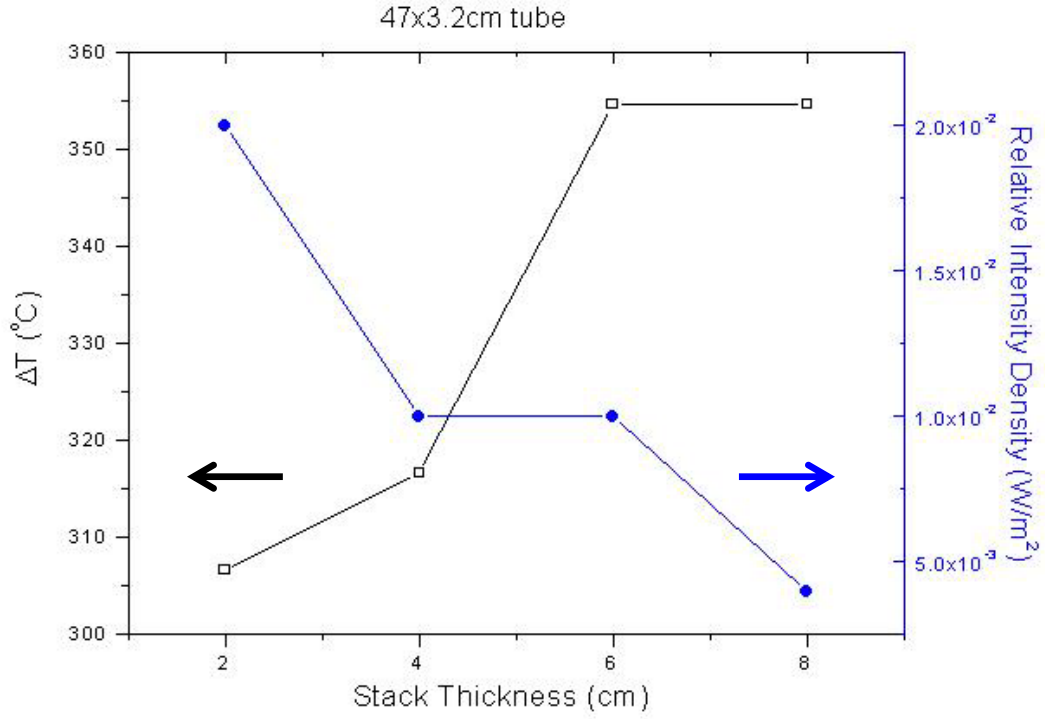

Fig. 11 Stack thickness plotted against minimum required temperature difference and produced sound intensity. 47cm long tube, diameter 3.2cm.

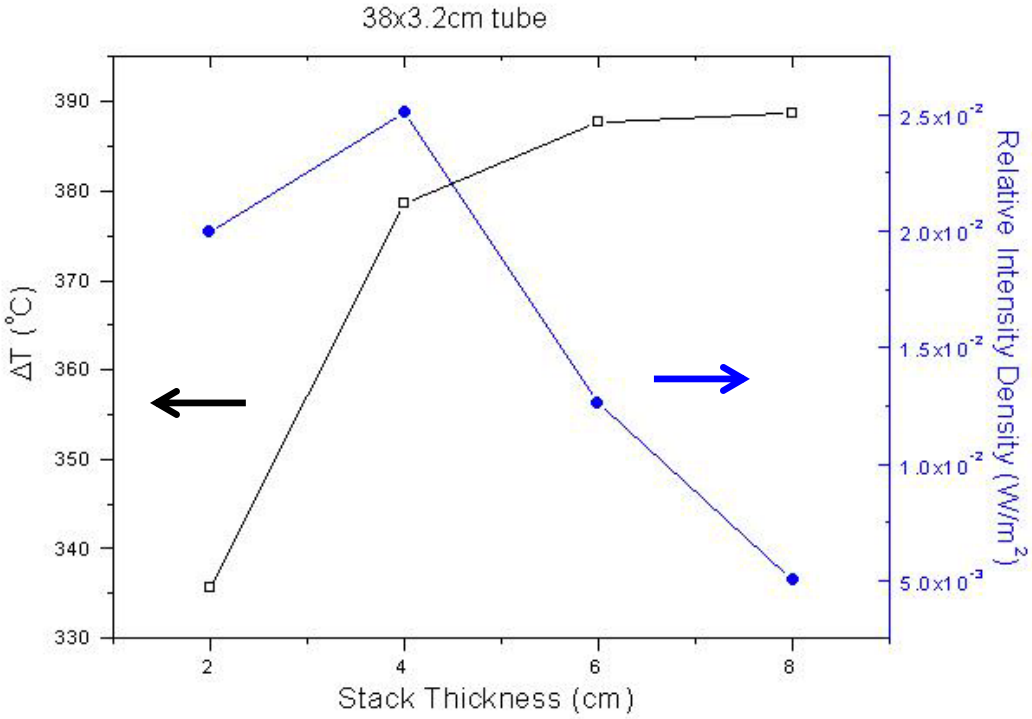

Fig. 12 Stack thickness plotted against minimum required temperature difference and produced sound intensity. 38cm long tube, diameter 3.2cm.

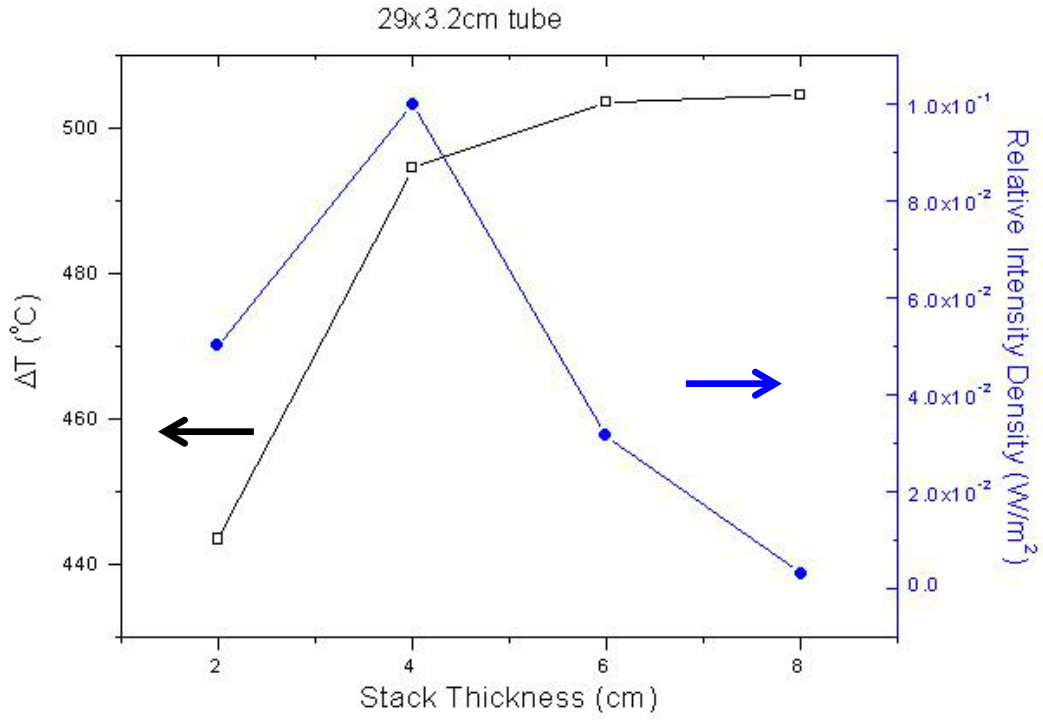

Fig. 13 Stack thickness plotted against minimum required temperature difference and produced sound intensity. 29cm long tube, diameter 3.2cm.

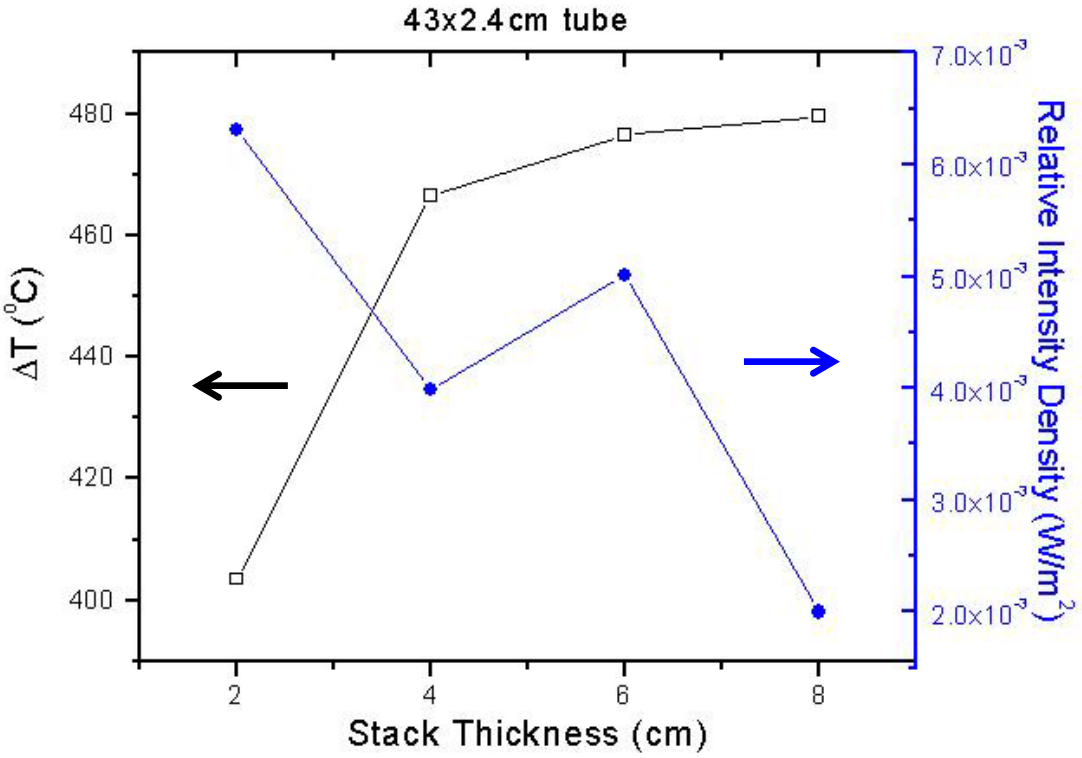

Fig. 14 Stack thickness plotted against minimum required temperature difference and produced sound intensity. 43cm long tube, diameter 2.4cm.

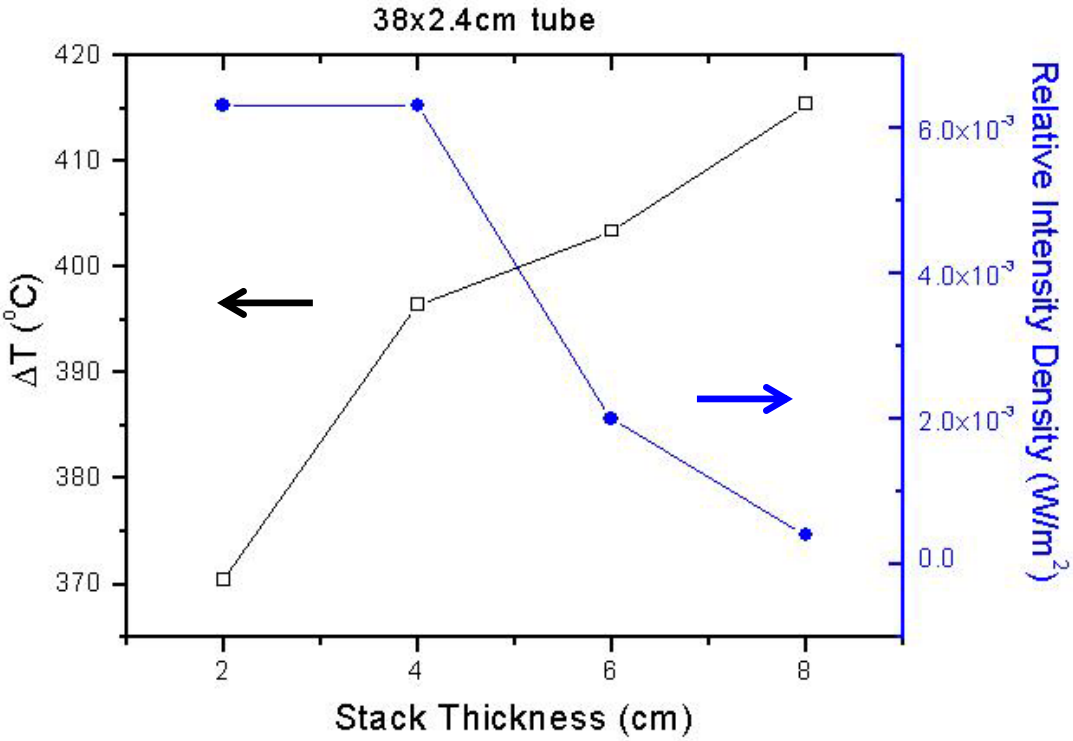

Fig. 15 Stack thickness plotted against minimum required temperature difference and produced sound intensity. 38cm long tube, diameter 2.4cm.

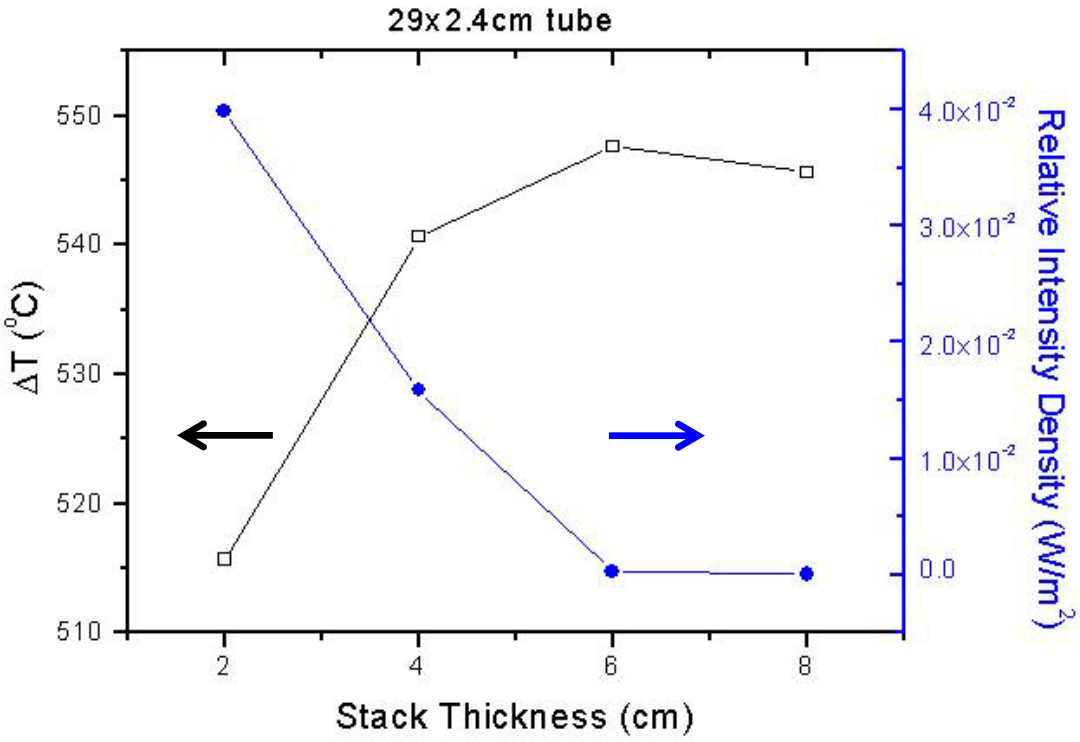

Fig. 16 Stack thickness plotted against minimum required temperature difference and produced sound intensity. 29cm long tube, diameter 2.4cm.

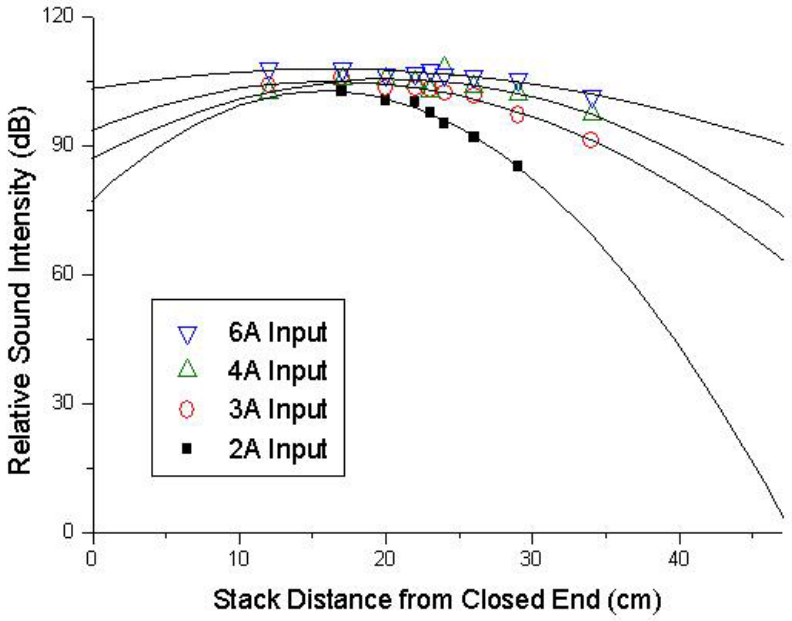

Fig. 17 Sound intensity drop when stack is moved away from the center of the resonance tube.

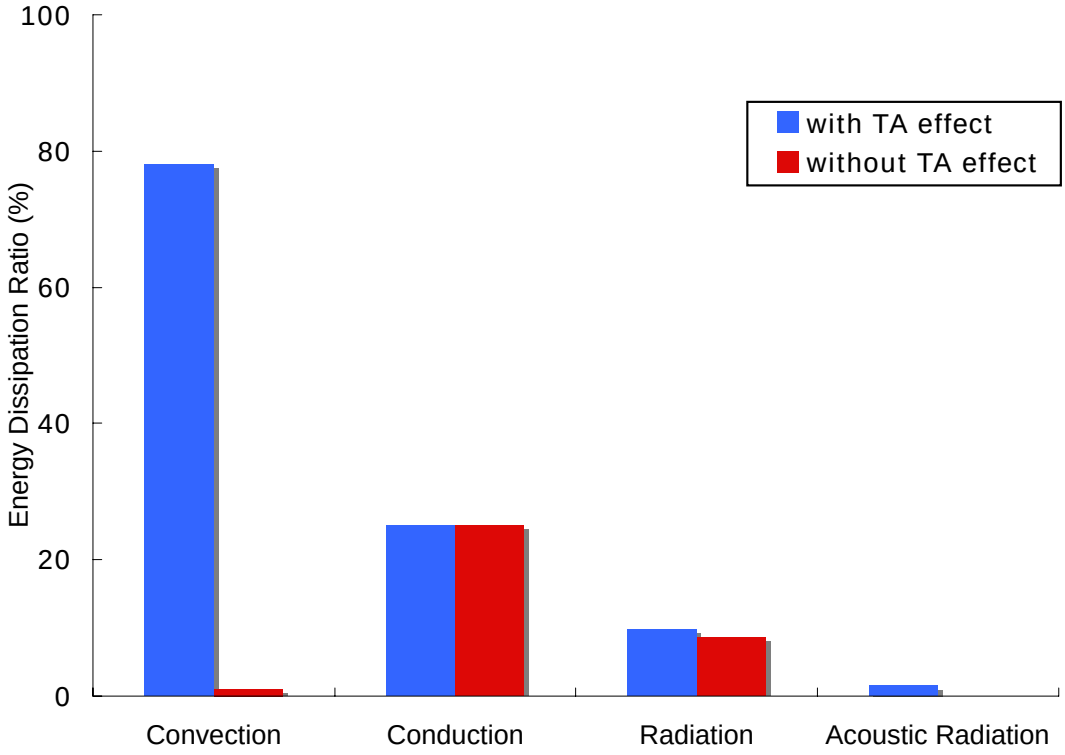

Fig. 18 The ratio of energy dissipation in the thermoacoustic engine apparatus, which primarily comprises of enhanced air convection induced by resonating sound.

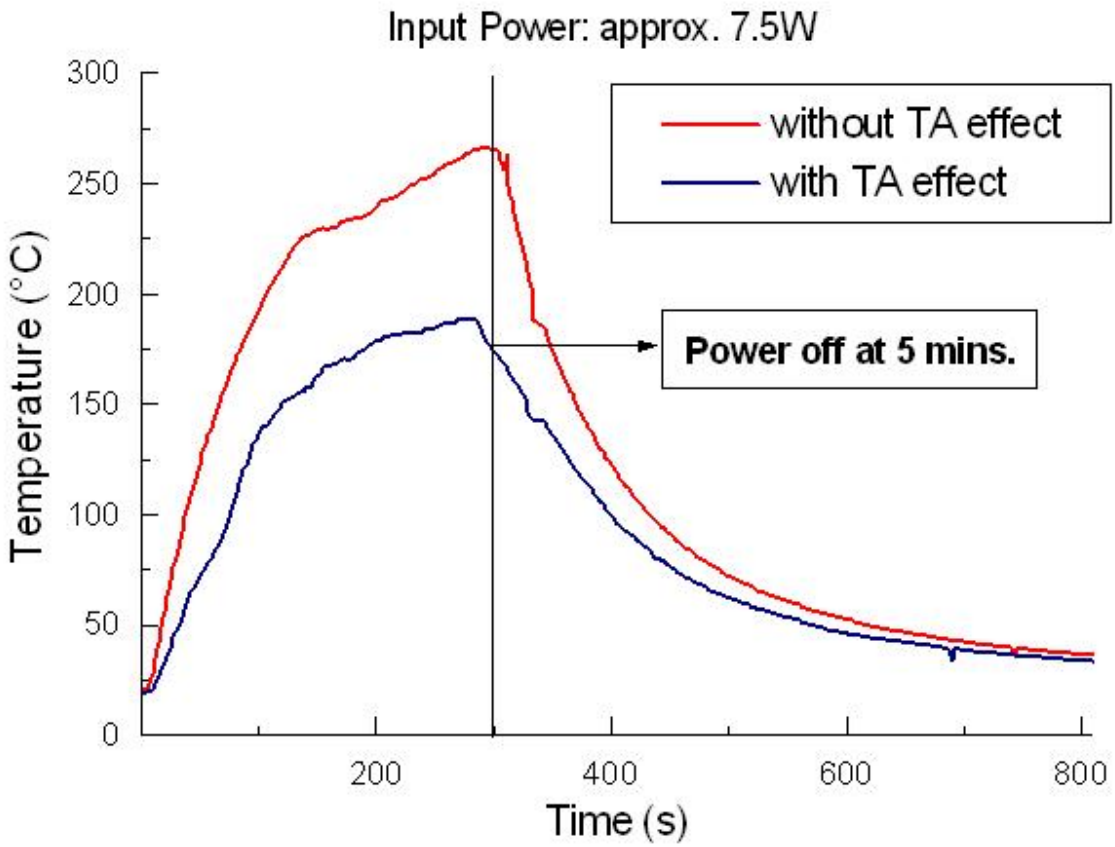

Fig. 19 Passive cooling caused by the thermoacoustic effect, a maximum temperature drop of about 80℃ was observed.

VI. Bibliography

[1]Lord Rayleigh (1945). *The Theory of Sound, Vol.II*. Dover, New York: Dover Publications.

[2]Swift, G. W. (1988). Thermoacoustic Engines. *Journal of the Acoustical Society of America*, *88*, 1145-1180.

[3]Garrett, S. L., J. A. Adeff & T. J. Hofler (1993). Thermoacoustic refrigerator for space applications. *Journal of Thermophysics and Heat Transfer*, *7*, 595-599.

[4]Garrett, S. L. (1997). *High-power thermoacoustic refrigerator*. U.S. Patent 5,647,216.

[5]Tijani, M.E.H., Zeegers, J.C.H., de Waele , A.T.A.M. (2002). Design of thermoacoustic refrigerators. *Cryogenics*, *42*, 49-57.

[6]Tijani, M.E.H., Zeegers, J.C.H., de Waele , A.T.A.M. (2002). Construction and performance of a thermoacoustic refrigerator. *Cryogenics*, *42*, 59-66.

[7]Qiu, T., Qing, L., Feng, W., Fang, Z. G. (2003). Network model approach for calculating oscillating frequency of thermoacoustic prime mover. *Cryogenics*, *43*, 351-357.

[8]Qiu, T., Qing, L., Fang, Z. G., Ji, H. W., Jun, X. L. (2003). Temperature difference generated in thermo-driven thermoacoustic refrigerator. *Cryogenics*, *43*, 515-522.

[9]Symko, O. G., Abdel-Rahman, E., Kwon, Y. S., Emmi, M., Behunin, R. (2004). Design and development of high-frequency thermoacoustic engines for thermal management in microelectronics. *Microelectronics Journal*, *35*, 185-191.

[10]Sakamoto, S., Watanabe, Y. (2004). The experimental studies of thermoacoustic cooler. *Ultrasonics*, *42*, 53-56.

[11]Chen, G.H. (2000). *Design and Experiment of a thermoacoustic refrigerator*. Unpublished master's dissertation, National Taiwan University, Taipei, Taiwan R.O.C.

[12]Huang, P.C. (2004). *Experimentation and Numerical Simulation of a Sonic Refrigerator*. 2004 Energy and Refrigeration Conference. Taipei, Taiwan R.O.C. (September 10th, 2004).

[13]Sarpotdar, S. M., Ananthkrishnan, N., Sharma, S. D. (2003). The Rijke Tube - A Thermo-acoustic Device. *Resonance, 8*, 59-71.

[14]*Thermoacoustics - Sounds Cool!* (n.d.). Retrieved October 10th, 2004 from Ben & Jerry's Ice Cream website: http://www.benjerry.com/our_company/sounds_cool/

[15]Garrett, S.L., Backhaus, S. (2000). The Power of Sound. *American Scientist*, *88*, 516-525.

[16]*Penn State "Acoustic Laser" Kit Instructions*. (2003). State College, PA: Graduate Program in Acoustics, Applied Research Laboratory, Pennsylvania State University.

[17]Cheng, Y.Z. (2002). Applications of Infrared Thermography. *Safety, Health and Environment*, 7. Retrieved September 17th, 2004, from the Industrial Development Bureau, Ministry of Economic Affairs website: http://she.moeaidB.gov.tw/issue/issue7/tec7_2.htm

[18]Lin, M.D., et al. (2002). *High School Material Science: Physics Vol. II*. Tainan, Taiwan: Nani Publishing.

[19]*Pyrex Properties*. (n.d.). Retrieved September 19th, 2004, from the Präzisions Glas & Optik GmbH website: http://www.pgo-online.com/intl/jse/frameroute/genericset.html?Content=/intl/katalog/pyrex.html

[20]Wolfe, J. (1998). *What is a decibel?* Retrieved August 23rd, 2004, from the University of New South Wales website: http://www.phys.unsw.edu.au/~jw/dB.html

[21]Çengel, Y. A. (1998). *Heat Transfer: A Practical Approach*. Hightstown, NJ: WCB/McGraw-Hill.

[22]McGlen, R. J., Jachuck, R., Lin, S. (2004). Integrated thermal management techniques for high power electronic devices. *Applied Thermal Engineering, 24*, 1143-1156.

VII. Appendix

1. Computer software used in this project

[1]Mac OS X 10.3.9 Panther, Copyright© 2003, Apple Computer, Inc.
[2]Microsoft Windows XP Professional, Copyright© 1981-2001 Microsoft Corporation.
[3]Microsoft Word 2002, Copyright© 1983-2001 Microsoft Corporation.
[4]Microsoft Excel 2002, Copyright© 1983-2001 Microsoft Corporation.
[5]Graph 3.3, Copyright© 2004 Ivan Johansen.
[6]Voice Spectrograph, http://www.voicesync.org .
[7]Microsoft Calculator 5.1, Copyright© 1981-2001 Microsoft Corporation.
[8]Microsoft Paint 5.1, Copyright© 1981-2001 Microsoft Corporation.
[9]Adobe Illustrator CS 11.0.0, Copyright© 1987-2001 Adobe Systems, Inc.
[10]MSN Messenger 6.2, Copyright© 1997-2004 Microsoft Corporation.
[11]Microsoft Internet Explorer 6.0 SP-2, Copyright© 1995-2004 Microsoft Corporation.
[12]WinZip 9.0 SR-1 (6224), Copyright© 1991-2004 WinZip Computing, Inc.
[13]Microsoft Notepad 5.1, Copyright© 1981-2001 Microsoft Corporation.
[14]CorelDraw Version 12.0.0.458, Copyright© 2003 Corel Corporation.
[15]Microcal Origin 5.0 Professional, Copyright© 1991-1997 Microcal Software, Inc.
[16]Microsoft Photo Editor 3.0.2.3, Copyright© 1989-2000 Microsoft Corporation.
[17]AutoCAD 2006 Z.54.10, Copyright© 1982-2005 Autodesk, Inc.

2. Materials and equipment used in this project

[1]Cordierite ceramic composite
[2]Pyrex test tubes
[3]Nichrome (NiCr) wiring
[4]Copper wires
[5]Stainless steel tube
[6]ABM 9306D Dual-Tracking Power Supply
[7]Philips Corded Electret Microphone SBC-ME570
[8]Extech Digital Sound Level Meter 407727
[9]Nippon Avionics Co., Ltd. Avio Handy Thermo TVS-100 Infrared Thermography
[10]Hola TM-906 k-type thermocouple thermometer
[11]Samsung Kenox Digmax V4 digital camera
[13]Stopwatch
[14]Water